

2013 RSNA (Filtered Schedule)

Sunday, December 01, 2013

10:45-12:15 PM • **SSA12** • Room: S504CD • ISP: Molecular Imaging (Oncology I)
12:30-01:00 PM • **CL-MIE-SU5A** • Room: S503AB • Vein Graft Implantable Contrast Initiative: Enhanced Vessel Wall Imaging
12:30-01:00 PM • **CL-MIS-SUA** • Room: S503AB • Molecular Imaging - Sunday Posters and Exhibits (12:30pm - 1:00pm)
01:00-01:30 PM • **CL-MIS-SUB** • Room: S503AB • Molecular Imaging - Sunday Posters and Exhibits (1:00pm - 1:30pm)

Monday, December 02, 2013

08:30-10:00 AM • **MSMI21** • Room: S406B • Molecular Imaging Symposium: Preparing for Tomorrow: The Application of Novel and Advanced Imaging in Clinical...
08:30-10:00 AM • **RC220** • Room: S104A • Molecular and Functional Imaging/Surrogate Markers in Radiation Oncology
10:30-12:00 PM • **MSMI22** • Room: S406B • Molecular Imaging Symposium: Radiogenomics - The Next Logical Step in 'Rad-Path' Correlation for Clinical Imag...
12:15-12:45 PM • **CL-MIE-MO5A** • Room: S503AB • PET-MRI in Alzheimer Disease
12:15-12:45 PM • **CL-MIS-MOA** • Room: S503AB • Molecular Imaging - Monday Posters and Exhibits (12:15pm - 12:45pm)
12:45-01:15 PM • **CL-MIS-MOB** • Room: S503AB • Molecular Imaging - Monday Posters and Exhibits (12:45pm - 1:15pm)
01:30-03:00 PM • **MSMI23** • Room: S406B • Molecular Imaging Symposium: Imaging Cellular Subpopulations - Current Progress and Future Directions
03:30-05:00 PM • **MSMI24** • Room: S406B • Molecular Imaging Symposium: Molecular Brain Imaging: From Research to Clinical Applications

Tuesday, December 03, 2013

10:30-12:00 PM • **SSG01** • Room: E451A • ISP: Breast Imaging (Nuclear/Molecular Imaging)
10:30-12:00 PM • **SSG09** • Room: S504CD • Molecular Imaging (Subspecialties)
12:15-12:45 PM • **CL-MIE-TU5A** • Room: S503AB • Recurrent Brain Tumors v/s Radiation Necrosis: PET MRI as a Rescue
12:15-12:45 PM • **CL-MIS-TUA** • Room: S503AB • Molecular Imaging - Tuesday Posters and Exhibits (12:15pm - 12:45pm)
12:45-01:15 PM • **CL-MIS-TUB** • Room: S503AB • Molecular Imaging - Tuesday Posters and Exhibits (12:45pm - 1:15pm)
12:45-01:15 PM • **LL-MIS-TUB** • Room: Lakeside Learning Center • Molecular Imaging - Tuesday Posters and Exhibits (12:45pm - 1:15pm)
03:00-04:00 PM • **SSJ15** • Room: S504CD • Molecular Imaging (Neurosciences)

Wednesday, December 04, 2013

10:30-12:00 PM • **SSK12** • Room: S504CD • ISP: Molecular Imaging (Oncology II)
10:30-12:00 PM • **SSK21** • Room: S404AB • Physics (Molecular Imaging)
12:15-12:45 PM • **CL-MIE-WE5A** • Room: S503AB • PET Imaging of Neuroendocrine Tumors-Clinical State of the Art
12:15-12:45 PM • **CL-MIS-WEA** • Room: S503AB • Molecular Imaging - Wednesday Posters and Exhibits (12:15pm - 12:45pm)
12:45-01:15 PM • **CL-MIS-WEB** • Room: S503AB • Molecular Imaging - Wednesday Posters and Exhibits (12:45pm - 1:15pm)
03:00-04:00 PM • **SSM12** • Room: S504CD • Molecular Imaging (Imaging Probes)

Thursday, December 05, 2013

10:30-12:00 PM • **SSQ12** • Room: S504CD • Molecular Imaging (Oncology and Subspecialties)
12:15-12:45 PM • **CL-MIE-TH5A** • Room: S503AB • Characterization of Breast Cancer Using PET Molecular Imaging: A Clinical Perspective
12:15-12:45 PM • **CL-MIS-THA** • Room: S503AB • Molecular Imaging - Thursday Posters and Exhibits (12:15pm - 12:45pm)
12:45-01:15 PM • **CL-MIS-THB** • Room: S503AB • Molecular Imaging - Thursday Posters and Exhibits (12:45pm - 1:15pm)
04:30-06:00 PM • **RC717** • Room: S504CD • Ultrasound/Opto-Acoustic Molecular Imaging

Friday, December 06, 2013

08:30-10:00 AM • **RC817** • Room: S505AB • Essentials of Molecular Imaging

PET-CT Scan Features in Extrapulmonary Tuberculosis: A Case Series Review

[Back to Top](#)

CL-MIE3041

Ricardo Becerra Ulloa, MD
Leslie Elizabeth Rocha Mendez
Luis Felipe Alva Lopez, MD

PURPOSE/AIM

The purpose of this exhibit is: 1. To review the features in extrapulmonary tuberculosis (Tb) detected by positron emission tomography in conjunction with (F-18) fluoro-2-deoxy-D-glucose (FDG) as a tracer. 2. To review the advantages of PET-CT scan over the CT for diagnosis of extrapulmonary Tb and the disease activity level. 3. To review the combined use of 18 -FDG and 11-c acetate for the differentiation of neoplasm versus infection.

CONTENT ORGANIZATION

1. Incidence of tuberculosis infection in patients with fever of unknown origin (FUO) 2. Justification of PET-CT use in patients with FUO 3. PET-CT features found in patients with extrapulmonary Tb, showing our experience 4. Discussion of the use of new tracers in infectious and oncological diseases.

SUMMARY

One-third of global population is infected with M. Tuberculosis. The radiological features depend more of host immunity than the time transpired since infection. PET-CT plays an important role in the evaluation of patients with impaired host immunity and FUO, due to the atypical manifestations, both, clinical and radiological, present in Tb. The major teaching points of this exhibit are: 1) Features of extrapulmonary Tb detected by PET-CT scan 2) Utility of PET-CT in FUO and TB with different tracers.

Primary Brain Tumors: Potential Role of 18F-Fluorothymidine PET-CT in Treatment Monitoring

[Back to Top](#)

CL-MIE3042

Digna Pachuca Gonzalez, MD
Juan C Garcia Reyna
Yeni Fernandez De Lara Barrera, MD
Ricardo Becerra Ulloa, MD
Rocio C Brom-Valladares, MD
Luis Felipe Alva Lopez, MD
Carlos G Sarco, MD

PURPOSE/AIM

To review current applications of imaging in cell-proliferation with 18F-Fluorothymidine (18F-FLT) PET-CT for primary brain tumors screening, staging, restaging, and response evaluation.

CONTENT ORGANIZATION

1.To explain the utility of MRI and PET-CT in brain tumors.2.Role of 18F-FLT PET-CT in staging and assessment of therapy response in primary brain tumors as compared to 18F-FDG.3.Potential role of 18F-FLT and other amino acid tracers in tumor proliferation imaging.

SUMMARY

MR is currently the imaging gold standard for the diagnosis and follow up of treatment of brain tumors. MR limitations in differentiating recurrent or residual tumor are: fibrosis, scar tissue, postsurgical changes, and tumor necrosis after radiation therapy. Reports of 18F-FLT PET-CT show better characterization of tumors than 18F-FDG PET-CT. The new tracer is used in cases of radionecrosis and when MR is inconclusive. We show our initial experience with 18F-FLT PET-CT and review the current literature existing about 18F-FLT and other tracers by brain cancer. The major teaching points of this exhibit are: 1. MRI limitations in primary brain cancer. 2. Potential 18F-FLT PET-CT indications in brain tumors. 3. Controversy of tumor cell proliferation imaging: 18F-FLT vs 18F-FDG PET-CT

Is Fused PET/MRI Imaging Better than Whole-body MRI or PET/CT Alone for Oncological Patients Evaluation?

[Back to Top](#)

CL-MIE3043

Marcos D Guimaraes , MD

Almir Bitencourt , MD

Alex D Oliveira

Eduardo N Lima

Rubens Chojniak , MD, PhD

Myrna C Godoy , MD, PhD

Jefferson Gross , MD, PhD

PURPOSE/AIM

To evaluate the role of fused imaging between 18F-fluorodeoxyglucose (FDG) positron emission tomography/computed tomography (PET/CT) and whole-body magnetic resonance imaging (WB MRI) for evaluation of oncologic patients.

CONTENT ORGANIZATION

18F-FDG PET/CT - Indications - Advantages - Limitations WB MRI - Indications - Advantages - Limitations FUSED PET/MRI - Technique - Indications - Advantages - Limitations

SUMMARY

Accurate malignancy evaluation is essential for choosing the appropriate treatment strategy. PET/CT and WB MRI shown to be appropriate tools for evaluation of oncological patients, each with its own particular characteristics. Recent published data demonstrate that the combined use of both techniques add greater value in evaluation of cancer patients due different advantages at different sites considering that PET/CT is better than WB MRI in detecting bone and lymph node metastasis whereas WB MRI is better than PET/CT in detecting brain or liver metastasis, for example. Combined use of WB-MRI and PET/CT may correct some diagnostic misunderstandings and improve the diagnostic accuracy of WB-MRI or PET/CT when they are performed and analysed separately.

68Ga-DOTATOC PET-CT: A Promising Tool in Non-Radioiodine Avid Differentiated Thyroid Carcinomas

[Back to Top](#)

CL-MIE3044

Ali Salavati , MD, MPH

Hendra Budiawan , MD

Harshad Kulkarni

Richard P Baum , MD, PhD

PURPOSE/AIM

To describe our experience and the current literature on PET imaging in patients with non-radioiodine avid differentiated thyroid carcinomas.

CONTENT ORGANIZATION

To compare different imaging modalities used for the staging and restaging of non-iodine avid differentiated thyroid carcinomas and describe our experience on sixteen non-radioiodine-avid / radioiodine therapy refractory patients who studied before and after treatment using 68Ga-DOTATOC PET/CT.

SUMMARY

In patients with progressive metastatic or recurrent differentiated thyroid carcinoma that do not take up radioiodine, staging is difficult and treatment options are few. The high and consistent expression of somatostatin receptor subtypes in thyroid carcinoma cell suggests the feasibility of somatostatin receptor imaging and therapeutic options. In this exhibition we will review current literature on different radiopharmaceuticals used for the staging and restaging of these patients and illustrate our experience on the role of 68Ga-DOTATOC PET-CT for monitoring treatment response in patients with non-radioiodine avid differentiated thyroid carcinomas.

MRI and CT Perfusion Techniques Better Correlate with Newly Published Glycolytic Vasculogenesis Concept ALPHA (Acidic Lactate Sequentially Induces Lymphangiogenesis, Phlebogenesis, Arteriogenesis) than the Traditional Oxygen Vasculogenesis Theory

[Back to Top](#)

CL-MIE3045

John R Haaga , MD

Rebecca Haaga

Ji Y Bueche , MD

Nicholas L Fulton , MD

Nathan Bohnert , MD

PURPOSE/AIM

Purposes of this exhibit are to review CT and MRI perfusion techniques and correlate them with vasculogenesis concepts, traditional and the newly introduced ALPHA.

CONTENT ORGANIZATION

1) Review of aerobic and glycolytic metabolism, i.e. Warburg Principle 2) Discuss traditional vasculogenesis concept and newly described glycolytic vasculogenesis concept ALPHA 3) Hypoxia and Lactate stimulates vascular growth factors and these growth factors stimulate vessel development. For lactate drainage, veins develop before arteries 4) Describe the technical basis of perfusion imaging parameters including: blood volume, permeability, 'kinetic' curve analysis, and 'washout' of contrast enhanced CT and MRI 5) Explain how time density curves provide the basis for perfusion parameters 6) Discuss current perfusion parameters used clinically and correlate to show they are more consistent with venous flow than arterialization.

SUMMARY

Cancer uses both aerobic and glycolytic metabolism which produce complementary vasculogenesis processes. Traditional vasculogenesis is based on hypoxia and glycolytic ALPHA is based on lactate. Veins are given preferential development by ALPHA. Current imaging perfusion studies are more based on venous drainage favored by ALPHA.

Molecular, Functional, and Structural Imaging of Tumor Angiogenesis

[Back to Top](#)

CL-MIE4114

Roberto Garcia Figueiras , MD

Anwar R Padhani , MD *

Ambros J Beer , MD *
Sandra Baleato Gonzalez , MD
Dow-Mu Koh , MD, FRCR
Joan C. Vilanova , MD, PhD
Antonio Luna , MD

PURPOSE/AIM

Antiangiogenic (AA) therapies are validated for use in the clinic but recent data shows that progression free survival does not translated into overall survival for a number of cancers with no consistent predictive efficacy biomarkers (BMs) emerging. It is likely that BMs for AA efficacy will be multiparametric (imaging combined with wet BMs). This exhibit compares the complementary nature of the information derived from targeted imaging techniques (for assessing molecules selectively expressed on neoangiogenic vessels) to those directly assessing microvessel permeability and blood flow (dynamic CT/MRI/US).

CONTENT ORGANIZATION

Review of relationships between biology and imaging findings in tumor angiogenesis. Methods used of data acquisition and analysis for assessing angiogenesis: targeted or functional imaging techniques. Imaging in the evaluation of oncologic therapies and drug development. Multiparametric evaluation.

SUMMARY

Imaging approaches use a variety of modalities and are aimed at either assessment of the functional integrity of tumor vasculature or assessment of its molecular status before and in response to therapies. The major teaching points of this exhibit are: Summary of the imaging techniques in the assessment of angiogenesis. Correlation between information derived from targeted and functional imaging techniques.

Searching for Fingerprint Images: Magnetic Resonance Spectroscopy in Oncology

[Back to Top](#)

CL-MIE4115

Roberto Garcia Figueiras , MD
Sandra Baleato Gonzalez , MD
Carlos Cobas , MD *
Laura Oleaga
Joan C. Vilanova , MD, PhD
Pedro Ramos-Cabrer , PhD
Antonio Luna , MD

PURPOSE/AIM

Abnormal metabolites represent emerging tumor biomarkers. Magnetic resonance spectroscopy (MRS) is a non-invasive method that allows measurement of metabolite concentration that can be utilized to characterize the metabolic changes associated with cancer. Most clinical MR scanners have routine sequences for 1H-MRSI measurements and quantitative 1H-MRSI measurements of specific metabolites are implemented in the clinic. This exhibit is focused on: 1)To perform a systematic approach to image acquisition and interpretation of MRSI for cancer evaluation. 2)To evaluate the strengths and limitations of MRSI. 3)To correlate metabolite peaks at MRSI with diagnostic and prognostic parameters of cancer in CNS, H&N, breast, liver, rectum, prostate, testicles, uterus, and ovary.

CONTENT ORGANIZATION

Pre-acquisition set-up of MRS. Spectral acquisition techniques. Post-processing steps. Main metabolites in cancer imaging. Clinical applications of proton MRS: diagnosis, prognosis, prediction of treatment response to therapy, and monitoring patient with cancer after treatment. Advantage and limitations of MRSI

SUMMARY

1H-MRS studies can aid in the management of cancer patients. The major teaching points of this exhibit are: Summary of the technical features and clinical value of MRSI in cancer. Correlation between tumor biology, patient outcome and MRSI findings

Somatostatin Receptor Imaging with Ga-68 DOTATATE PET/CT: Clinical Utility, Normal Patterns, Pearls and Pitfalls in Interpretation

[Back to Top](#)

CL-MIE4116

Michael S Hofman , MBBS
Eddie W Lau , FRANZC
Rodney Hicks , MBBS

PURPOSE/AIM

Ga-68 DOTATATE PET/CT has high impact in a range of tumours with high somatostatin receptor (SSTR) expression. The purpose of this exhibit is:

1. To review clinical applications in neuroendocrine tumours, phaeochromocytoma / paraganglioma, neuroblastoma, meningioma and oncogenic osteomalacia.
2. Describe advantages compared to In-111 octreotide SPECT/CT and standalone CT or MRI.
2. Discuss the pearls and pitfalls in the interpretation of this new modality.
3. Explain complementary role of FDG PET/CT in limiting false negative interpretation

CONTENT ORGANIZATION

-Physiologic distribution / variants

-Indications

-Samples cases with pearls and pitfalls, and correlative imaging

-Role of FDG PET/CT

SUMMARY

The major teaching points of this exhibit are:

1. Advantages compared to conventional imaging include vastly superior sensitivity and specificity, and quantitation of SSTR expression
2. Causes of interpretative pitfalls include prominent pancreatic uncinata activity, inflammation (reactive nodes, prostatitis), osteoblastic activity (degenerative bone disease, fracture, vertebral hemangioma, growth plates), splenunculi and benign meningiomas
3. DOTATATE and FDG PET/CT are complementary and identify well- and poorly-differentiated poorly phenotypes enabling tumor characterisation and better selection of appropriate therapy for an individual patient

PET MRI for Evaluation of Movement Disorder

[Back to Top](#)

CL-MIE4117

Hemant T Patel , MD
Ankur Shah , MD
Manas Mayank , MD
Megha Sanghvi , MD
Nishat Goyal , MBBS, DMRD
Jay V Shah , MBBS

PURPOSE/AIM

The purpose of this exhibit is:

1. To review limitations of CT and MRI in various Movement disorders
2. To outline the advantages and limitations of PET-MRI

3. To discuss PET MRI findings in Movement disorders and its impact on management

CONTENT ORGANIZATION

- Corelation of PET imaging with structural images of MRI for evaluation of functional changes
- Matching of images through digital atlas templates that provide normative values from representative image sample may enhance quantitative evaluation substantially
- PET MRI findings in common movement disorders like Parkinsonism, Atypical Parkinsonism disease including Multisystem Atrophy, Progressive Supranuclear Palsy, Corticobasal Degeneration and Diffuse Lewy body disease
- Future direction and summary

SUMMARY

The major teaching points of this exhibit are:

1. PET MRI is an excellent tool for imaging work up of certain movement disorders which require functional metabolic evaluation
2. Proper technical parameters, coregistration techniques and matching of images are essential for better delineation of disease process
3. This exhibit will help for recognition of certain movement disorders in their early form which eventually helps for better management.

SPECTacular Tc-99m- Sestamibi Dual Phase Parathyroid SPECT Imaging Combined with Dual Bolus Single Acquisition (sa) Contrast Enhanced(ce)-CT. Usefulness and Limitations of SPECT/ sa- ceCT in Parathyroid Adenomas

[Back to Top](#)

CL-MIE4118

Victor V Iyer , MD
Pia Afzelius , MD, PhD
Rune Fisker , MD
Ramune Aleksyniene , MD, PhD

PURPOSE/AIM

The purpose of this exhibit is: 1: Define the concept of SPECT /sa-ceCT of parathyroid glands 2.:Define the role of multimodality hybrid molecular imaging in parathyroid adenomas 3: To review the SPECT/ (sa-ce) CT findings and correlate them with surgical and pathological findings in our study population of 128 patients with query parathyroid adenoma. 4. To discuss the reduction in radiation dose in comparison to conventional 4 D -CT imaging

CONTENT ORGANIZATION

The role of single-isotop, double phase SPECT/sa-ceCT in parathyroid imaging Describe how to perform and interpret SPECT/sa-ceCT for preoperative localisation of parathyroid adenomas. Show representative cases with surgical and anatomical correlation with SPECT/sa-ce CT Review imaging findings with cases - false positive - false negative Discuss the limitations of this method Summary

SUMMARY

Hybird molecular imaging with SPECT/4 D CTof the neck is associated with a high radiation exposure to patient. Teaching points of our exhibit 1) Low radiation exposure and shorter scanning time, 'one stop shop'. 2) Better identification of parathyroid adenomas 3) Increase in confidence levels in reporting parathyroid adenomas, enabling the ENT surgeon to perform minimal invasive neck surgery with lesser comorbidity and shorter inpatient time.

Cancer Immunotherapy: Functional and Anatomic Imaging Assessment of Treatment Response and Immune-related Adverse Events

[Back to Top](#)

CL-MIE4119

Jennifer J Kwak , MD
Sreeharsha Tirumani , MBBS, MD
Phillip J Koo , MD
Christopher Sakellis , MD
Nikhil H Ramaiya , MD
Heather Jacene , MD

PURPOSE/AIM

Immunotherapy treatment of cancer is changing the imaging evaluation of treatment response and toxicities. Ipilimumab, recently FDA approved for melanoma treatment, is a prototype example. This presentation reviews important concepts of cancer immunotherapy and illustrates the immune-related response patterns and immune-related adverse events to aid in the interpretation of post treatment imaging with PET/CT, CT and MRI.

CONTENT ORGANIZATION

Immunotherapy

- Current strategies and mechanisms of action: monoclonal antibodies against cancer associated antigens (e.g. rituximab), recombinant cytokines (interferon alpha, IL-2), immune checkpoint inhibitors (ipilimumab), and vaccinations (sipuleucel-T)

Immune-related response criteria

- Treatment response differs from cytotoxic agents
- 4 patterns of response

Immune-related adverse events

- Multimodality pictorial overview of a wide-range of immune-mediated treatment toxicities such as colitis, hepatitis, sarcoid-like reaction, hypophysitis, and pancreatitis

SUMMARY

Advancements in cancer immunotherapy challenge the current approach to the evaluation of tumor response to treatment Imagers must recognize treatment response patterns and be cognizant of a wide-range of toxicities which should not be mistaken for disease progression and referred for appropriate clinical management

PET/MRI: When Will the Hybrid Agents Be?

[Back to Top](#)

CL-MIE4120

Anita Kiani
Aurore Esquevin , MD
Florence Le Jeune , MD, PhD
Nicolas Lepareur
Jean-Yves Gauthier , MD

PURPOSE/AIM

To describe the different hybrid agents existing in positron emission tomography (PET) and magnetic resonance imaging (MRI) hybrid imaging, as well as their future applications.

CONTENT ORGANIZATION

This exhibit is an exhaustive presentation of the different PET and MRI hybrid agents developed. Agents and techniques used for their development are detailed. The combination of MRI contrast agents as super paramagnetic iron oxide (SPIO), Gadolinium or microbubbles and PET radiotracers as ⁶⁴Cu, ¹²⁴I or ¹⁸F are detailed. The future clinical applications they have been created for are presented, as well as the prospects with antibodies and theranostic agents.

SUMMARY

The aim of developing PET and MRI hybrid imaging is to combine the high sensitivity of the PET imaging with the high resolution of MRI, required for diagnosis accuracy. The solution used for creating a hybrid agent is to add a PET radiotracer on the surface of an MRI contrast agent. The 124I-SA-MnMEIO is an example, the aim of which is to identify lymph nodes. Applications fields are large, mainly in oncology and in cardio-vascular imaging. Prospects are very open, especially since the development of PET/MRI hybrid machines.

Evolving Role of Preclinical Imaging in Cancer Drug Discovery and Development in the Era of Molecular Targeted Agents

[Back to Top](#)

CL-MIE4121

Kyung Won Kim, MD
Nancy Kohl, PhD
Jeffrey T Yap, PhD *
Yanping Sun, PhD
Jen-Chieh Tseng, PhD
Tanya Tupper

PURPOSE/AIM

1. To review recent advances in mouse tumor models and preclinical trials for development of molecular targeted agents for the treatment of cancer
2. To review the role of preclinical imaging for cancer drug discovery

CONTENT ORGANIZATION

1. New generation of mouse models for cancer drug discovery
 - Mouse models: conventional cell-line xenograft models
 - patient-derived xenograft models
 - genetically-engineered mouse models
2. Recent advances in preclinical trials for development of molecular targeted agents
 - Advantages and pitfalls of various mouse models
 - How to bridge the gap between animal data and human data
 - Preclinical trial design: validation of potential drug targets, discovery of predictive biomarkers, linkage to clinical trial
3. Role of preclinical imaging
 - reflecting physiological, functional, and molecular mechanism
 - validation of imaging endpoints with pathologic correlation or survival
 - translation between preclinical and clinical trials

SUMMARY

Recent advances in mouse modeling of cancer and preclinical trial design enables prediction of outcomes in human clinical trials, provides insights into mechanisms of drug effect and resistance, and readily translates preclinical data into the clinic. The importance of preclinical imaging has been growing in the era of molecular targeted agents.

Whole-body Diffusion-weighted MRI in Caring for Patients with Hodgkin and Diffuse Large B-Cell Lymphoma: Acquisition Parameters, Imaging Findings, Pitfalls, and Limitations

[Back to Top](#)

CL-MIE4122

Sarah M Toledano-Massiah
Chieh Lin, MD
Emmanuel Itti, MD
Violaine Safar
Alain Luciani, MD, PhD *
Bertrand Bresson
Karim Belhadj
Pierre Zerbib
Benhalima Zegai
Julien Moroch
Michel Meignan, MD, PhD
Corinne Haioun, MD
Alain Rahmouni, MD

PURPOSE/AIM

- To understand the basic principles of whole body diffusion-weighted MRI (WB-DW-MRI).
To learn how to optimize the acquisition parameters of WB-DW-MRI at 1.5 and 3T, and to generate reliable parametric ADC images.
To be familiar with native and parametric diffusion-weighted images, and be able to apply it in routine lymphoma imaging and patient care.
To enumerate and learn how to avoid the pitfalls of WB-DW-MRI in imaging lymphoma patients.

CONTENT ORGANIZATION

Basic principles of DW-MRI and its application in oncology. Optimization of acquisition parameters in WB-DW-MRI at 1.5 and 3T. ADC mapping. Imaging findings at diagnosis and during treatment. Pitfalls. Limitations.

SUMMARY

Recent improvements in MR technology such as moving examination table, multichannel surface coils, echo-planar sequences and respiratory gating, have resulted in clinically feasible protocols for WB-DW-MRI. As a result, WB-DW-MRI with ADC mapping has become a promising tool in staging and response assessment of patients with malignant lymphoma. Based on our experience of 60 patients with Hodgkin and diffuse large B-cell lymphoma having undergone both WB-DW-MRI and 18FDG-PET/CT, we expose the spectrum of imaging findings and discuss the pitfalls, limitations, and potential challenges of WB-DW-MRI in caring for lymphoma patients.

Molecular Imaging Case of the Day

[Back to Top](#)

LL-EDE3015

Umar Mahmood, MD, PhD
David A Mankoff, MD, PhD
Hannah M Linden, MD
David M Schuster, MD
Katja Pinker-Domenig, MD
Edwin L Palmer, MD
Mukesh G Harisinghani, MD
Pedram Heidari, MD

PURPOSE/AIM

- 1) Participants will gain a better understanding, through example cases, of cutting edge clinical applications of molecular imaging using novel techniques.

Molecular Imaging Case of the Day

[Back to Top](#)

LL-EDE3015

Umar Mahmood, MD, PhD
David A Mankoff, MD, PhD
Hannah M Linden, MD
David M Schuster, MD
Katja Pinker-Domenig, MD
Edwin L Palmer, MD
Mukesh G Harisinghani, MD
Pedram Heidari, MD

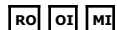
PURPOSE/AIM

1) Participants will gain a better understanding, through example cases, of cutting edge clinical applications of molecular imaging using novel techniques.

ISP: Molecular Imaging (Oncology I)

Sunday, 10:45 AM - 12:15 PM • S504CD

[Back to Top](#)



SSA12 • AMA PRA Category 1 Credit™:1.5 • ARRT Category A+ Credit:1.5

Moderator

Daniel C Sullivan, MD

Moderator

Heike E Daldrop-Link, MD

SSA12-01 • Molecular Imaging Keynote Speaker: Multi-modal Molecular Imaging of Cancer

Heike E Daldrop-Link MD (Presenter)

SSA12-02 • Utilization of Ultrasound Molecular Imaging Targeted to Thy1(CD90) for the Detection of Pancreatic Ductal Adenocarcinoma in an Orthotopic Murine Xenograft Model

Steven B Machtaler PhD (Presenter); **Kira Foygel** PhD; **Huaijun Wang** MD, PhD; **Ru Chen**; **Teresa A Brentnall** MD; **Juergen K Willmann** MD *

PURPOSE

To describe the identification of Thy1/CD90 as vascular tumor marker for human pancreatic ductal adenocarcinoma (PDAC) and assess the feasibility of using ultrasound (US) molecular imaging directed against human Thy1 (hThy1) to detect pancreatic tumors in an orthotopic murine xenograft model.

METHOD AND MATERIALS

Proteomic analysis of whole tissues from patients with PDAC (n=5), chronic pancreatitis (n=5), and normal pancreas (n=10) using a LTQ-Orbitrap hybrid mass spectrometer identified Thy1 as a pancreatic tumor marker. Expression of Thy1 in human PDAC vasculature was verified by IHC of pancreatic tissue obtained from normal, primary chronic pancreatitis, and PDAC patient samples. An orthotopic murine xenograft tumor model was created to assess human (h) CD90-specific *in vivo* microbubble (MB) binding. Murine vascular endothelial (MS1) cells stably expressing hCD90 and human AsPC1 PDAC cells were co-injected into the tail of the pancreas of nude mice. In all PDAC xenografts, intra-animal comparisons of ultrasound imaging signals were performed following injection of both MB_{Thy1} and MB_{Control} in a randomized order during the same imaging session using a VEVO2100 US system.

RESULTS

IHC analysis validated the proteomic data showing that hThy1 was expressed on the vasculature and significantly increased in PDAC tumors (score: 2.1±0.1, 81% of tumors were Thy1-positive) in contrast to normal pancreata (score: 0.5±0.1; *In vivo* binding of MB_{Thy1} to PDAC xenografts was assessed using US molecular imaging. A targeted signal using MB_{Thy1} of 7.7±2.3 au was observed in hThy1 expressing PDAC xenografts compared to 1.9±1.8 in control tumors and 1.4±2.2 using non-targeted MBs.

CONCLUSION

These results illustrate the development of a translational US-MB directed against a vascular tumor marker and the development of a novel, orthotopic human PDAC model expressing hThy1 within the tumor vasculature, which may eventually aid in earlier detection of PDAC.

CLINICAL RELEVANCE/APPLICATION

This work provides the first steps towards the development of an US molecular imaging contrast agent targeted to a vascular tumor marker for the detection of pancreatic tumors in humans.

SSA12-03 • Characterization of Perfusion and Therapeutic Resistance in a Renal Cell Carcinoma Mouse Model with Hyperpolarized 13-C-tert-butanol

Leo L Tsai MD, PhD (Presenter) *; **Xiaoen Wang** MD; **Gopal Varma** PhD; **David C Alsop** PhD *; **Rupal Bhatt**; **Aaron K Grant** PhD

PURPOSE

METHOD AND MATERIALS

12 mice were implanted with A498 RCC tumors. 5 were treated with sunitinib, 5 controls were administered phosphate-buffered saline (PBS), and 2 were untreated. Sunitinib-treated mice were imaged pretreatment, 5-7 days after treatment initiation, and at resistance. Control mice were imaged pre-PBS, 5-7 days with PBS treatment, and at a tumor limit of 20 mm. Tumors were harvested after final images for immunohistological analysis. MRI was performed at 4.7 T using: (1) 1H-T2-weighted rapid acquisition with refocused echoes for anatomical localization, TR/TE=3000/80ms, 128x128 matrix, 2mm slice, 3.5cm FOV, (2) h13C-tert-butanol imaging with 2D balanced steady state free precession (bSSFP), 128x128 matrix, 8.5cm FOV, 3.3 mm slice, 512ms/frame for 100 frames, (3) arterial-spin-label (ASL) perfusion mapping with flow-sensitive inversion-recovery.

RESULTS

Fig (a) and (b) show interval growth of a control tumor (outlined in red, over an axial T2-weighted 1H image) and increased perfusion (green overlay). Sunitinib-treated tumors are vascular at pretreatment (c) but demonstrate unperceivable perfusion and growth at post-treatment day 7 (d). Reperfusion is seen at resistance (e). The peak intratumoral h13C-tert-butanol SNR of 7.9 exceeds ASL by ~2-fold. Moreover, multiple h13C-tert-butanol frames can be averaged to obtain perfusion-weighted images with greater SNR. Peripheral tumor enhancement was consistent with central necrosis as seen on 1H imaging and histopathology. Increased perfusion during resistance was detected in all mice using h13C-tert-butanol.

CONCLUSION

h13C-tert-butanol MRI provides high-SNR *in vivo* perfusion mapping of RCC and detects reperfusion with sunitinib resistance in a xenograft mouse model.

CLINICAL RELEVANCE/APPLICATION

h13C-tert-butanol provides quantitative perfusion mapping with improved detection of vascular tumor progression and therapeutic resistance, with high potential for translation into clinical use.

SSA12-04 • Next-generation Nanoparticle Allows Accurate Prediction of Nodal Status in Pre-operative Patients with Pancreatic Adenocarcinoma

Shaunagh McDermott FFRCSI (Presenter) ; **Sarah Thayer** ; **Carlos Fernandez-Del Castillo** MD ; **Mari Mino Kenudson** MD ; **Ralph Weissleder** MD, PhD ; **Mukesh G Harisinghani** MD

PURPOSE

The purpose of this study was to assess the ability of a lymphotropic nanoparticle-enhanced MRI to preoperatively detect lymph node metastases in patients with pancreatic cancer.

METHOD AND MATERIALS

This exploratory study was performed as a prospective, pilot study and was approved by the Institutional Review Board. All patients with known or high index of suspicion of pancreatic cancer and who were scheduled for surgical resection were eligible for enrollment in this study. The study group consisted of thirteen patients (6 males, 7 females) with a mean age of 64 years; range 40 -91 years. Eleven patients underwent surgery with an average of 23 lymph nodes resected; range 7 - 42. In total 264, lymph nodes were resected and available for analysis. In two patients liver metastases were identified on the pre-operative MRI and therefore they did not undergo resection. Patients underwent MRI before, and immediately and 48 hours after the intravenous administration of ferumoxytol. Signal-to-noise ratios and subjective nodal characterization were determined based on the T2*-weighted sequences. Following resection, the pathologic and imaging findings were compared on a regional basis.

RESULTS

CONCLUSION

Lymphotropic nanoparticle-enhanced MRI is an accurate and safe method for detecting nodal metastases in patients with pancreatic cancer.

CLINICAL RELEVANCE/APPLICATION

The ability to preoperatively identify metastatic lymph nodes in patients with pancreatic cancer could alter management, possibly making an extended lymphadenectomy or systemic therapy a better option

SSA12-05 • Targeted Biodegradable Nanoparticles MRI Contrast Agent for Enhanced Tumor Imaging and Non-viral Gene Delivery

Xiaolong Gao PhD (Presenter) ; **Peijun Wang** MD, PhD ; **Chao Lin** ; **Guoliang Wang**

PURPOSE

To prepare targeted biodegradable nanoparticles to connect folic acid MRI contrast agent with appropriate size. To explore the feasibility of the macromolecular contrast agent for tumor targeting and the characteristics of imaging in vivo and in vitro with folic receptor-positive tumor cells in nude mice models.

METHOD AND MATERIALS

RESULTS

CONCLUSION

In summary, SSPUA-DTPA-FA-PEG-Gd was successfully developed as a target specific, biodegradable and non-toxic delivery system of siRNA therapeutics. Treatment with SSPUA-DTPA-FA-PEG-Gd/siVEGF complex reduced VEGF mRNA and protein expression in vitro and in vivo, and it also retarded tumor growth in vivo. The SSPUA-DTPA-FA-PEG-Gd helps to intensify the effect in MR enhancement in nude mice models. Therefore, SSPUA-DTPA-FA-PEG-Gd might be effective non-viral gene vector for gene therapy.

CLINICAL RELEVANCE/APPLICATION

no

SSA12-06 • In Vivo Reporter Imaging in a Large Animal Pre-clinical Model Demonstrates that Angiotensin II Improves Gene Expression Upon Intra-arterial Adenovirus Delivery

Vikas Kundra MD, PhD (Presenter) * ; **Murali Ravoori** ; **Lin Han** ; **Sheela Singh** ; **Katherine Dixon** RT ; **Rajesh Uthamanthil** DVM, PhD ; **Sanjay Gupta** MD ; **Kenneth C Wright** PhD *

PURPOSE

Gene therapy has been hampered by low levels of gene expression upon in vivo delivery. Using a somatostatin receptor type 2 (SSTR2)-based reporter, we assessed whether angiotensin II can improve gene expression by adenovirus upon intra-arterial delivery.

METHOD AND MATERIALS

A SSTR2-based reporter that can be imaged with the FDA approved radiopharmaceutical¹¹¹In-octreotide was used to assess gene expression in vivo. 8 rabbits bearing VX2 tumors in each thigh were randomly injected intra-arterially with adenovirus containing a human somatostatin receptor type 2A (Ad-CMV-HA-SSTR2A) gene chimera + angiotensin II or control adenovirus containing green fluorescent protein (Ad-CMV-GFP). 3 days later, ¹¹¹In-octreotide was given IV after CT imaging using a clinical CT scanner and intravenous contrast. Tumor uptake of ¹¹¹In-octreotide was evaluated the next day using a clinical gamma camera. Gene expression was normalized to tumor weight and morphology from CT to obtain in vivo biodistribution.

RESULTS

SSTR2-based expression was readily visualized. VX2 tumors infected with Ad-CMV-HA-SSTR2 upon intra-arterial delivery with angiotensin II had greater in vivo biodistribution, thus greater gene expression, than without angiotensin II (P

CONCLUSION

Angiotensin II can improve in vivo gene expression by adenovirus upon intra-arterial delivery. In vivo SSTR2-based reporter imaging can be used to compare methodologies for improving gene expression.

CLINICAL RELEVANCE/APPLICATION

SSTR2-based reporter imaging may be useful in comparing methods for improving gene expression. Intra-arterial co-delivery of angiotensin II with adenovirus may improve gene therapy efficacy.

SSA12-07 • PSMA Imaging with 18F-DCFBC PET for Detection of Primary Prostate Cancer: Initial Evaluation Using MRI and Pathologic Analysis

Kenneth L Gage MD, PhD (Presenter) ; **Sheila Friedrich Faraj** MD ; **George Netto** MD ; **Katarzyna J Macura** MD, PhD * ; **Martin G Pomper** MD, PhD * ; **Steve Cho** MD * ; **Ronnie Mease** PhD ; **Enrico Munari** MD ; **Akimosa Jeffrey-Kwanisai** MBA

PURPOSE

¹⁸F-DCFBC (DCFBC) is a novel low-molecular weight PET agent targeted to prostate specific membrane antigen (PSMA) that has previously demonstrated uptake at sites of metastatic prostate cancer (PC). We present our preliminary findings evaluating quantitation of DCFBC for the detection of primary PC.

METHOD AND MATERIALS

Eight patients with biopsy-proven PC with Gleason score (GS) \geq 6 were imaged with both DCFBC PET and pelvic MRI (T2 and DWI) prior to prostatectomy. PET imaging with 35 min pelvic imaging (30 min 2D and 5 minute 3D) and whole body imaging was started 2 hrs after injection of 370 MBq (10 mCi) of DCFBC. Post-surgical prostatectomy specimens were sectioned in 4mm planar increments from apex to

base, divided into quadrants and analyzed by both HandE and PSMA immunohistochemistry (IHC). PET and MRI were visually correlated and co-registered for analysis, and compared with the anatomically reassembled pathology results. The area of highest GS (postsurgical) determined the location for analysis. The PET ROI (SUVmax) was correlated using Spearman's rank correlation with Gleason score, MRI ADC values, H-score for PSMA IHC staining, degree of staining (strong, moderate, weak), and lesion size.

RESULTS

Three pts showed strongly positive (pos) intraprostatic DCFBC PET signal which correlated with signal on MRI and prostatectomy pathology with dominant GS of 4+5=9 tumor. Three pts were negative (neg) by DCFBC PET with low-grade disease (GS 6, 4+3=7, 3+4=7). Two additional patients had discernible but subtle uptake which also correlated with signal on MRI and pathology with dominant GS 4+3=7 and GS 3+4=7 PC. DCFBC PET SUVmax on WB and 2D pelvic imaging was positively correlated with GS (? coeff=0.85, p=0.0079; ? coeff=0.72, p=0.045, respectively), and trended toward significance when compared to PSMA IHC H-score results in this small dataset. MRI DWI imaging was able to localize sites of prostate cancer but ADC values did not correlate significantly with PC GS or PSMA IHC.

CONCLUSION

DCFBC PET imaging of primary PC demonstrates tumor PET SUVmax is positively correlated with GS and trended toward significance with tumor PSMA expression by IHC. These findings will need further confirmation in our ongoing clinical trial.

CLINICAL RELEVANCE/APPLICATION

PSMA imaging with DCFBC PET may provide a novel biomarker for noninvasive detection of high-grade primary prostate cancer and tumor PSMA expression.

SSA12-08 • MR Colonography with Intestine-absorbable Nanoparticle Contrast Agents in Evaluation of Colorectal Tumors

Yin Jin (Presenter) ; **Jihong Sun** MD, PhD ; **Xia Wu** ; **Xiaozhe Shi** ; **Peng Hu** ; **Xiaoming Yang** MD, PhD

PURPOSE

To develop a novel nanoparticle-based magnetic resonance (MR) colonography technique, which enabled us to evaluate colorectal tumors via transrectal administration of intestine-absorbable nanoparticle contrast agents.

METHOD AND MATERIALS

Solid lipid nanoparticles (SLNs) were synthesized with loading of gadolinium (Gd) diethylenetriaminepenta acetic acid (Gd-DTPA) and otcadecylamine fluorescein isothiocyanate (FITC) to construct Gd-FITC-SLNs for histologic confirmation of MR findings. Twelve APCMin/+ female mice were treated with 1-2 administration cycles of 2% dextran sulfate sodium in the drinking water for 5-7 days to create the colorectal tumors. The neoplastic mice were administered by a transrectal enema with Gd-FITC-SLNs (40mg/ml). T1-weighted MR colonographies using spin echo sequence (TR/TE, 840/15 msec) were then performed to detect various Gd-carrying SLNs within the colonic walls. MRI findings were correlated with subsequent histological confirmation.

RESULTS

MR colonographies displayed mild enhancement of the tumor masses and significant enhancement of normal colorectal walls. Confocal fluorescence microscopy demonstrated the delivered Gd-FITC-SLNs as highly-concentrated green fluorescent spots into the surface of the tumor mass with less spots within the tumor of APCMin/+ mice (Figure).

CONCLUSION

This study establishes the ♦proofs-of-principle♦ of a new MR colonography technique, which enables the differentiation of colorectal tumors from the normal colorectal walls based on various absorption capability of nanoparticle contrast agents. Solid lipid nanoparticle-based MR colonography may open new avenues for efficient management of colorectal tumors.

CLINICAL RELEVANCE/APPLICATION

Solid lipid nanoparticle-based MR colonography may open new avenues for efficient management of colorectal tumors.

SSA12-09 • Interventional Optical Molecular Imaging: Intra-procedural Imaging Guidance via a Translatable Handheld Device for Percutaneous Sampling of Focal Hepatic Lesions

Rahul A Sheth MD (Presenter) ; **Shadi A Esfahani** MD, MPH ; **Pedram Heidari** MD ; **Umar Mahmood** MD, PhD

PURPOSE

As a real-time, high resolution imaging modality, optical molecular imaging has the potential to significantly advance image guidance during interventional radiology (IR) procedures. The clinically approved optical molecular imaging agent indocyanine green (ICG) has recently been shown to localize to both primary and metastatic malignant hepatic lesions. We assessed the ability of ICG to serve as a molecular beacon for hepatic malignancy by highlighting lesions with high target-to-background ratios (TBRs). We also evaluated the ability of custom-designed, translatable, catheter-based handheld imaging system to perform intra-procedural measurements of ICG fluorescence intensity during the percutaneous sampling of focal hepatic lesions.

METHOD AND MATERIALS

A handheld optical molecular imaging device was constructed to pass through the introducer needle of a standard 18 gauge percutaneous biopsy kit. Intrahepatic colorectal cancer metastases (human colorectal cancer cell line HT-29) were generated in nude mice (n = 25). Epifluorescence imaging of the tumors was performed 4 weeks post-implantation at multiple time points following the intravenous administration of 0.5mg/kg ICG. The mice were then imaged using the custom designed handheld imaging device, and measurements of fluorescence intensity within normal liver versus tumor were acquired.

RESULTS

There was avid localization of ICG to the focal hepatic lesions at all time points by epifluorescence imaging. Similarly, fluorescence intensity within the tumors was significantly greater than within normal liver as detected by the handheld imaging system, with a TBR of 3.9 ± 0.2 at 24 hours. A core biopsy of tumor and normal adjacent liver using a standard 18 gauge biopsy needle demonstrates a sharp margin of fluorescence intensity at the tumor-liver interface, with a 10%-90% rise distance of 4mm.

CONCLUSION

The custom-designed molecular imaging device, in combination with ICG, was able to readily differentiate between normal versus malignant tissue, an ability that is of tremendous potential utility in IR. Both the device and imaging agent are ready for immediate clinical translation.

CLINICAL RELEVANCE/APPLICATION

Optical molecular imaging may improve the accuracy and obviate the need for cytologic ♦wet reads♦ or frozen section analysis during percutaneous biopsy procedures.

Vein Graft Implantable Contrast Initiative: Enhanced Vessel Wall Imaging

Sunday, 12:30 PM - 01:00 PM • S503AB

CL-MIE-SU5A

Oscar R Miranda
Frank J Rybicki, MD, PhD *
C K Ozaki, MD *
Jeffrey Karp, PhD

[Back to Top](#)

Peng Yu , MD
Dimitris Mitsouras , PhD
Praveen K Vemula , PhD
Ming Tao
Chengwei Liu
Robert V Mulkern , PhD

PURPOSE/AIM

To describe the current and potential role of molecular imaging approaches for enhancing the magnetic resonance (MR) properties of vascular tissues.

CONTENT ORGANIZATION

1. Review of signal-to-noise ratio and contrast-to-noise ratio constraints in the context of the MR properties of vessel wall tissues, and the consequent limitation in sensitivity to detect disease in small and medium caliber vessels.
2. Review of current molecular imaging approaches that can be used to enhance sensitivity of MR for differentiation of diseased and normal wall tissues.
3. Review of validated animal models of vascular disease that can be used to test MRI sensitivity hypotheses.
4. Description of current and future approaches and findings where covalently bound contrast agents have successfully enhanced vessel wall MR signal properties.
5. Imaging examples confirming validity of molecular-imaging enhanced vessel wall MRI including ex vivo and in vivo platforms.

SUMMARY

1. The current role and testing of molecular approaches for covalent binding of MR contrast media to vascular tissues will be reviewed.
2. These targeted MR approaches using novel contrast agents enhance noninvasive differentiation of wall tissues, not otherwise possible in small and medium sized vessels. Future applications can potentially enhance tissue characterization for human cardiovascular imaging.

Molecular Imaging - Sunday Posters and Exhibits (12:30pm - 1:00pm)

Sunday, 12:30 PM - 01:00 PM • S503AB

[Back to Top](#)



CL-MIS-SUA • AMA PRA Category 1 Credit™:0.5

Host

Heike E Daldrop-Link , MD

CL-MIS-SU1A • Measuring Renal Oxygenation in a Mouse Model of Volume-dependent Hypertension Using BOLD MRI

Darah N Wright MS (Presenter) ; **Stephen Lin** ; **Ping-Chang Lin** ; **Dan Zhang** ; **Chung-Shieh Wu** ; **Paul Wang** ; **Andre J Duerinckx** MD, PhD ; **Dexter Lee**

PURPOSE

Purpose: Hypertension is closely associated with the progression of kidney damage and dysfunction. Tissue hypoxia in the hypertensive kidney contributes to the progression of kidney damage. Peroxisome proliferator activated receptor α ? (PPAR- α) is a nuclear receptor that plays an important role in reducing volume-dependent hypertension. The goal of this study was to determine the role of PPAR- α on renal oxygenation using blood oxygen level-dependent (BOLD) MRI in a model of volume-dependent hypertension.

METHOD AND MATERIALS

Materials and Methods: Wild-type (WT) and PPAR- α knockout (KO) mice were imaged using a multiple gradient echo BOLD sequence (12 echoes from 3.2-54ms, TR=900ms) on a 9.4T MRI to measure functional changes in renal oxygenation. Imaging was performed during baseline, day 12 of Ang II (400 ng/kg/min), and 9 days after Ang II-treatment (recovery). T2* relaxation time was measured in the cortex and medulla of the kidney.

RESULTS

Results: Cortex T2* values were lower in KO vs WT during baseline (11.0 ± 1.1 ms vs 13.1 ± 1.5 ms), day 12 of Ang II (11.6 ± 1.2 ms vs 16.2 ± 1.5 ms) and 9 days after Ang II (12.5 ± 0.7 ms vs 15.2 ± 0.3 ms). Medulla T2* values were lower on day 12 of Ang II in KO (16.5 ± 2.5 ms) vs WT (20 ± 1.6 ms) mice. Medulla T2* values were similar between KO and WT mice during baseline and the recovery period. In KO and WT mice, cortex T2* values were lower than that of the medulla, indicative of different metabolic functions between the two tissues.

CONCLUSION

Conclusion: PPAR- α plays an important role in blood pressure regulation and renal oxygenation in the cortex and medulla of the kidney during Ang II-induced hypertension.

CLINICAL RELEVANCE/APPLICATION

Hypertension is a risk factor for chronic kidney disease when untreated. BOLD MRI can aid in monitoring renal oxygenation changes during hypertension and determine therapeutic interventions in humans.

CL-MIS-SU2A • Frontal Watershed Sign: A Novel SPECT Imaging Finding in CNS LUPUS

Avetis Azizyan MD (Presenter) ; **Paul Linesch** ; **Alessandro D'Agnolo** ; **Alan D Waxman** MD *

PURPOSE

Single-photon emission computed tomography (SPECT) is routinely utilized for the evaluation of systemic lupus erythematosus (SLE) patients with acute neurological symptoms, however, a clear anatomic distribution of disease has not been found. In this study, 3D rendering of SPECT imaging was performed to determine whether a specific cortical distribution of disease is present.

METHOD AND MATERIALS

37 consecutive SLE patients who presented with acute neurological symptoms underwent surface rendered brain SPECT. All studies were performed on a three detector SPECT camera (Prism 3000) following 20mCi Tc-99m ethyl cysteinate dimer. 3D stereotactic surface projection (3D SSP) analysis was conducted on Neurostat software comparing the 37 lupus patients averaged as a group to 19 patients from a normal database. Differences in cortical perfusion were presented as a color map of standard deviations from the mean. Standardized 3D rendered SPECT images from the lupus group along with 11 normal studies were then reviewed by a radiologist blinded to any history or laboratory findings. The images were scored on a numerical scale with 10 being the most abnormal pattern and 0 being a normal pattern. Scores of 5 and above were considered as positive while 4 and below were negative.

RESULTS

3D SSP analysis demonstrates decreased perfusion in the medial frontal lobes and along the watersheds between the anterior and middle cerebral arteries which is 6 standard deviations below the mean. There is sparing of the parietal and occipital lobes as well as the inferior temporal lobes. When the radiologist reviewed and scored the SPECT images individually, an abnormality in the frontal lobes was detected with a specificity of 100%, but sensitivity of 64%.

CONCLUSION

3D surface rendered brain SPECT detects markedly decreased perfusion in the anterior watershed territories of the frontal lobes in lupus patients, which has not been previously described. Furthermore, blinded reading of the surface rendered imaging demonstrates that this finding is specific for lupus when present.

CLINICAL RELEVANCE/APPLICATION

The finding of diminished perfusion in the frontal watersheds on 3D surface rendered SPECT imaging is novel and helps elucidate the pathophysiology of acute CNS lupus.

CL-MIS-SU3A • Conventional vs. Dedicated Head SPECT System: Image Quality Comparison

William F Sensakovic PhD (Presenter) ; **Matthew C Hough** MSc ; **Elizabeth Kimbley**

PURPOSE

To compare a new SPECT system with a scanning geometry specialized for the head with a conventional SPECT system under similar clinical scanning conditions.

METHOD AND MATERIALS

A dedicated head SPECT scanner (Neurologica inSPira HD) consisting of 72 detectors with focused cone collimators in a rotating ring geometry was compared to a conventional GE millennium VG SPECT scanner. A small ACR phantom was scanned in the inSPira HD and GE millennium VG. Images were acquired with both high and low activities of Tc-99m with acquisition parameters selected to simulate a clinical ictal scan. Resolution, contrast, noise, and uniformity were compared.

RESULTS

The inSPira was able to resolve rods 7.9mm and greater vs. 11.1mm and greater for the VG. Noise was increased from a coefficient-of-variation of 2.1 in the VG to 3.0 in the inSPira. Contrast was 24% better on the inSPira on average over all spheres. Spheres 12.7mm and larger were visible on the VG vs. 6.4mm and larger on the neurologica. Spheres appeared larger in VG images due to lower resolution and increased partial volume artifact. Integral uniformity of the inSPira was 6.9 compared to 4.6 in the VG.

CONCLUSION

The dedicated head SPECT system demonstrated substantially better resolution, contrast, and less partial volume artifact. Subjectively, the improvement of these characteristics in the inSPira produced qualitatively better images than the conventional SPECT scanner despite increased noise and lower uniformity.

CLINICAL RELEVANCE/APPLICATION

The improved resolution and contrast of the dedicated head SPECT system may lead to more accurate mapping of the brain and improved localization and size estimation of lesions.

CL-MIS-SU4A • Quantitative Evaluation of FDG-PET Lesions with Low Dose Protocol

Wenli Wang PhD (Presenter) * ; **Ting Xia** PhD * ; **Hongwei Ye** PhD * ; **Xiaofeng Niu** PhD * ; **Changguo Ji** PhD * ; **Mark L Winkler** MD ; **Manabu Teshigawara** PhD * ; **Yasuhiro Noshi** ; **Edward Haines** PhD * ; **Daniel Gagnon** PhD *

PURPOSE

Advancements of PET scanner design and reconstruction algorithm offer the opportunity to reduce patient's radiotracer dose and/or imaging time. The purpose of this paper is to evaluate how low the dose reduction can be without sacrificing the FDG-PET lesion's detectability and quantitative accuracy.

METHOD AND MATERIALS

Several lung and/or breast cancer patients' FDG-PET data are used, with IRB approval and patient's consent. The data were acquired from a PET/CT prototype scanner, where the PET data is reconstructed with 3D list-mode time-of-flight ordered-subset expectation-maximization algorithm with full physical corrections, and low-dose CT data for PET attenuation correction. The original PET data was acquired with whole-body imaging protocol with regular injection dose and imaging time (i.e., default-dose protocol). The PET data with different levels of lower injection dose and shorter imaging time (i.e., low-dose protocol) is then mimicked from the original data by taking a uniform sub-sampling. Different levels of smoothing post-filters will be applied to the PET image to achieve similar signal-to-noise-ratio in soft tissue among different dose protocols. The lesion's standard-uptake-values (SUV) are then measured and compared for different dose protocols to represent the lesion's detectability.

RESULTS

Moderate size and spherical-shape lesions will be used for the SUV analysis. The percentage change of lesion's SUV (referenced to the default-dose) will be plotted for different levels of dose protocols and also as a function of the post-filter kernel for the default dose. Different metrics of SUVs, such as SUV_{max} , SUV_{mean} and SUV_{peak} , or total lesion glycolysis, will be compared.

CONCLUSION

The most stable SUV metric will be proposed and the lowest dose protocol with acceptable SUV degradation will be recommended. More patients needed to be recruited in the study in the future to indicate any statistical significance.

CLINICAL RELEVANCE/APPLICATION

Provide objective guidelines on imaging protocol and image quality metric for dose reduction of FDG-PET oncology application.

Molecular Imaging - Sunday Posters and Exhibits (1:00pm - 1:30pm)

Sunday, 01:00 PM - 01:30 PM • S503AB



[Back to Top](#)

CL-MIS-SUB • AMA PRA Category 1 Credit™:0.5

CL-MIS-SU2B • The Diagnostic Value of DTI and Fiber Tractography Parameters in Differentiating Solitary Intracranial Masses

Paloma Puyaito MD (Presenter) ; **Juan Jose Sanchez** MD, PhD ; **Montserrat Virumbrales** ; **Carles Aguilera** ; **Angel Olazabal Zudaire** ; **German Camilo** ; **Magally Padilla**

PURPOSE

To establish the parameters that differentiate metastases and primary high grade glial tumors by diffusion-tensor sequences.

METHOD AND MATERIALS

51 patients with solitary intracranial mass were analyzed: 24 metastasis and 27 GBM. Fractional anisotropy (FA), medium diffusion (MD), pure anisotropic diffusion (q^*) and total magnitude of the diffusion (L) were studied, both in the contrast enhanced tumor area and the affected adjacent white matter region. These measures were reproduced in the contralateral unaffected side of the brain by obtaining mirror images.

RESULTS

DTI sequences and mainly q^* (P

CONCLUSION

Differentiating the etiology of brain tumors and achieving an accurate measurement of their real extension (discriminating peritumoral edema from tumor infiltration beyond the enhanced area) will have a great repercussion in the decrease of the number of the cerebral biopsies, reduction of the extension of the surgical resections, as well as an indirect reduction of the hospitable stay and better therapeutic decisions.

CLINICAL RELEVANCE/APPLICATION

DTI and fiber tractography add valuable information for the differential diagnosis between glioblastoma multiforme (GBM) and metastases in patients with a solitary cerebral expansive lesion.

CL-MIS-SU3B • Temporal Subtraction of Torso FDG-PET Images by Using Anatomical Standardization Approach

Takeshi Hara PhD (Presenter) ; **Daisuke Fukuoka** PhD ; **Tetsuro Katafuchi** ; **Xiangrong Zhou** PhD ; **Chisako Muramatsu** PhD ; **Hiroshi Fujita** PhD ; **Shinichiro Kumita** MD ; **Kenta Hakozaki** ; **Satoshi Itoh** MD, PhD

PURPOSE

To develop a new computer-aided diagnosis system with temporal subtraction technique for FDG-PET scans and to show the fundamental usefulness based on an observer performance study.

METHOD AND MATERIALS

The computerized system consists of the following steps: (1) Anatomical standardization of normal FDG-PET scans, (2) Normal model construction from the normal FDG-PET scans, (3) Z-score mapping based on statistical image analysis, (4) Automated detection of abnormal region, (5) Comparison of detected regions between previous and current scans, and (6) Image subtraction of previous and current scans. An automated detection technique has been applied to each scan of previous and current examinations independently at the fourth step. The detection technique is based on SUV and Z-score thresholding. The detected regions were compared between two scans to show the changes of activities. Observer performance study based on ROC (receiver operating characteristics) was also performed without and with the system results to shows the usefulness of the computerized scheme.

RESULTS

The recognition performance of the computer outputs for the 43 pairs was 96% sensitivity with 31.1 false-positive marks per scan. The average of area under-the-ROC-curve (AUC) from 4 readers in the observer performance study was increased from 0.85 without computer outputs to 0.90 with computer outputs ($p=0.0389$, DBM-MRMC). The average of interpretation time was slightly decreased from 42.11 to 40.04 seconds per case ($p=0.625$, Wilcoxon test).

CONCLUSION

We concluded that the computerized scheme for torso FDG-PET scans with temporal subtraction technique might improved the diagnostic accuracy of radiologist in cancer therapy evaluation.

CLINICAL RELEVANCE/APPLICATION

New application of anatomical standardization method to torso region. Temporal subtraction of 3D torso FDG-PET scans to enhance temporal changes of SUV.

CL-MIS-SU4B • F-18 Fluoroacetate PET Imaging -Biodistribution in Healthy Subjects and Preliminary Study for Diagnosis of Liver Tumors

Ryuichi Nishii MD, PhD (Presenter) ; **Tatsuya Higashi** MD ; **Shinya Kagawa** ; **Masaaki Takahashi** MD ; **Yoshihiko Kishibe** ; **Hiroshi Yamauchi** MD, PhD ; **Shigeki Nagamachi** MD, PhD ; **Shozo Tamura** MD, PhD

PURPOSE

F-18 Fluoroacetate (FACE) is a potential tracer for the quantitative evaluation of TCA cycle/membrane metabolism of cancers. Based on our previous reports of this PET tracer, we have started to investigate FACE PET imaging in normal volunteers and in patients with liver tumors as preliminary studies.

METHOD AND MATERIALS

The clinical trial studies were conducted with a total of twenty-four healthy volunteers and eight patients with liver tumor. All subjects were injected FACE and dynamic PET were acquired, followed by whole body static scans. In the study of patients with liver tumor, FDG PET was also performed on each day respectively. Qualitative analysis and quantitative analysis of tumors (4 hepatocellular carcinoma/HCC, 1 cholangiocellular carcinoma/CCC, 3 metastatic tumors from colon cancer and P-NET) was performed using SUVmax and TNR (Tumor-to-normal Liver Ratio).

RESULTS

Dynamic PET imaging demonstrated that the renal and hepatobiliary systems were the principal pathways of clearance of FACE. The average SUVmean values in the brain, lung, myocardium, liver, muscle and fat tissue at 1hr imaging were 1.34, 0.46, 2.20, 1.76 1.28 and 0.44, respectively. There was no deposition of radioactivity in the skeletal structures, indicating metabolic stability over 1 to 2hr post-injection of the radiotracer. FDG uptake of liver tumors (SUVmax: 6.1 ± 3.9 , TNR: 2.4 ± 1.5) was significantly higher than that of FACE (2.7 ± 0.6 , 1.5 ± 0.4), while normal physiological uptake of FACE (SUVmean: 1.8 ± 0.2) was lower than that of FDG (SUVmean: 2.5 ± 0.2). In qualitative analysis, FDG was positive in 3 tumors (2 HCC, 1 CCC) and negative in the other 5 tumors, while FACE was also positive in 3 tumors which were the same tumors with positive FDG uptake. Pathological results showed that a case of moderately differentiated HCC showed high FACE uptake (SUVmax=3.0), while FDG also showed high uptake (SUVmax=5.7).

CONCLUSION

FACE PET would be suitable and promising imaging as a tumor seeking molecular imaging. Tumor FACE uptake was positive in three patients with HCC and CCC, but the uptake pattern was similar to FDG. Further evaluation was needed.

CLINICAL RELEVANCE/APPLICATION

FACE PET would be suitable and promising imaging for the quantitative evaluation of TCA cycle/membrane metabolism of cancers. Tumor FACE uptake was positive in patients with HCC and CCC.

Molecular Imaging Symposium: Preparing for Tomorrow: The Application of Novel and Advanced Imaging in Clinical Oncology

Monday, 08:30 AM - 10:00 AM • S406B

OI MJ BQ

[Back to Top](#)

MSMI21 • AMA PRA Category 1 Credit™:1.5 • ARRT Category A+ Credit:1.5

Moderator

Ronald L Korn, MD, PhD

MSMI21A • Fluorescence and Optoacoustic Imaging Heads to the Clinics

Vasilis Ntziachristos PhD (Presenter) *

LEARNING OBJECTIVES

1) Learn the technology basics and assess the current state of the art in fluorescence and optoacoustic imaging. 2) Understand the imaging performance achieved and major improvements over past approaches. 3) Learn on how this new-generation imaging performance offers a paradigm shift in optical and clinical imaging. 4) Link the developments described to unique contrast generation in clinical and pre-clinical applications. 5) Gain insights into current clinical pilot studies using these approaches.

MSMI21B • CT Biomarkers and How to Use Them

Kenneth Miles (Presenter) *

LEARNING OBJECTIVES

1) Describe the oncological imaging biomarkers available from CT. 2) Demonstrate knowledge of the processes required for qualification of CT biomarkers in oncological drug development and clinical practice. 3) Compare the applications of CT biomarkers for prognosis, response prediction and response assessment.

ABSTRACT

By measuring size and attenuation with or without contrast material, CT can provide a range of oncological biomarkers including T-stage, RECIST, enhancement, CT perfusion and CT texture analysis. Implementation of these biomarkers requires prior assessments of technical/biological performance and establishment of biomarker performance characteristics. For clinical applications, assessments of therapeutic and health impact are also required. Technical/biological validation includes assessments of test-retest performance and identification of relevant biological correlates. Evaluations of biomarker performance should report cross-validated diagnostic/prognostic thresholds, hazard ratio and biomarker prevalence. Based on these parameters, modelling studies can evaluate the potential therapeutic and health impacts that would result from clinical deployment. Current evidence supporting the use of CT biomarkers in drug development and clinical practice are summarised.

MSMI21C • The Use of Novel PET Tracers. What is in the Pipeline for Approval

Jonathan E McConathy MD, PhD (Presenter) *

LEARNING OBJECTIVES

1) Describe the PET tracers in late phase clinical trials for oncologic imaging in terms of their molecular targets and potential clinical indications. 2) Identify the major regulatory and financial challenges encountered during the translation of PET tracers into widespread clinical use. 3) Compare the properties, strengths, and weaknesses of PET tracers for prostate cancer imaging as case studies.

ABSTRACT

Positron emission tomography (PET) with the glucose analogue 2-deoxy-2-[F-18]fluoro-D-glucose (FDG) combined with computed tomography (CT) is currently the workhorse for clinical molecular imaging in oncology. While very successful, FDG-PET/CT has limitations in certain cancers and provides a readout of only one aspect of cancer biology. Novel PET tracers have great promise to improve diagnostic imaging, and a wide range of small molecule, peptide, antibody, and nanoparticle-based PET tracers are in development for oncologic imaging. This presentation will provide an overview of PET tracers in late phase clinical development with an emphasis on mechanism of action and potential clinical indications. Additionally, some of the key challenges to the widespread clinical use of PET tracers including regulatory and financial issues will be reviewed. Finally, several classes of PET tracers for prostate cancer imaging will be discussed in greater depth to illustrate key points.

MSMI21D • Systems Diagnostics - The Future of Diagnostic Medicine?

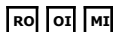
Michael D Kuo MD (Presenter) *

LEARNING OBJECTIVES

1) To understand systems diagnostics as a new diagnostics paradigm. 2) To explore clinical applications and future directions of systems diagnostics.

Molecular and Functional Imaging/Surrogate Markers in Radiation Oncology

Monday, 08:30 AM - 10:00 AM • S104A



[Back to Top](#)

RC220 • AMA PRA Category 1 Credit™:1.5 • ARRT Category A+ Credit:1.5

Nina A Mayr, MD
Carryn Anderson, MD
Jinxing Yu, MD
William T Yuh, MD

LEARNING OBJECTIVES

1) To understand challenges in the optimal and timely assessment of tumor response in clinical cancer therapy and in clinical trial testing new therapy regimens. 2) To understand the role and the potential of functional and molecular imaging modalities and techniques used prior, during or after cytotoxic therapy in headandneck, brain, lung, prostate and gynecologic malignancies. 3) To apply and integrate imaging modalities into the therapeutic management of cancer. 4) To review the role of imaging as predictors of tumor control and survival and their emerging role as short-term surrogate markers for long-term therapeutic outcome of cancer treatment regimens and its potential for adaptive therapy.

ABSTRACT

Molecular Imaging Symposium: Radiogenomics - The Next Logical Step in 'Rad-Path' Correlation for Clinical Imaging?

Monday, 10:30 AM - 12:00 PM • S406B



[Back to Top](#)

MSMI22 • AMA PRA Category 1 Credit™:1.5 • ARRT Category A+ Credit:1.5

Moderator
King C Li, MD

MSMI22A • Radiogenomics: Merging Molecular Diagnostics and Clinical Imaging in Cancer

Michael D Kuo MD (Presenter) *

LEARNING OBJECTIVES

1) To understand the fundamental concepts behind radiogenomics. 2) To explore the current and evolving landscape of radiogenomics. 3) To understand how radiogenomics can be implemented in current clinical practice.

MSMI22B • Linking Molecular and Imaging Data in Lung Cancer

Olivier Gevaert PhD (Presenter)

LEARNING OBJECTIVES

1) Learn how image features are defined and extracted from non small cell lung cancer CT and PET images. 2) Learn the complexity and dimensionality reduction of gene expression data. 3) Learn how to correlate image features with gene expression data and establishing a radiogenomics map.

ABSTRACT

Radiogenomics is an emerging field that attempts to correlate and integrate radiological information from medical images and molecular data from tissue. Typically medical image features are extracted from a wide range of imaging modalities such as MRI, CT or PET images.

Similarly, recent developments in molecular technologies have unleashed a myriad of technologies to produce diverse biological data types such as gene expression, microRNA expression, DNA methylation, and DNA mutation data. Radiogenomics is defined as the integration of these two developments. We demonstrate our approach on non-small cell lung carcinoma patients for whom CT, PET/CT and gene expression data were obtained. We extracted 149 computational features, 30 semantic features and PET-SUV from the imaging data. The microarray data was processed using an advanced clustering algorithm and 56 high quality clusters were represented using metagenes. We found several though provoking associations between imaging features and metagenes. 115 of 180 image features were predicted by a sparse regression on 56 metagenes with an accuracy of 65-86%. After mapping the predicted image features to a public gene expression dataset, we found 26 image features were significantly associated with recurrence-free survival and 22 with overall survival. A multivariate survival analysis identified prognostic image features independent of clinical covariates. Our results show that we have developed a method that can be used as a non-invasive way for rapid prognostic assessment of imaging. This motivates investing in larger studies that collect and store medical images and tissue of the same patients in NSCLC and other diseases such that our method can be used to assess immediately the prognostic relationship of new imaging biomarkers or technologies without the need for follow-up data. Our bioinformatics strategy for identifying imaging biomarkers may be most relevant to the clinical evaluation of emerging and evolving

MSMI22C • A Radiogenomic Analysis of the TCGA Glioma Data Set

David Gutman MD, PhD (Presenter)

LEARNING OBJECTIVES

1) Understand how to access large public data sets with imaging, genomics, and clinical data available. 2) Learn the steps involved in generating a controlled vocabulary to describe and annotate imaging data sets. 3) Review of current findings in associating MRI features with patient outcome and genomic profile. 4) Become familiar with 2-D and 3-D volumetric methods to extract quantitative features to describe tumors.

PET-MRI in Alzheimer Disease

Monday, 12:15 PM - 12:45 PM • S503AB

[Back to Top](#)

CL-MIE-MOSA

Hemant T Patel , MD
Ankur Shah , MD
Megha Sanghvi , MD
Manas Mayank , MD
Laxmi V Bhobe , DMRD
Jay V Shah , MBBS

PURPOSE/AIM

The purpose of this exhibit is:

1. To review limitations of CT and MRI in detection of Alzheimer disease
2. To outline the advantages and limitations of PET-MRI
3. To demonstrate various appearances of PET MRI in Alzheimer disease and its impact on management

CONTENT ORGANIZATION

- ◆ Classification of dementia and etiopathogenesis of Alzheimer disease
- ◆ Correlation of PET imaging with structural images of MRI for evaluation of functional changes in presenile and advanced cases of Alzheimer disease
- ◆ Discuss PET MRI findings in Alzheimer disease : Sample cases and images
- ◆ Overlapping appearances and limitations of PET-MRI
- ◆ Future directions and summary : Role of PET MRI in diagnosis of other causes of dementia

SUMMARY

The major teaching points of this exhibit are:

1. PET MRI is an excellent tool for imaging work up of dementia with Alzheimer disease in particular which requires functional metabolic evaluation
2. This exhibit will help for recognition of Alzheimer disease in its early form which eventually helps for better management

Molecular Imaging - Monday Posters and Exhibits (12:15pm - 12:45pm)

Monday, 12:15 PM - 12:45 PM • S503AB

[Back to Top](#)



CL-MIS-MOA • AMA PRA Category 1 Credit™:0.5

Host
Vikas Kundra , MD, PhD *

CL-MIS-MO1A • CT Imaging Biomarker for Evaluation of Emodin as a Potential Drugs on LPS-induced Osteoporosis Mice

Han Ah Lee (Presenter) ; Kwon-Ha Yoon MD, PhD ; Dong Min Kang MD ; Ju-Young N Kim ; Jae Min Oh ; Myung Soo Lee ; Seong Tae Jung ; Seon Kwan Juhng ; Young Hwan Lee MD

PURPOSE

This study was designed to identify CT imaging biomarker for evaluation of the effect of emodin as a potential drugs to treat osteoporosis on lipopolysaccharide (LPS)-mediated bone resorption mice model

METHOD AND MATERIALS

We examined TRAP staining, or alkaline phosphatase (ALP) and Alizarin Red-mineralizaion staining to analyze the role of emodin on osteoblasts or osteoclasts differentiation in vitro. Twenty male DBA/1J mice were induced bone osteoporosis by intraperitoneal injection of LPS (5 mg/kg) on days 1 and 4. Of the twenty mice, ten were administered emodin (50 mg/kg) 1 day prior to LPS injection and every other day for 8 days. Five were administered emodin only, and other five mice were injected saline as a control group. After 8 days, the mice were sacrificed, and micro-CT images were obtained in the proximal femur. The images were analyzed using a software to calculate the bone parameters such as BV/TV(%), Tb.Sp(◆m), Tb.Th(◆m), and trabecular number as CT imaging biomarkers. Histomorphometric analysis was performed using hematoxylin and eosin and TRAP immunohistochemistry methods.

RESULTS

In vitro results, emodin inhibited RANKL-induced osteoclast differentiation in bone marrow macrophages and bone resorbing activity of mature osteoclasts. Emodin also increased osteoblastic differentiation marker, ALP and Alizarin Red-mineralizaion activity on osteoblasts. Mice treated with emodin demonstrated marked suppression effect of lipopolysaccharide-induced bone resorption (BV/TV: 29.7% vs 39.5%, Tb.Sp: 0.283 ◆m vs 0.227 ◆m, Tb.Th 0.098 ◆m vs 0.099 ◆m, Tb. N: 2.673 vs 3.314). On TRAP immunohistologic analysis of femurs, the number of osteoclasts per field of tissue were revealed as 43 vs 25. The imaging biomarker of BV/TV(%) and trabecular number were well correlated to histomorphometric analysis

CONCLUSION

This findings reveal a novel effect of emodin in bone remodeling in LPS-induced mice model. CT imaging biomarkers can offer as a

promising tool for assessment of therapeutic effect of a potential drugs in osteoporosis

CLINICAL RELEVANCE/APPLICATION

Micro-CT imaging biomarkers can offer as a promising tool for assessment of therapeutic effect of a potential drug in osteoporosis.

CL-MIS-MO2A • Assessment of ¹¹C-Acetate PET for Response Monitoring of Indirect Modulators of Fatty Acid Synthase in Prostate Cancer

Pedram Heidari MD (Presenter) ; Umar Mahmood MD, PhD ; Giorgia Zadra PhD ; Massimo Loda MD

PURPOSE

It has been previously shown that the uptake of ¹¹C-acetate in PET strongly correlates with the expression of fatty acid synthase (FASN) in the native prostate cancer (PCa) tumor models and following treatment with direct FASN inhibitors such as C75. We performed a study to evaluate the utility of ¹¹C-acetate PET for monitoring of the response to therapy in indirect FASN modulators specifically AMPK activators.

METHOD AND MATERIALS

In this study we imaged nu/nu mice bearing subcutaneous LNCaP tumors using ¹¹C-acetate PET at baseline and following treatment with vehicle, MT 63-78 (30 mg/kg), AICAR (400 mg/kg) and C75 (30 mg/kg), at 24h and 1h before follow-up imaging. MT 63-78 and AICAR are AMPK activator and C75 is FASN inhibitor. We also performed western blotting for measuring FASN expression on cells following treatment with vehicle, MT 63-78, and AICAR. Moreover we measured ¹⁴C incorporation in lipids and ¹⁴C-CO₂ release from cells following incubation with ¹⁴C-acetate and treatment with vehicle, MT 63-78 and AICAR.

RESULTS

We observed that the mean SUVmean of tumors in ¹¹C-acetate PET minimally changed following treatment with vehicle and MT 63-78, increased 16% with AICAR and decreased 20% with C75 treatment. Western blots showed a pronounced decrease in FASN expression in MT 63-78 and to a smaller extent in AICAR. There was a significant decrease in ¹⁴C incorporation in cell lipids following treatment with MT 63-78 while there was a significant increase in ¹⁴C-CO₂ release from cells with MT 63-78 and to a higher extent with AICAR treatment.

CONCLUSION

Acetate is used as a substrate precursor during FA and cholesterol synthesis in cancer cells with increased lipogenesis (e.g. PCa) but can also be metabolized through the tricarboxylic acid (TCA) cycle. These results suggest that AMPK activation (with MT 63-78 and AICAR) not only causes the inhibition of FASN, but also increases of catabolic activity of enzymes of TCA cycle and mitochondrial biogenesis, which compensates/overcompensates for the reduction in ¹¹C-acetate uptake observed with the FASN inhibitors such as C75. Thus, ¹¹C-acetate may not be an adequate marker for monitoring the response to therapy with indirect inhibitors of FASN such as AMPK activators in PCa.

CLINICAL RELEVANCE/APPLICATION

This study helps clarify when ¹¹C-acetate PET imaging is useful for monitoring response of prostate cancer to new targeted therapeutics that modulate FASN directly or indirectly.

CL-MIS-MO3A • Decision Modelling in the Identification of Potential Clinical Applications for Prognostic Imaging Biomarkers in Oncology: Methods and Preliminary Results

Kenneth Miles (Presenter) * ; Thida Win ; Balaji Ganeshan PhD * ; Ashley M Groves MBBS *

PURPOSE

To describe a decision modeling approach for the identification of potential clinical applications for prognostic imaging biomarkers in oncology.

METHOD AND MATERIALS

An approach that uses decision modeling to identify potential applications for prognostic imaging biomarkers was defined. The approach requires cross-validated data indicating the hazard ratio and proportion of high risk patients identified by the imaging biomarker along with the 95% confidence intervals (CI). The biomarker also needs to be prognostic independent of tumor stage and other potential imaging biomarkers. Decision modeling is then used to assess potential health outcomes and costs from proposed biomarker deployments with Monte Carlo analysis quantifying the likelihood of realizing beneficial outcomes. The approach was used to assess potential applications of CT texture analysis (CTTA) for the personalization of chemotherapy for patients with advanced non-small cell lung cancer.

RESULTS

The cross-validated mortality hazard ratio (95% confidence interval) for CTTA was 1.99 (1.14 ♦ 3.44) with 52.5% (95% CI: 43.2 ♦ 61.7%) categorized as high risk. Decision modeling identified CTTA-based strategies with high, intermediate and low likelihoods of clinical benefit and/or cost-effectiveness. Two strategies that used CTTA to identify sub-sets of patients with EGFR-negative tumors for 2-agent platinum based chemotherapy increased the survival benefit of this treatment to 5.3 months (95% CI: 3.3 -7.3 months) and were most likely to be cost-effective (Net monetary benefit \$540; 95% CI: \$369-702 and \$762; 95% CI: \$351-1154 respectively).

CONCLUSION

Decision modeling can be useful in the identification of potential clinical applications for prognostic imaging biomarkers in oncology.

CLINICAL RELEVANCE/APPLICATION

Methods that aid the identification of clinical applications for prognostic imaging biomarkers will promote their translation to personalized medicine.

Molecular Imaging - Monday Posters and Exhibits (12:45pm - 1:15pm)

Monday, 12:45 PM - 01:15 PM • S503AB



CL-MIS-MOB • AMA PRA Category 1 Credit™:0.5

CL-MIS-MO1B • Comparing Photoacoustically Derived Hemoglobin and Oxygenation Measurements and Ultrasound Contrast Agent Derived Vascularity Measurements to Immunohistochemical Staining in a Breast Cancer Xenograft Model

John R Eisenbrey PhD (Presenter) ; Andrew Marshall ; Daniel A Merton ; Ji-Bin Liu MD * ; Traci B Fox MS, RT ; Anush Sridharan ; Flemming Forsberg PhD *

PURPOSE

To compare tumor oxygenation levels derived by photoacoustic imaging (PA) and tumor vascularity measurements derived by contrast-enhanced ultrasound (CEUS) with immunohistochemical markers in a murine subcutaneous breast cancer model.

METHOD AND MATERIALS

Subcutaneous MDA-MB-231 breast tumors implanted in the mammary pads of 11 nude rats were imaged in nonlinear contrast mode on a Vevo 2100 ultrasound scanner (Visualsonics, Toronto, Canada). Rats received a bolus 36 ?l injection of Definity (Lantheus Medical

[Back to Top](#)

Imaging, N Billerica MA) during CEUS imaging (acoustic power=4%, frequency=24 MHz, gain=35 dB). Maximum intensity projections were then generated over the tumor area using the VevoCQ software as a measure of tumor vascularity. PA was performed using a PA probe (MS-250-PA, Visualsonics) on the Vevo2100. The laser was operated at 100% output power at wavelengths of 750 and 850 nm with a PA gain of 40 dB. Hemoglobin signal (HbT), oxygenation levels in detected blood (SO2 Avg), and oxygenation levels over the entire tumor area (SO2 Tot) were then calculated for 20 frames using the Oxygenation-Hemoglobin measurement package. Post imaging, rats were sacrificed and the tumors stained for VEGF, Cox-2, and CD-31.

RESULTS

When comparing CEUS to PA measurements, significant correlation was observed between CEUS derived vascularity and both HbT and SO2 Tot (R=0.61 and R=0.64 respectively, p<0.32). Similarly, no significant correlation was observed between either HbT or SO2 Tot and any immunohistochemical marker (p>0.18). SO2 Avg did show significant inverse correlation with Cox-2 (R=-0.65; p=0.03), but not with either VEGF or CD-31 (p>0.5).

CONCLUSION

PA modes that rely on the total detection of hemoglobin appear to correlate with CEUS vascularity measurements, but not with the studied immunohistochemical markers. Oxygenation levels within detected blood determined via PA appear to correlate with Cox-2 expression.

CLINICAL RELEVANCE/APPLICATION

Depending on the imaging mode, PA may be useful for detecting changes in tumor vascularity or expression of the angiogenic marker Cox-2.

CL-MIS-MO2B • Radiation-free Whole Body MR Imaging of Children with Cancer: A Solution to the Conundrum of Long-term Side-effects from CT Scans

Christopher Klenk MD (Presenter) ; Rakhee S Gawande MD ; Deqiang Qiu PhD ; Andrew Quon MD ; Michael E Moseley PhD ; Heike E Daldrop-Link MD

PURPOSE

Standard CT and radiotracer-based staging procedures of children with cancer are associated with considerable radiation exposure and risk of secondary cancer development later in life. The purpose of this study was to develop an alternative radiation-free staging technique, based on whole body diffusion-weighted magnetic resonance (WB-DW MR) imaging and the iron supplement ferumoxytol, used as an MR contrast agent.

METHOD AND MATERIALS

A novel concept for WB-DW MR was established based on color-encoded, iron oxide nanoparticle-enhanced diffusion weighted MR scans for tumor detection, which were co-registered with nanoparticle-enhanced T1-weighted MR scans for anatomical orientation. Following pulse sequence optimizations in nine healthy volunteers, 16 children and young adults with malignant lymphoproliferative disorders underwent WB-DW MR and 18F-FDG PET/CT scans. The presence or absence of tumors in different anatomical areas was determined separately for WB-DW MR and clinical routine 18F-FDG PET/CT staging exams. Histopathology and follow-up imaging served as the standard of reference. The agreement between tumor staging results of the two imaging tests was evaluated using Cohen's kappa statistics, with a score of 1.0 indicating perfect agreement.

RESULTS

Evaluation of healthy volunteers revealed optimal pulse sequence parameters for WB-DW MR as follows: TR 3400 ms, TE 45-55 ms, b-values 50 and 600 s/mm², and bandwidth of 0.25kHz. Duration of the diagnostic procedure was 1-1.5 hours for WB-DW MR scans and 1.5-2.5 hours for 18F-FDG PET/CT scans (radionuclide injection + imaging). WB-MRI/DWIBS and 18F-FDG-PET/CT showed very good inter-observer agreement for tumor staging according to the Ann Arbor classification with a weighted k value of 0.889.

CONCLUSION

Ferumoxytol-enhanced WB-DW MR imaging provides a radiation-free alternative to 18F-FDG PET/CT for staging of children with malignant lymphomas. To the best of our knowledge, this is the first study that integrates an MRI technique for tumor detection (WB-DW) with an MR technique for anatomical orientation, in accordance with the concept of integrated 18F-FDG PET/CT scans.

CLINICAL RELEVANCE/APPLICATION

Since our new WB-DW MR approach is radiation free, it may solve the conundrum of mandatory radiographic imaging for cancer staging, but associated risk of developing radiation-induced secondary cancer

CL-MIS-MO3B • Three-dimensional Angiogenesis Imaging Using Molecular Ultrasound in Colon Cancer: Preliminary Feasibility Study in a Mouse Model

Osamu F Kaneko MD (Presenter) ; Huaijun Wang MD, PhD ; Vijay Shamdasani MS, PhD * ; Dimitre Hristov PhD * ; Juergen K Willmann MD *

PURPOSE

To explore the feasibility of three-dimensional (3D) targeted contrast-enhanced (molecular) ultrasound (US) imaging using a 3D clinical transducer in a human colon cancer xenograft model in mice undergoing vascular disrupting treatment.

METHOD AND MATERIALS

Subcutaneous human colon cancer LS174T xenografts were induced in 14 female nude mice. Mice were randomly assigned to either 1) a treatment group receiving the vascular disrupting agent ASA404 (n=8; single dose of 15 mg/kg i.v.) or 2) a control group (n=6; saline only) with no treatment. All mice were scanned with US at baseline (day 0) and at day 1 after treatment. 3D US molecular imaging was performed with a clinical US system (IU22 xMATRIX; Philips Healthcare, Bothell, WA) and a clinical transducer (X6-1; center frequency, 3.2 MHz) at 4 min after i.v. injection of 5x10⁷ VEGFR2-targeted microbubbles (MB-VEGFR2) or non-targeted control microbubbles (MB-Control) administered at the same dose in the same imaging session. After imaging, all mice were sacrificed and tumors were analyzed for VEGFR2 expression levels on ex vivo immunofluorescence.

RESULTS

3D US molecular imaging was feasible in all 14 tumors. In the treatment group, US molecular imaging signal with MB-VEGFR2 following a single treatment with ASA404 was significantly lower (81% decrease, P

CONCLUSION

Volumetric US molecular imaging using a clinical US system and 3D transducer is technically feasible. Preliminary data show good correlation of in vivo VEGFR2-targeted US imaging signal with ex vivo VEGFR2 expression levels in human colon cancer xenografts in mice undergoing vascular disrupting treatment.

CLINICAL RELEVANCE/APPLICATION

3D imaging capabilities of US may further expand its future clinical role in molecular imaging of cancer, particularly for more accurate monitoring of treatment response in complete tumor volumes.

Molecular Imaging Symposium: Imaging Cellular Subpopulations - Current Progress and Future Directions

Monday, 01:30 PM - 03:00 PM • S406B



[Back to Top](#)

Moderator
Michael D Kuo , MD *

MSMI23A • Using Imaging to Track the In Vivo Contribution of Lgr5 Stem Cells in GI Cancer

Nick Barker PhD (Presenter)

LEARNING OBJECTIVES

1) To learn about in vivo lineage tracing as a technique to document endogenous stem cell activity.

ABSTRACT

Lgr5 Stem Cells in Epithelial Self-Renewal and Cancer Nick Barker: Institute of Medical Biology, 8A Biomedical Grove, 06-06 Immunos, Singapore 138648 The intestinal epithelium is subjected to a constant barrage of mechanical and chemical assault, imposing a requirement for regular self-renewal. This renewal is driven by a small population of adult stem cells residing in epithelial pockets known as crypts of Leiberkuhn. Lgr5 is a Tcf/?-catenin (Wnt) target gene specifically expressed on crypt-base columnar cells located at the base of the intestinal crypts. Employing in vivo lineage tracing we have proven these cells to be the stem cells of the small intestine and colon. The same rapid turnover of the intestinal epithelium also makes it particularly susceptible to cancer-forming mutation. Using Lgr5-CreERT2 mice to selectively induce deletion of the APC tumor suppressor gene in the intestinal stem cells, we recently proved that these Lgr5+ve stem cells are the cell-of-origin of colon cancer. This work also revealed the presence of a minor population of Lgr5+ve cells within intestinal tumors. Multicolor lineage tracing from these tumor-resident Lgr5+ve cells has demonstrated these to be cancer stem cells contributing to tumor growth in vivo.

MSMI23B • CLARITY and Beyond: Towards Complete Structural and Molecular Investigation of Large-Scale Intact Biological Systems

Kwanghun Chung PhD (Presenter)

LEARNING OBJECTIVES

1) To understand the limitations of current imaging-based approaches in understanding disease processes. 2) To understand how CLARITY overcomes these limitations and allows cellular and subcellular imaging/molecular phenotyping while maintaining a whole system-wide perspective. 3) To explore potential clinical applications and future directions of CLARITY.

MSMI23C • Imaging Immune Cell Subsets Using ImmunoPET

Anna M Wu PhD (Presenter) *

LEARNING OBJECTIVES

1) To delineate the advantages and disadvantages of using an antibody-based imaging approach for cell tracking. 3) To identify appropriate combinations of antibody formats and radionuclides for specific immunoPET applications.

ABSTRACT

Antibodies are attractive candidates as imaging agents due to their exquisite specificity. Recent advances in protein engineering have enabled optimization of antibodies for noninvasive imaging applications such as immunoPET, through reduction of immunogenicity, acceleration of clearance to enable rapid, same-day imaging, and provision of site-specific radioconjugation. Broader availability of non-standard PET radionuclides, including Cu-64, Zr-89, and I-124 and others, has expanded the range of biological targets and processes that can be imaged. The cell-surface CD markers provide a well-characterized set of targets that can be used to distinguish lineage, differentiation, and activation state of hematopoietic and immune cells. Corresponding antibodies can readily be converted into engineered fragments for PET imaging, and can be used to profile immune responses such as expansion, trafficking, homing, and activation of immune cell subsets. Examples of profiling immune cells and responses in mouse models will be presented, as well as the potential for clinical translation.

MSMI23D • New Strategies for Using Smart MRI Contrast Agents for Monitoring Cell Therapy

Michael T McMahon PhD (Presenter)

LEARNING OBJECTIVES

1) Describe the Chemical Exchange Saturation Transfer (CEST) MRI contrast mechanism and how to modify an imaging sequence to obtain this contrast. 2) List the properties that make a compound a successful CEST MRI contrast agent. 3) Describe the various methods to employ CEST MRI contrast for monitoring cell therapy.

ABSTRACT

Hydrogels have facilitated cell therapies by protecting therapeutic cells from immune responses and providing a physical cue to support the grafts. A non-invasive imaging technique that allows the monitoring of engrafted cell viability is needed as these therapies move into the clinic. Chemical Exchange Saturation Transfer (CEST) imaging is sensitive to changes in pH and ion concentrations, and as a result is well suited as a tool to obtain information on the status of these cells. We have incorporated organic CEST contrast agents into alginate hydrogels for this purpose and have developed a magnetization transfer image collection scheme suitable for obtaining high quality CEST contrast maps in the abdomen. The in vivo results upon transplanting these hydrogels into mice will be discussed.

Molecular Imaging Symposium: Molecular Brain Imaging: From Research to Clinical Applications

Monday, 03:30 PM - 05:00 PM • S406B

MI BQ NR

[Back to Top](#)

MSMI24 • AMA PRA Category 1 Credit™:1.5 • ARRT Category A+ Credit:1.5

Moderator
Satoshi Minoshima , MD, PhD *

LEARNING OBJECTIVES

1) To discuss molecular brain imaging technologies that have been translated from research developments to clinical applications.

ABSTRACT

MSMI24A • Amyloid Imaging: Translational Research to Clinical Applications

Alexander Drzezga MD (Presenter) *

LEARNING OBJECTIVES

1) Pathophysiological background: Role of amyloid-aggregation in the development of Alzheimer's disease. Concept of modern anti-amyloid therapy options. Time course of amyloid-aggregation as compared to the appearance of clinical symptoms. Value of amyloid-imaging as compared to other biomarkers of Alzheimer's disease. 2) Methodological principles of amyloid imaging: Development, mechanism, available tracers. Proof of concept, in vivo versus ex vivo histopathological confirmation. 3) Clinical value and interpretation of amyloid-imaging results, pitfalls and artefacts, value of amyloid-imaging with regard to early diagnosis, differential diagnosis and therapy monitoring. 4) Amyloid imaging in comparison to other imaging biomarkers (MRI, FDG-PET), value of multioimodal imaging.

MSMI24B • How Molecular Imaging Contributes to Movement Disorders? Current and Future

Kirk A Frey MD, PhD (Presenter) *

LEARNING OBJECTIVES

View learning objectives under main course title.

MSMI24C • Quantitative Analysis and Interpretation of Molecular Brain Imaging

Satoshi Minoshima MD, PhD (Presenter) *

LEARNING OBJECTIVES

1) To explain various quantification methods applied in the field of molecular brain imaging. 2) To discuss how such quantification methods can be used in clinic.

MSMI24D • Making Molecular Brain Imaging Available in the Clinic: FDA and CMS

Peter Herscovitch MD (Presenter)

LEARNING OBJECTIVES

1) To discuss new molecular brain imaging techniques that are available in the clinic. 2) To explain how basic research has been translated to clinical applications. 3) To discuss approval processes that are necessary to establish clinical molecular brain imaging.

ISP: Breast Imaging (Nuclear/Molecular Imaging)

Tuesday, 10:30 AM - 12:00 PM • E451A

NM MI BR

[Back to Top](#)

SSG01 • AMA PRA Category 1 Credit™:1.5 • ARRT Category A+ Credit:1.5

Moderator

David A Mankoff , MD, PhD

Moderator

D. David Dershaw , MD

SSG01-01 • Breast Imaging Keynote Speaker: Molecular Imaging of Breast Cancer-Clinical and Biological Considerations

David A Mankoff MD, PhD (Presenter)

SSG01-03 • Comparison of FDG-PET/CT and FDG-PET/MRI for Local Staging of Breast Cancer

Johannes Grueneisen (Presenter) ; James Nagarajah ; Sonja Liebeskind ; Kai Nassenstein ; Sonja Kinner MD

PURPOSE

To compare the diagnostic potential of FDG-PET/MRI mammography and FDG-PET/CT for local staging in breast cancer patients.

METHOD AND MATERIALS

43 Patients with biopsy-proven invasive breast cancer were included in our study. In addition to a clinically indicated FDG-PET/CT all patients subsequently underwent contrast enhanced FDG-PET/MR mammography (Biograph mMR, Siemens) using a 16-channel breast coil. Two readers evaluated separately both imaging methods concerning lesion detection and size measurement of the primary tumor as well as detection of multifocality / multicentricity and bilateral lesions. All patients underwent surgery; histopathology examination served as a reference of standard.

RESULTS

A total of 52 lesions, including 49 primary tumor lesions and three contralateral lesions were detected. While PET/CT allowed for identification of 46/52 cases (88,5%), PET/MRI offered correct identification of 50/52 (96,2%) breast cancer lesions. PET/MRI enabled a correct assessment of the T stage in 44/52 cases (84,6%); compared to PET/CT (31/52; 59,6%). In five cases the same lesion at T2 stage was falsely diagnosed as T1 stage by both diagnostic modalities.

CONCLUSION

The results demonstrate the superiority of PET/MRI in detecting malignant lesions and in its size estimation compared to PET/CT while both diagnostic methods reveal the tendency to underestimate the tumor size.

CLINICAL RELEVANCE/APPLICATION

PET/MRI seems to be a powerful tool in detecting and rating primary breast cancer lesions as well as accessory lesions and should be diagnostic modality of choice for staging primary breast cancer.

SSG01-04 • Meta-analysis of Molecular Breast Imaging (MBI) Studies

James W Hugg PhD (Presenter) *

PURPOSE

Molecular Breast Imaging (MBI) uses planar imaging of single gamma photon emission from intravenous injection of Tc99m-sestamibi or tetrofosmin to visualize breast cancers that are often occult on mammography in the 40-50% of women with radiographically dense breasts. Clinical results published since 2002 support a meta-analysis of the MBI studies in three clinical applications: diagnostic workup, extent of disease, and high-risk screening.

METHOD AND MATERIALS

MBI consists of a pair of opposed semiconductor (CZT) gamma photon cameras. Breast-Specific Gamma Imaging (BSGI) consists of a single scintillator (NaI or CsI with PS-PMT or photodiode) gamma camera and a compression paddle. In both MBI and BSGI the breast is mildly compressed in standard planar mammographic views. We culled the literature until we had 19 studies and 4948 patients for diagnostic workup, 8 studies and 1507 patients for extent of disease, and 5 studies and 3013 patients for dense-breast screening. The analysis pools studies performed by BSGI (Dilon) and MBI (Gamma Medica or GE Healthcare).

RESULTS

Patient injected doses were 8-20 mCi for MBI and 20-44 mCi for BSGI, with a general reduction in dose over time. The diagnostic workup studies, including primarily women with suspicious lesions on screening mammography, had a sensitivity of 94% for the detection of 1652 cancers and a specificity of 85%. The extent of disease studies in women with biopsy-proven cancer yielded additional cancers in 8% of women, changing clinical treatment in many cases. The high dense-breast screening studies detected a prevalence of 12.9 cancers per 1000 asymptomatic women screened by MBI or BSGI, compared to an incidence of 3.0 per 1000 for annual screening mammography.

CONCLUSION

MBI and BSGI are more sensitive and specific than mammography, especially in dense breasts, and should be considered as an adjunct diagnostic and screening tool in breast cancer. Efforts to improve the technology and reduce the patient dose will further encourage the adoption of this new breast imaging modality.

CLINICAL RELEVANCE/APPLICATION

MBI and BSGI are more sensitive and specific than mammography, especially in dense breasts, and should be considered as an adjunct diagnostic and screening tool in breast cancer.

SSG01-05 • Correlation between Quantitative 18F-FDG Uptake on PET/CT with Prognostic Factors in Triple-negative Breast Cancers

Hye Ryoung Koo MD ; Woo Kyung Moon ; Nariya Cho MD ; Jung Min Chang MD ; Mirinae Seo MD ; Hye Mi Gweon MD (Presenter) ; Keon Wook Kang

PURPOSE

We aimed to investigate whether a correlation exists between quantitative 18F-FDG uptake on PET/CT and prognostic factors in triple-negative breast cancer

METHOD AND MATERIALS

Between January 2009 and December 2012, 1109 patients with newly diagnosed breast cancer underwent 18F-FDG PET/CT for initial staging followed by surgical treatment. This retrospective study involved 112 triple-negative invasive ductal cancers (mean tumor size 2.64cm, range 1 to 6.5cm) in 112 patients (mean age, 50.04 years; range, 28-77 years). Correlations between quantitative 18F-FDG uptake on PET/CT, expressed as maximum standardized uptake value (SUVmax), and prognostic factors including tumor size, axillary lymph node involvement status, histologic grade, nuclear grade, expression of Ki-67, p53, bcl-2, EGFR, CK5/6 were analyzed. Triple-negative breast cancer was defined as estrogen receptor (ER)-negative, progesterone receptor (PR)-negative, and human epidermal growth factor 2 (HER2)-negative.

RESULTS

The mean SUVmax value of the 112 tumors was 10.05 ± 5.8 (range: 1.4-32.8). Tumors with high nuclear grade (mean SUVmax 10.39 ± 5.75 , n=106) showed higher FDG uptake than tumors with low nuclear grade (mean SUVmax 3.96 ± 2.31 , n=6). There was a positive correlation between 18F-FDG uptake and tumor size (Spearman's correlation coefficient = 0.38) as well as Ki-67 (Spearman's correlation coefficient = 0.22), whereas this relationship was not observed among the axillary lymph node involvement status, histologic grade, p53, bcl-2, EGFR, and CK5/6. In a multivariate logistic regression analysis, tumor size (P

CONCLUSION

Increased FDG uptake on PET/CT correlates with tumor size, nuclear grade, and Ki-67 proliferation index in triple-negative breast cancer.

CLINICAL RELEVANCE/APPLICATION

FDG uptake relates to biologically important prognostic factors in triple-negative breast cancer. FDG uptake on PET/CT might be a useful tool to define the heterogeneity of triple-negative breast cancer.

SSG01-06 • Molecular Breast Imaging: The Sensitivity of Breast-specific Gamma Imaging (BSGI) as a Diagnostic Adjunct to Mammography and Ultrasound in a Triple Assessment Protocol

Jean M Weigert MD (Presenter) * ; Douglas A Kieper BS * ; Marcela Bohm-Velez MD

PURPOSE

BSGI is a diagnostic breast imaging procedure becoming more common in clinical breast practice. The goal of this work is to quantify its performance as an addition to mammography and ultrasound in detection of breast carcinoma when used in the community breast center setting.

METHOD AND MATERIALS

A multi-center patient registry was maintained for all patients routinely sent to BSGI as part of their diagnostic work up. From the registry data, patients who had a mammogram followed by ultrasound and BSGI were selected for evaluation. The BIRADS rating schematic was used for mammography and sonography and a similar category system was used for the BSGI images. For each modality, the reports were classified as positive (categories 4 - 6) or Negative (categories 0 - 3). Needle and/or surgical biopsy were conducted as deemed clinically necessary and all patients who had a malignant diagnosis by pathology were entered into this analysis.

RESULTS

731 patients had all three imaging modalities as part of their diagnostic work up resulting in 180 malignancies confirmed by pathology: 29 ductal carcinoma in-situ, 110 infiltrating ductal carcinoma, 11 infiltrating lobular carcinoma, 9 papillary carcinoma and 21 mixed component malignancies. Mammography was positive in 130 (sensitivity = 72%) while ultrasound was positive in 114 (sensitivity = 63%) and BSGI was positive in 147 (sensitivity = 82%). Mammography and ultrasound were positive in 163 cases (sensitivity = 90%). BSGI provided positive findings for 177 malignancies resulting in a sensitivity of 98%. A breast MRI detected one lesion missed by the three modalities while two lesions were found by pathology alone

CONCLUSION

Of the three imaging modalities, BSGI provided the highest independent sensitivity and when added to the diagnostic workup, BSGI detected an additional 14 malignancies, increasing the sensitivity from 90% to 98%. Although it is beyond the scope of this work, it is interesting to note that the cost of the BSGI procedure is relatively low, about \$320, and that in this population the BSGI specificity was 74%. In summary, when added to the diagnostic work up of patients in the community breast cancer, BSGI can improve the detection of breast malignancy when compared to mammography and ultrasound alone.

CLINICAL RELEVANCE/APPLICATION

BSGI can improve the detection of breast malignancy when compared to mammography and ultrasound alone.

SSG01-07 • False Positive Findings on Adjunct Screening Molecular Breast Imaging with Tc-99m Sestamibi

Carrie B Hruska PhD (Presenter) * ; Amy L Connors MD ; Katie N Jones MD ; Michael K O'Connor PhD * ; Deborah J Rhodes MD

PURPOSE

To determine the rates and histopathologic subtypes of false positive imaging findings and benign biopsies generated from adjunct screening with molecular breast imaging (MBI).

METHOD AND MATERIALS

Screening MBI was performed in asymptomatic women presenting for screening mammography who had dense breasts (>50% fibroglandular) on past prior mammogram. Intravenous injection of 8 mCi Tc-99m sestamibi was administered; bilateral 2-view MBI was performed using a dual-head CZT-based gamma camera. MBI studies were interpreted with access to the current screening mammogram and assigned an assessment of 1-5 that parallels BI-RADS. Assessment of 3 or higher was considered test positive. Participants with negative reference standard (benign biopsy result or negative/benign imaging at one year) were analyzed.

RESULTS

Of 1638 eligible participants, 1578 (96%) had complete reference standard, of which 1557 had no diagnosis of cancer. In 1557 participants with negative reference standard, 105 (6.7%) had test positive screening MBI and were recalled for diagnostic workup. Of these 105, 70 (67%) were resolved with benign findings on immediate diagnostic mammogram/ultrasound and follow-up MBI at 6 months. Final impressions included: stable background uptake (24) or resolved focal uptake (16); appearance of fibrocystic change (14), fibroadenoma (5), lymph node (3), post-operative change (4), or stable mass (2); and previously biopsied papilloma (2). The remaining 35 of 105 (33%) underwent biopsy: ultrasound-guided in 26, magnetic resonance imaging-guided in 7, and stereotactic in 2. Pathologic findings included fibroadenoma (11), benign breast parenchyma (6), fibrocystic change (5), papilloma (4), radial scar (3), stromal fibrosis (2), pseudoangiomatous stromal hyperplasia (2), atypical ductal hyperplasia (2).

CONCLUSION

For non-cancer cases, adjunct MBI had a recall rate of 6.7% and benign biopsy rate of 2.3%. The most common false positive imaging finding was benign background uptake of Tc-99m sestamibi in fibroglandular tissue; the most common biopsied benign lesion was fibroadenoma.

CLINICAL RELEVANCE/APPLICATION

MBI demonstrated a relatively low additional false positive rate compared to that reported for other modalities under consideration for supplemental screening in the dense breast.

SSG01-08 • Improved Diagnostic Yield in Dense Breasts with Supplemental Screening Molecular Breast Imaging

Deborah J Rhodes MD (Presenter) ; Carrie B Hruska PhD * ; Amy L Conners MD ; Katie N Jones MD ; Michael K O'Connor PhD *

PURPOSE

We previously demonstrated that addition of Molecular Breast Imaging (MBI) using 20 mCi Tc-99m sestamibi to screening mammography (SM) increased diagnostic yield for breast cancer in dense breasts (supplemental yield of 7.5/1000 screened). After implementing radiation dose reduction techniques, we are comparing performance of incident SM and prevalent screen MBI in women with dense breasts.

METHOD AND MATERIALS

Women presenting for SM with heterogeneously or extremely dense breasts on past prior SM were enrolled and underwent digital SM and MBI. MBI was performed with 8 mCi Tc-99m sestamibi and dual-head cadmium zinc telluride detectors. SMs were read independently; MBIs were read in comparison with SM. MBIs were assigned an assessment score of 1-5 which parallels BI-RADS; scores of 3-5 on MBI were considered positive.

RESULTS

In 1651 women enrolled, 1578 (96%) completed imaging and had reference standard of pathology findings within 365 days or negative imaging at >300 days. In 1578 analyzable participants, 21 had breast cancer diagnosed. Sensitivity was 5/21 (24%) for SM alone and 19/21 (91%) for the combination of SM and MBI. Diagnostic yield was 3.2 for SM and 12.0 for the combination ($p = 0.0001$). Diagnostic evaluation was prompted by SM alone in 174 (11%) patients and by the combination in 280 (18%). Biopsy was prompted by SM in 21 (1.3%) patients and by the combination in 67 (4.3%). The number of breast cancers diagnosed per number of biopsies (PPV) was 24% for SM and 28% for combination. Specificity was 88% for SM alone and 82% for the combination ($p = 0.0001$). Fourteen patients had cancer detected only on MBI: 4 ductal carcinoma in situ (DCIS); 8 invasive ductal carcinoma (IDC); and 2 invasive lobular carcinoma (ILC); median pathologic tumor size was 12 mm; range 4-62 mm. Three of 14 were node positive. The 4 MBI occult cancers were node negative and included 1 DCIS, 1 IDC, and 2 ILC; median pathologic tumor size was 6 mm, range 3-7 mm. Two patients had cancers detected on neither modality, including a 6 mm ILC detected on MRI and a 7 mm ILC detected on prophylactic mastectomy.

CONCLUSION

Low dose MBI as an adjunct to SM in women with dense breasts provided a supplemental yield of 8.8 per 1000 with a modest decline in specificity.

CLINICAL RELEVANCE/APPLICATION

The supplemental yield of adding screening MBI to SM in women with dense breasts is preserved at a lower administered dose of 8 mCi Tc-99m sestamibi.

SSG01-09 • Background Parenchymal Uptake of Tc-99m Sestamibi on Molecular Breast Imaging in Mammographically Dense Breasts

Carrie B Hruska PhD (Presenter) * ; Amy L Conners MD ; Katie N Jones MD ; Deborah J Rhodes MD ; Michael K O'Connor PhD * ; Celine M Vachon *

PURPOSE

Background parenchymal uptake (BPU), or uptake of Tc-99m sestamibi in normal fibroglandular tissue (FT), has been observed on molecular breast imaging (MBI). We describe categories of BPU and examine associated factors, including mammographic density.

METHOD AND MATERIALS

Screening MBI exams between April 2010-March 2012 from women with BI-RADS D3/D4 density on last mammogram were reviewed. Participants with breast implants or cancer diagnosed at screening were excluded. BPU intensity was subjectively categorized by two radiologists as photopenic (uptake in FT < subcutaneous fat), mild (uptake in FT = fat), moderate (uptake in FT up to 2x fat), or marked (uptake in FT > 2x fat). Association of BPU with age, current BI-RADS mammographic density, menopausal status, and use of hormonal medications was examined.

RESULTS

In 1274 screening MBI exams, BPU was photopenic in 273 (21%), mild in 826 (65%), moderate in 136 (11%), and marked in 39 (3%). Moderate/marked BPU occurred in 31% (99/315) of women age 40-49 compared to 8% (76/959) of women age 50 and older (p

CONCLUSION

Moderate/marked BPU occurred more often in denser breasts and in women who were younger, pre- or perimenopausal, or on exogenous hormones. In each density category, substantial proportions of both moderate/marked and photopenic BPU were observed, establishing that similar-appearing FT on mammography can demonstrate considerable differences in BPU on MBI.

CLINICAL RELEVANCE/APPLICATION

BPU may reflect underlying functional activity of mammographically dense tissue. Additional studies are needed to determine if BPU can help predict an individual's density-related breast cancer risk.

Molecular Imaging (Subspecialties)

Tuesday, 10:30 AM - 12:00 PM • S504CD



[Back to Top](#)

SSG09 • AMA PRA Category 1 Credit™:1.5 • ARRT Category A+ Credit:1

Moderator

Vikas Kundra, MD, PhD *

SSG09-01 • Noninvasive Assessment of Myocardial Inflammation by Cardiac Magnetic Resonance Imaging in a Rat Model of Cardiorenal Syndrome Type IV

Di Chang (Presenter) ; Sheng Hong Ju MD, PhD

PURPOSE

Cardiorenal syndrome (CRS) type IV is a condition of primary chronic kidney disease (CKD) worsening cardiac function, which in turn further accelerates the failure progression of both. Monocyte-macrophages contribute to the myocardial inflammatory progression caused by CKD. The purpose of this study was to detect and quantify macrophage-related inflammation within the inflamed heart in a CRS type IV rat model using magneto-fluorescent nanoparticles (MNPs) enhanced, high-resolution cardiac magnetic resonance (CMR) imaging.

METHOD AND MATERIALS

RESULTS

CONCLUSION

MNPs enhanced CMR imaging can noninvasively assess myocardial monocyte-macrophages burden and potentially monitor therapy-mediated myocardial changes in CRS type IV.

CLINICAL RELEVANCE/APPLICATION

MNPs enhanced CMR imaging can noninvasively assess myocardial monocyte-macrophages burden and potentially monitor therapy-mediated myocardial changes in CRS type IV

SSG09-02 • Black Blood 3D DCE-MR to Examine Permeability and Predict Nanoparticle Targeting in Experimental Atherosclerosis

Mark E Lobatto MD (Presenter) ; Claudia Calcagno PhD ; Antoine Millon ; Max Senders ; Francois Fay PhD ; Phil Robsom PhD ; Sarayu Ramachandran MS ; Erik Stroes MD, PhD ; Zahi A Fayad PhD * ; Willem J Mulder MS, PhD

PURPOSE

Atherosclerotic disease is a major cause of global morbidity and mortality that might benefit from targeted therapy to the vessel wall¹. Recent studies have shown efficient and local drug delivery with nanoparticles, though the targeting method in atherosclerosis has not been clarified². In the current study we used in and ex vivo imaging methods to investigate nanoparticle targeting and the role of permeability in a rabbit model of atherosclerosis. ¹Tabas I, Glass CK, Science 2013
²Lobatto ME et al. Nat Rev Drug Discovery 2011

METHOD AND MATERIALS

To achieve this we developed a novel black-blood 3D Dynamic Contrast Enhanced (DCE)-MRI technique that allows the assessment of endothelial permeability over a large vascular region, e.g. the infra-renal aorta of an atherosclerotic rabbit. Atherosclerotic rabbits (n=8) were subjected to a DCE-MRI scan on a 3T clinical scanner and injected with nanoparticles labeled with the fluorescent dye Cy7 (Cy7-LN) that we allowed to circulate different time points (½-hour, 6 hours and 24 hours). Next, we injected a fluorescent dye (Evans Blue (EB)) that extravasates at sites with enhanced permeability, after which rabbits were sacrificed. Near infrared fluorescence imaging was then used to quantify both Cy7-LN and EB in excised aortas.

RESULTS

Excellent correlation was observed between the accumulation of Cy7-LN at a ½-hour and permeability determined with EB ($r^2=0.8, p=0.65, p=0.47, p=0.007$; DCE: $r^2=0.53, p=0.003$), but became insignificant after 24 hours (EB: $r^2=0.08, p=0.33$; DCE: $r^2=0.08, p=0.33$). With fluorescence microscopy we found Cy7-LN confined to the vasculature when circulated for a ½-hour, while gradual extravasation from the lumen and neovessels was seen at 6 hours. At 24 hours LN was found diffusely throughout the plaque, clarifying the aforementioned decrease in correlation between LN accumulation and endothelial permeability.

CONCLUSION

3D DCE-MRI allowed the visualization of permeability within atherosclerotic plaques, which similarly correlated with nanoparticle uptake.

CLINICAL RELEVANCE/APPLICATION

As nanoparticles may be employed for local drug delivery to atherosclerotic plaques, 3D DCE-MRI might be a valuable in vivo tool to predict if a subject is amenable to nanoparticle therapy.

SSG09-03 • Cardiac PET/MRI with 18F-FDG: Feasibility and Initial Results in Patients with Acute Myocardial Infarction

Felix Nensa MD (Presenter) ; Thorsten D Poeppel ; Karsten J Beiderwellen MD ; Juliane Schelhorn MD ; Amir A Mahabadi MD ; Philipp Heusch MD ; Kai Nassenstein ; Michael Forsting MD ; Thomas W Schlosser MD

PURPOSE

To assess the feasibility of hybrid imaging of the heart with ¹⁸F-fluorodeoxyglucose (¹⁸F-FDG) on an integrated 3 Tesla PET/MRI system and to discuss its potential clinical impact.

METHOD AND MATERIALS

Twenty patients with confirmed acute myocardial infarction underwent ¹⁸F-FDG PET/MRI with oral glucose loading within 2-7 days after interventional revascularization. Tracer accumulation in each myocardial segment was compared to regional wall motion abnormalities and to signal intensity in late gadolinium-enhanced (LGE) images with Cohen's χ^2 statistics. The size of the infarction zone was measured on LGE and PET images. In 10 patients additional PET/CT imaging was performed and PET data was visually and semi-quantitatively (SUV_{max}) compared between PET/CT and PET/MR.

RESULTS

Absolute parallelized scan time was 71 ± 3 min. Categorical inter-method agreement between PET and LGE over all patients and segments was $\chi^2=0.83$, and $\chi^2=0.81$ between PET and cine imaging. On average $20 \pm 17\%$ of the entire left ventricular myocardium was classified as infarcted in PET images and $19 \pm 19\%$ in LGE images ($p=0.65$). Bland-Altman analysis of tracer uptake in PET/MR and PET/CT yielded limits of agreement of -3.04 to 3.65 (SUV_{max} : 6.51 ± 3.42 vs. 6.82 ± 3.16 ; $p=0.21$), the coefficient of variation was 0.18.

CONCLUSION

Cardiac PET/MRI in patients with acute myocardial infarction is feasible on an integrated PET/MR scanner. Comparison of PET images from PET/CT and PET/MRI showed good concordance. A close match between PET and MRI regarding myocardial viability and infarct quantification was demonstrated. Further study will show, if hybrid PET/MRI with ¹⁸F-FDG yields added value in patients with ischemic cardiac disease.

CLINICAL RELEVANCE/APPLICATION

Cardiac PET/MRI provides quantitative information on metabolic processes that might be incorporated into cardiac MRI protocols to improve risk stratification in acute myocardial infarction.

SSG09-04 • Non-invasive Assessment of Inflammation in a Murine Model of Chronic Inflammatory Bowel Disease Using Ultrasound Molecular Imaging

Ferdinand Knieling (Presenter) ; Steven B Machtaler PhD ; Thierry Bettinger * ; Richard Luong ; Huaijun Wang MD, PhD ; Juergen K Willmann MD *

PURPOSE

Ultrasound (US) molecular imaging has shown promising results in imaging inflammation in murine models of acute inflammatory bowel disease (IBD). The purpose of this study was to evaluate the feasibility of US molecular imaging using a clinically translatable microbubble (MB) targeted to the inflammation markers P- and E-selectin (MBselectin) for monitoring inflammation in a chronic and a chronic flare model of murine colitis.

METHOD AND MATERIALS

Acute colitis was established by rectal 2,4,6-trinitrobenzene sulfonic acid (TNBS) administration in 23 mice. Chronic colitis was established by 3 repetitive cycles of oral dextran sodium sulfate (DSS) administration in an additional 23 mice; an acute inflammatory flare in the chronic colitis mice was simulated by rectal TNBS injection. All mice were imaged in contrast mode following i.v. injection of 5x10⁷ MBselectin and control microbubbles (MBcontrol) using a 21 MHz transducer (VisualSonics). In vivo imaging results were correlated with ex vivo immunofluorescence and histology.

RESULTS

CONCLUSION

Selectin-targeted US molecular imaging allows inflammation assessment in acute inflammation and chronic flare models of IBD in mice, which may simulate different disease states seen in patients with IBD.

CLINICAL RELEVANCE/APPLICATION

US molecular imaging is a clinically translatable approach to quantitatively assess inflammatory flares in both early and late stage IBD.

SSG09-05 • Inflammation Imaging Using Molecular Ultrasound in an Acute Terminal Ileitis Model in Swine

Huaijun Wang MD, PhD (Presenter) ; **Stephen A Felt** DVM, MPH ; **Ismayil Guracar** * ; **Steven B Machtaler** PhD ; **Thierry Bettinger** * ; **Juergen K Willmann** MD *

PURPOSE

To translate ultrasound (US) molecular imaging using a clinical grade contrast microbubble targeted at the inflammation markers P- and E-selectin (MB_{Selectin}) to a large animal model of acute terminal ileitis.

METHOD AND MATERIALS

An acute terminal ileitis porcine model was established in 9 female pigs using intraluminal 2,4,6-trinitrobenzene sulfonic acid (TNBS) installation. All pigs were imaged before (control), and 48 hours after induction of ileitis. US molecular imaging was performed after i.v. injection of either MB_{Selectin} or non-targeted MB_{Control} at a dose of 5×10⁸/kg b.w. each using a clinical US machine (Acuson Sequoia 512; Siemens) and a clinical transducer (15L8W; 7MHz). Four minutes after MB injection, images were acquired for 10 sec, followed by a 3-sec high power destruction pulse; this was followed by another 10-sec acquisition. Linearized imaging signal was expressed as intensity ratio, defined as average pre-destruction signal intensity divided by average post-destruction signal intensity. After imaging, pigs were sacrificed and the terminal ileum was analyzed for inflammation grade on HandE staining and for expression of P- and E-selectin using immunofluorescence.

RESULTS

US molecular imaging of the terminal ileum was feasible in all 9 pigs. Imaging signal intensity ratio using MB_{Selectin} was significantly higher (increased by 106%, P=0.005) in acute ileitis compared to normal control ileum. Also, imaging signal in acute ileitis using MB_{Selectin} was significantly higher (increased by 103%, P=0.002) compared to MB_{Control}. US imaging signal was not significantly different (P=0.06) when using MB_{Selectin} or MB_{Control} in normal control ileum. *Ex vivo* analysis on HandE stained tissue samples confirmed strong inflammation in the terminal ileum. Immunofluorescence showed overexpression of selectins on the vasculature of inflamed bowel.

CONCLUSION

US molecular imaging with MB_{Selectin} can be translated to large animal imaging in an acute terminal ileitis porcine model and molecular US imaging signal correlates well with extent of inflammation on histology.

CLINICAL RELEVANCE/APPLICATION

The feasibility of US molecular imaging in large animals with ileitis paves the way towards clinical translation of US molecular imaging for the accurate quantification of inflammation in the abdomen.

SSG09-06 • Optical Imaging for Real-time Detection of Cartilage Matrix Degeneration in Experimental Osteoarthritis Models

Shadi A Esfahani MD, MPH (Presenter) ; **Andrea Foote** ; **Averi A Leahy** ; **Li Zeng** ; **Umar Mahmood** MD, PhD

PURPOSE

Osteoarthritis (OA) is a degenerative disease due in part to permanent destruction of cartilage matrix, causing patients pain and immobility. This destruction occurs by highly activated proteases in the matrix, predominantly matrix metalloproteinase (MMP). We used an optical probe, cleaved and activated by MMP enzymes in the cartilage and assessed the ability of this probe for early detection and monitoring of OA progression in animal models.

METHOD AND MATERIALS

RESULTS

CONCLUSION

Our imaging and histopathology results showed that targeting MMP is a promising non-invasive method for early detection and monitoring of cartilage matrix degeneration in a wear-and-tear model of OA. The method is readily translatable to humans.

CLINICAL RELEVANCE/APPLICATION

Optical imaging of matrix metalloproteinase could aid in non-invasive detection of cartilage destruction in early stages of disease and in evaluation of treatment response in osteoarthritic patients.

SSG09-07 • Arterial Spin Labeling and T1-mapping for Evaluation of Renal Perfusion Impairment and Tissue Edema following Acute Kidney Injury in Mice-Comparison with Histopathology

Katja Hueper (Presenter) ; **Marcel Gutberlet** DiplPhys ; **Song Rong** MD ; **Dagmar Hartung** MD ; **Matti Peperhove** MD ; **Amelie Barmeyer** ; **Michael Mengel** ; **Hermann Haller** MD ; **Frank K Wacker** MD * ; **Martin Meier** PhD ; **Faikah Gueler** MD

PURPOSE

Acute kidney injury (AKI) leads to inflammation, decrease of renal perfusion, and loss of renal function. The purpose was to investigate whether arterial spin labeling (ASL) and T1-mapping allow monitoring renal perfusion impairment and acute tissue edema in a mouse model of ischemia induced AKI.

METHOD AND MATERIALS

AKI was induced in C57Bl/6 mice by transient unilateral clamping of the right renal pedicle for 35 min (n=10, moderate AKI) or 45 min (n=7, severe AKI). Animals underwent MRI prior to surgery and at different time points thereafter (d1, d7, d14, d21, d28) using a 7 Tesla magnet. Flow sensitive alternating inversion recovery (FAIR) EPI ASL sequences (13 inversion times) were acquired, and maps of renal perfusion and T1 relaxation time were calculated. Kidney volume was determined by segmentation of axial T2-weighted images. Renal pathology in the same animals after 4 weeks was assessed by histology. Statistical analysis comprised ANOVA for repeated measurements followed by multiple comparison with the Sidak method, unpaired t-tests and correlation analysis between MRI parameters, histology and kidney volume loss.

RESULTS

Renal perfusion at d7 was significantly reduced to 56±8% after moderate (p

CONCLUSION

ASL and T1-mapping allow non-invasive monitoring of renal perfusion impairment and tissue edema after AKI in mice. Changes of renal perfusion and T1 relaxation time are associated with the severity of renal pathology and kidney volume loss.

CLINICAL RELEVANCE/APPLICATION

Renal perfusion and T1 relaxation time measured by arterial spin labeling and T1-mapping may serve as non-invasive biomarkers to characterize renal pathology after acute kidney injury.

SSG09-08 • Visceral Obesity Assessed by 1H-MRS Predicts Cardiovascular Events in Chronic Kidney Disease Patients

Francesca Bolacchi (Presenter) ; Ettore Squillaci MD ; Fabrizio Chegai MD ; Marco Nezzo MD ; Giovanni Simonetti MD

PURPOSE

Cardiovascular disease is the leading cause of death among patients with chronic kidney disease (CKD). Although there is emerging evidence that excess visceral fat is associated with a cluster of cardiometabolic abnormalities in these patients, the impact of visceral obesity evaluated by a gold-standard method on future outcomes has not been studied. We aimed to investigate whether visceral obesity assessed by 1H-MRS was able to predict cardiovascular events in CKD patients.

METHOD AND MATERIALS

We studied 48 nondialyzed CKD patients [58% men; 29% diabetics; age 52.4 ± 9 years; body mass index (BMI) 26 ± 4.2 kg/m(2); estimated glomerular filtration rate (GFR) 32.7 ± 11.5 ml/min/1.72 m(2)]. Visceral and subcutaneous abdominal fat were analysed by single voxel magnetic resonance spectroscopy (MRS). The MRS lipid spectrum was analysed and a lipid polyunsaturation index (PUI) was calculated. Fifteen healthy subjects were enrolled as controls. Cardiovascular events including acute myocardial infarction, angina, arrhythmia, uncontrolled blood pressure, stroke and cardiac failure were recorded during 24 months.

RESULTS

Cardiovascular events were 3-fold higher in patients with higher PUI index. The Kaplan-Meier analysis indicated that patients with a high PUI index had shorter cardiovascular event-free time than those a normal PUI values (P = 0.031). In the univariate Cox analysis, PUI was associated with higher risk of cardiovascular events (hazard ratio = 3.4; 95% confidence interval = 1.1-10.5; P = 0.03). The prognostic power of PUI for cardiovascular events remained significant after adjustments for sex, age, diabetes, previous cardiovascular disease, smoking, sedentary lifestyle, BMI, GFR, hypertension, dyslipidemia and inflammation.

CONCLUSION

Visceral and subcutaneous fat as analysed by 1H-MRS is a valuable tool in predicting cardiovascular events in CDK patients.

CLINICAL RELEVANCE/APPLICATION

PUI index ased by 1-H MRS was a predictor of cardiovascular events in CKD patients.

SSG09-09 • C5b-9 Targeted Molecular MR Imaging in Rats with Heymann Nephritis: A New Approach in Evaluation of Nephrotic Syndrome

Wenbo Xiao MD ; Qiang Huang (Presenter) ; Song Wen ; Chuangen Guo ; Qidong Wang ; Rui Zhang

PURPOSE

To determine the feasibility of magnetic resonance imaging in rats with Heymann nephritis(HN) by using membrane attack complex C5b-9 targeted ultrasmall superparamagnetic iron oxide(USPIO)

METHOD AND MATERIALS

RESULTS

CONCLUSION

Anti-C5b-9-USPIO, as targeted molecular probe in MRI, could be used in specific imaging of rats with HN. Such a new molecular imaging method would be promising in the study of nephrotic syndrome diagnosis and treatment. [This study was supported by grants from the National Natural Science Foundation of P.R. China (81171388) to W.X. and partly from the Ministry of Health Research Foundation of P.R. China (WKJ2011-2-004) to W.X]

CLINICAL RELEVANCE/APPLICATION

C5b-9 targeted molecular MR imaging can be a promising noninvasive approach in study of glomerulonephritis.

Recurrent Brain Tumors v/s Radiation Necrosis: PET MRI as a Rescue

Tuesday, 12:15 PM - 12:45 PM • S503AB

[Back to Top](#)

CL-MIE-TU5A

Hemant T Patel , MD
Ankur Shah , MD
Megha Sanghvi , MD
Manas Mayank , MD
Mrunali I Shah , MBBS
Laxmi V Bhohe , DMRD

PURPOSE/AIM

The purpose of this exhibit is:

1. To review specific imaging of recurrent Brain tumor and radiation necrosis
2. To evaluate the accuracy of PET MRI in different recurrent brain tumors
3. To describe the pattern of local recurrence of brain tumors and radiation necrosis using PET MRI

CONTENT ORGANIZATION

- ◆ Pathophysiology of recurrent brain tumors after surgery and radiotherapy
- ◆ Limitations of conventional mode of imaging including MRI and MR perfusion
- ◆ Correlation of PET imaging with structural images of MRI for evaluation of functional changes
- ◆ Review of PET MRI findings for local tumour recurrence, radiation necrosis or co-existent pathologies
- ◆ Future direction and summary

SUMMARY

Major teaching points of this exhibit are:

1. Recurrence of brain tumor is relatively high and requires a precise and early diagnosis for better outcome
2. PET MRI is a very sensitive modality to depict recurrent brain tumor with high positive predictive value
3. This exhibit will help for understanding of functional method of tumour viability which eventually helps to differentiate it from radiation necrosis

Molecular Imaging - Tuesday Posters and Exhibits (12:15pm - 12:45pm)

Tuesday, 12:15 PM - 12:45 PM • S503AB

[Back to Top](#)



CL-MIS-TUA • AMA PRA Category 1 Credit™:0.5

Host
Michael S Gee , MD, PhD

CL-MIS-TU1A • In Vivo Monitoring of NIS-induction and Tumor Phenotyping Using Extrathyroidal Tumor Xenograft Mouse Models

Eva J Koziolok DO (Presenter) ; **Ivayla Apostolova** ; **Agnieszka Tarkowska** ; **Winfried Brenner** * ; **Udo Schumacher** ; **Gerhard B Adam** MD ; **Michael G Kaul**

PURPOSE

Despite the method of gene transfer, all trans retinoic acid (atRA), a vitamin A derivative, in combination with glucocorticoides has been used to stimulate sodium iodide symporter (NIS) expression in thyroid and breast cancer models. To apply I^{131} therapy to extrathyroidal tissue, functional and sufficient NIS-expression is a pre-condition. The purpose of this study was to evaluate the potential of atRA and prednisolone (PRED) to i) induce functional NIS-expression in a NIS-negative pancreatic cancer model ii) enhance functional NIS in a NIS-transfected breast cancer model.

METHOD AND MATERIALS

Mouse tumor xenograft models BxPC3 (pancreas), HT29 (colon) and NIS-transfected MCF7 (breast) were established over the right scapula. Daily injections of atRA/PRED (1.3/0.7 mg/day) treatment were given subcutaneously for up to 7 days. SPECT was performed on day 0, 5 and 7 using a nanoSPECT/CTplus (Bioscan/Medisso) and 100 MBq/mouse Tc99m pertechnetate. Tumor phenotyping (T2w, ADC, DCE-MRI) was performed prior to the treatment using a 7T MRI (ClinScan, Bruker).

RESULTS

In vivo imaging of tumor-specific NIS-induction after 5 and 7 days of atRA/PRED treatment was performed by SPECT and resulted in an increase in Tc99m-uptake. The NIS-negative pancreatic cancer model showed an up to 3 fold increase in tracer uptake (n=4) above the background or when compared to HT29 tumor xenografts. As expected, the NIS-transfected breast cancer model (n=4) showed an initial strong tracer uptake in the tumor tissue (3 and 4 % ID/ml) and further increased by 30-50%, on day 7 of treatment. T2w MR imaging allowed a precise delineation of tumor mass, and was used to place the ROI with high accuracy for SPECT analysis. Tumor phenotyping allowed a detailed characterisation of the tumor tissue prior to atRA/PRED treatment.

CONCLUSION

Functional NIS-expression in extrathyroidal tissues can be stimulated by atRA/PRED treatment and further increased in already NIS-transfected tissues, when tissues initially respond with NIS-expression after atRA treatment. In vivo tumor-specific NIS-induction can be visualized by SPECT/CT using a NIS-specific tracer. Multimodal imaging including SPECT and MRI generates useful complementary data.

CLINICAL RELEVANCE/APPLICATION

The combination of gene transfer and atRA-induced NIS expression represents a convenient way to further increase NIS levels in extrathyroidal tissues in order to achieve a therapeutic effect with I^{131}

CL-MIS-TU2A • Optimization for Combination of Peptide Receptor Radionuclide Therapy (PRRT) and Temozolomide Therapy Using SPECT/CT and MRI; A Mouse Study

Joost C Haeck MS (Presenter) ; **Sander Bison** ; **Stuart Koelewijn** ; **Harald C Groen** PhD ; **Marleen Melis** ; **Monique R Bernsen** PhD ; **Marion De Jong** PhD

PURPOSE

Successful treatment of patients with somatostatin receptor overexpressing neuroendocrine tumors (NET) with Lutetium-177-labelled octreotate, (PRRT) or temozolomide (TMZ) as single treatments has been described. Their combination might result in additive response, so we studied tumor characteristics and therapeutic responses after different administration schemes in mice to obtain the optimal strategy to combine PRRT and TMZ.

METHOD AND MATERIALS

Initially we performed imaging studies of nu/nu mice (n=5-8) bearing somatostatin receptor-expressing human H69 small cell lung carcinoma xenografts, after single administration of PRRT (30MBq/♂g) or TMZ therapy (50mg/kg/day (d) 5x/week for 2 weeks). Once a week tumor perfusion was measured by DCE-MRI and SPECT/CT images were acquired to determine tumor ^{111}In -uptake. Based on the imaging results, seven groups were included in a combination therapy study; 1: control (saline), 2: TMZ, 3: PRRT 4: PRRT + TMZ both d1, 5: PRRT d1, TMZ from d15, 6: TMZ from d1 PRRT d15, 7: PRRT d1 and d15. Study endpoint was tumor volume >1800-2000 mm³.

RESULTS

Single treatment with PRRT or TMZ therapy resulted in reduction of tumor size, which led to changes in MRI characteristics such as intrinsic T2, T2* and perfusion values. Moreover, TMZ treatment not only showed a reduction in tumor size 9d after start of treatment and an increase in MRI perfusion parameters but also an increasing uptake of ^{111}In -octreotide till d15 followed by a decrease thereafter. In the combination therapy study no complete cure was found in control, single TMZ and single or double PRRT groups, while in the TMZ/PRRT combination groups resp. 44%, 38% and 55% of mice (groups 4, 5 and 6) showed cure without recurrence of tumor growth during follow-up. The median survival time (MST) was vastly improved in combination groups with TMZ and PRRT in comparison to single dose groups. Controls showed the lowest MST.

CONCLUSION

MRI and SPECT/CT studies showed that administration of PRRT 15d after start of TMZ treatment to be optimal for TMZ and PRRT combinations, resulting in the best anti-tumor effects. All three combination groups, including fractionated PRRT administration, showed additional anti-tumor effect compared to the single treatment groups.

CLINICAL RELEVANCE/APPLICATION

From our results, treatment with TMZ prior to PRRT might be the best option in clinical practice to increase tumor responses in NET patients as well.

CL-MIS-TU3A • New Molecular Imaging Index Derived from Dynamic Susceptibility-weighted Contrast Enhanced MR Perfusion Imaging May Indicate p53 and IDH Mutation in Glioblastoma

Xiang Liu MD (Presenter) ; **Wei Tian** MD, PhD ; **Sven E Ekholm** MD

PURPOSE

The p53 and IDH mutations are important genetic biomarker in glioblastomas, as they had been reported to be associated with secondary GBM and longer survival. The dynamic susceptibility-weighted contrast enhanced MR perfusion imaging (DSC-MR PWI) is the most widely used clinical pre-operative molecular imaging technique, This study is to evaluate whether the DSC-MR PWI findings could be associated with p53 and IDH mutations in glioblastoma.

METHOD AND MATERIALS

DSC-PWI images (GRE sequence, TR/TE = 1500/50 milliseconds; flip angle, 80°; FOV = 24x 24cm²; matrix = 96 x 128; thickness = 5 mm and gap=0mm) in 65 pathology confirmed glioblastomas were reviewed. Maximal relative cerebral blood volume (rCBV) ratio and percentage of signal recovery (PSR) were measured. The p53 immunostaining and IDH mutations were analyzed.

RESULTS

There were 13 glioblastomas with PSR higher than 1 (mean value=1.26±0.17, range: 1.13-1.52), the PSR in other 56 cases was lower than 1 (mean value=0.74±0.22, range: 0.62-0.9). There was no significant difference of rCBV ratio between two groups (p=0.58, M-W U test). The 4/13 glioblastomas with higher PSR presented negative IDH mutation; in contrast to 9/13 cases with positive IDH mutation. Kaplan-Meier survival plots (log rank test) showed that the patients with higher PSR had longer survival times. However, Cox proportional hazards regression analysis, showed that the higher PSR as a weak predictor of longer survival (p=0.047) after adjustment for age, tumor size, tumor number, resection extent, and post-operation therapies.

CONCLUSION

The PSR is a novel molecular imaging biomarker, which may potentially indicate information of IDH mutant status.

CLINICAL RELEVANCE/APPLICATION

Novel non-invasive DSC-PWI derived index of PSR may reveal IDH mutation induced pathologic changes.

CL-MIS-TU4A • Spectral Molecular Imaging of Multiple Intrinsic and Gold Nano-particle Labelled Bio-markers in Ex-vivo Atheroma in Diagnostic Energy Range

Nigel G Anderson MBBCh, FRANZCR (Presenter) * ; **Raj Kumar Panta** PhD ; **Karen Alt** ; **Christopher Bateman** ; **Raja Aamir** BSc ; **Joe Healy** ; **Niels De Ruiter** ; **Christoph Hagemeyer** ; **Karlheinz Peter** ; **Steven Gieseg** ; **Anthony P Butler** MBChB *

PURPOSE

Spectral molecular imaging is a new x-ray based 3D imaging modality which can specifically identify and measure components of biological tissues due to its energy resolution. We aimed to simultaneously distinguish multiple intrinsic and gold nano-particles labelled biomarkers in ex-vivo vulnerable plaque in the diagnostic energy range.

METHOD AND MATERIALS

Excised human carotid plaques were incubated in specific single chain antiLIBS antibodies (scFv) containing 30nm gold nanoparticles which specifically target activated platelets. A MARS small animal spectral molecular imaging scanner incorporating a Medipix3RX energy resolved (spectral) photon counting x-ray detectors bonded to CdTe or GaAs sensor layer with a pixel pitch of 110 μm was used to acquire energy resolved images of the intact plaques. Multiple projections, with eight lower threshold energies of 30, 35, 40, 45, 50, 60, 70 and 80 KeV at 120 kVp x-ray tube voltage were acquired by placing a 10 mm Aluminium filter at the exit window of the x-ray tube. The filter was used to simulate energy absorption of a human neck. Images were reconstructed with algebraic reconstruction methods. Quantification of calcium deposits, soft tissue components (water-like and lipid-like) and gold nanoparticles was performed by analysing their spectral attenuation profiles.

RESULTS

Gold labelled antiplatelet antibody-antigen complexes, calcium and iron, lipid-like, and water-like components of plaque have distinguishable and quantifiable energy responses to x-rays in diagnostic energy range, visible on spectral molecular imaging at 110 μm resolution.

CONCLUSION

We have demonstrated proof of concept that a gold labeled biomarker and intrinsic biomarkers of intact excised vulnerable atherosclerotic plaque can be quantified simultaneously using spectral x-ray molecular imaging at high spatial resolution in the diagnostic energy range. The imaging technique and methodology is likely to be applicable for human neck imaging.

CLINICAL RELEVANCE/APPLICATION

Spectral molecular imaging of carotid plaque is feasible. When spectral molecular imaging is available clinically, it could be used to detect vulnerable plaque then monitor efficacy of its treatment.

Molecular Imaging - Tuesday Posters and Exhibits (12:45pm - 1:15pm)

Tuesday, 12:45 PM - 01:15 PM • S503AB



[Back to Top](#)

CL-MIS-TUB • AMA PRA Category 1 Credit TM:0.5

CL-MIS-TU1B • Peptide-decorated Microbubbles for Ultrasound Molecular Imaging: Translatable Preparations for VCAM-1 and AVB3 Detection on Tumor Vascular Endothelium

Sunil Unnikrishnan MS ; **Zhongmin Du** PhD ; **Galina Diakova** MS ; **Alexander L Klivanov** PhD (Presenter) *

PURPOSE

Targeted microbubbles are investigated as promising ultrasound molecular imaging agents. A simple and efficient procedure for microbubble preparation and covalent attachment of targeting ligands is crucial for rapid translation to clinical use.

METHOD AND MATERIALS

Microbubbles were prepared by amalgamation in a sealed vial with perfluorobutane gas headspace and aqueous saline/propyleneglycol micellar dispersion of DSPC, PEG stearate and peptide-PEG-DSPE (1:1.1:0.2 mass ratio). For VCAM-1 targeting, VHPKQHRGGSK(FITC)GC-PEG3400-DSPE was synthesized by reacting C-terminal cysteine thiol with maleimide-PEG-DSPE. For the formulation of $\alpha\text{v}\beta_3$ integrin-targeted bubbles, cycloRGDFK or control cycloRADfK were reacted with NHS-PEG3400-DSPE. In vitro microbubble targeting was investigated in a flow chamber (1 dyn/cm²) in an $\alpha\text{v}\beta_3$ -coated dish or albumin control. In vivo targeting was tested in a subcutaneous murine tumor model (C57BL/6, MC38, J. Schlom, NIH). Contrast ultrasound imaging (7 MHz, CPS mode) of the tumor and contralateral hindleg muscle was performed simultaneously 10 min after iv bolus of 2.10⁷ microbubbles.

RESULTS

Fluorescence spectroscopy of FITC-peptide-lipid conjugate confirmed high efficacy (>85 %) of peptide transfer from aqueous micellar media to the bubble shell. Peptide-targeted (but not control) microbubbles selectively adhered to receptor-coated but not control surfaces in a flow chamber in vitro. CycloRDGFK-microbubbles, but not control cyclo-RADfK-microbubbles, bound to $\alpha\text{v}\beta_3$ surface (p

CONCLUSION

A simple and efficient procedure for the preparation of peptide-targeted microbubbles for molecular imaging studies was developed. VCAM-1-targeted and $\alpha\text{v}\beta_3$ -targeted microbubbles, but not control microbubbles, selectively accumulated in murine tumor vasculature.

CLINICAL RELEVANCE/APPLICATION

Peptide-microbubbles are useful probes for tumor vasculature biomarker molecular imaging, formulated from FDA DMF-list materials. Rapid bedside preparation ensures efficient clinical translation.

CL-MIS-TU2B • Standardized Comparison of Glucose Metabolism and Late Gadolinium-enhancement in Patients with Acute Myocardial Infarction Using Parametric Polar Maps in Cardiac PET/MRI

Felix Nensa MD (Presenter) ; **Thorsten D Poeppel** ; **Ercan Tezgah** ; **Philipp Heusch** MD ; **Kai Nassenstein** ; **Thomas W Schlosser** MD

PURPOSE

To design and implement a method for quantification and comparison of myocardial ¹⁸F-FDG uptake and late gadolinium-enhancement (LGE) in cardiac PET/MRI and to assess its feasibility in patients with acute myocardial infarction (AMI).

METHOD AND MATERIALS

Volumetric PET data and segmented 2D inversion recovery Turbo-FLASH sequences for the assessment of myocardial LGE in contiguous short-axis views were simultaneously acquired on an integrated 3 Tesla PET/MRI system in 10 patients with AMI. PET data was resampled to match the slice thickness and orientation of the LGE images using OsiriX imaging software (OsiriX Foundation, Geneva, Switzerland). The left ventricular myocardium (LVM) was delineated in LGE images and the resulting regions of interest were transferred to the corresponding PET images. LVM areas showing LGE were detected using an automated thresholding algorithm. Cylindrical sampling perpendicular to the long-axis was performed in all PET and LGE slices (100 segments/slice). The fraction of enhancing myocardium was

calculated for each segment in LGE images. The mean standardized uptake values (SUV_{mean}) were calculated for each segment in PET images and normalized with the maximum standardized uptake value (SUV_{max}) of the entire left ventricle. The sampled data was mapped to color space using lookup tables and rendered into polar coordinate system plots. Segment wise inter-method correlation was calculated using weighted Spearman's rank correlation ?. Binary inter-method agreement in infarct delineation was calculated using Cohen's ?.

RESULTS

The software successfully produced visually conclusive LGE and PET polar plots in all examinations. A negative segment wise correlation between LGE fraction and SUV_{mean} with moderate to good correlation coefficients (?: -0.47 to -0.74) was found. Binary inter-method agreement was substantial (=?=0.63) to very good (=?=0.81).

CONCLUSION

A new software for the standardized and semi-automatic translation of image data from two inherently different cardiac imaging modalities into a unified data representation was created. This enables consistent and reproducible comparison of LGE and PET on a visual and quantitative level in simultaneously acquired PET/MRI data.

CLINICAL RELEVANCE/APPLICATION

The introduction of cardiac imaging on integrated PET/MR devices requires new tools allowing for the cohesive interpretation of PET and MR images based on a unified data representation.

CL-MIS-TU3B • Patterns of MR Dynamic Susceptibility-weighted Contrast Enhanced MR Perfusion Imaging and Diffusion Tensor Imaging in Patients with Progressive/Recurrent Glioblastomas after Bevacizumab Treatment

Xiang Liu MD (Presenter) ; **Wei Tian** MD, PhD ; **Ali H Hussain** MD, FRCR ; **Sven E Ekholm** MD

PURPOSE

Bevacizumab-induced MRI changes are still full of conflicting controversies, including findings of advanced imaging techniques of MR dynamic susceptibility-weighted contrast enhanced MR perfusion imaging (DSC-PWI) and diffusion imaging. The purpose of this study was to evaluate patterns of DSC-PWI and diffusion tensor imaging (DTI) in patients with progressive/recurrent glioblastomas after Bevacizumab treatment.

METHOD AND MATERIALS

52 cases with pathology or radiological confirmed progressive/recurrent glioblastomas after Bevacizumab treatment were reviewed. Serial DSC-PWI and DTI examinations were performed after Bevacizumab treatment. The maximal rCBV ratios and minimal apparent diffusion coefficient (ADC) value in the examinations when the glioblastomas presenting minimal enhancement after Bevacizumab treatment and recurrence/progression were evaluated.

RESULTS

The mean maximal rCBV ratio of reference in glioblastomas after Bevacizumab treatment was 1.65 ± 0.52 ; there were 41 patients with the mean maximal rCBV ratio of recurrent/progressive glioblastomas was significant higher, 6.11 ± 4.58 , p value of paired t test was 0.013. There were 11 patients whose maximal rCBV ratio at recurrence/progression was relative lower, 1.26 ± 0.29 , without significant difference compared to reference, $p = 0.71$. All patients showed new restricted diffusion after Bevacizumab treatment. The mean minimal ADC value of reference was 0.49 ± 0.17 , the mean minimal ADC value of 41 and 11 patients at recurrence/progression were 0.63 ± 0.19 and 0.71 ± 0.57 respectively, and there was no significant difference compared to reference, p value of 0.22 and 0.09 respectively.

CONCLUSION

There are different patterns of MR PWI/DTI changes in recurrent/progressive glioblastomas after Bevacizumab treatment. Combing multiple imaging biomarkers is necessary for imaging interpretation.

CLINICAL RELEVANCE/APPLICATION

Understanding patterns of MR PWI/DTI changes in patients with recurrent/progressive glioblastomas after Bevacizumab treatment is important for imaging diagnosis and clinical management.

CL-MIS-TU4B • 1HMRS Characteristics of Cerebral Alveolar Echinococcosis

Jian Wang (Presenter)

PURPOSE

Purpose: To evaluate the 2D multi-voxel proton magnetic resonance spectroscopy (1HMRS) Characteristics in patients with Cerebral Alveolar Echinococcosis (CAE).

METHOD AND MATERIALS

RESULTS

CONCLUSION

Multi-voxel 1HMRS can reflect pathological characteristics of CAE. 1HMRS provides metabolic information for diagnosis of CAE and may be a necessary supplement of routine magnetic resonance examination.

CLINICAL RELEVANCE/APPLICATION

Molecular Imaging - Tuesday Posters and Exhibits (12:45pm - 1:15pm)

Tuesday, 12:45 PM - 01:15 PM • Lakeside Learning Center



[Back to Top](#)

LL-MIS-TUB • AMA PRA Category 1 Credit™:0.5

Molecular Imaging (Neurosciences)

Tuesday, 03:00 PM - 04:00 PM • S504CD



[Back to Top](#)

SSJ15 • AMA PRA Category 1 Credit™:1 • ARRT Category A+ Credit:1

Moderator

Satoshi Minoshima, MD, PhD *

Moderator

Peter Herscovitch, MD

SSJ15-01 • Development and In Vivo Assessment of an Optimized EGFR Targeted PET Probe for Glioma Imaging

Eric Wehrenberg-Klee MD (Presenter) ; **Navid Redjal** MD ; **Alicia Leece** ; **Pedram Heidari** MD ; **Nafize S Turker** PhD ; **Khalid**

PURPOSE

Distinguishing true progression of glioblastoma multiforme (GBM) from pseudoprogression after surgery with chemoradiation is quite challenging using current imaging techniques. EGFR is overexpressed on 40% of GBMs, and we hypothesized that targeted imaging could provide a novel mechanism for distinguishing recurrence from pseudoprogression in the large fraction of patients with confirmed baseline EGFR expression. We developed and preclinically tested a novel PET probe, ^{64}Cu -DOTA-EGFR F(ab)'₂, for direct tumor imaging based on EGFR expression, with optimized pharmacokinetics for clinically translatable PET imaging.

METHOD AND MATERIALS

An EGFR-specific imaging probe, ^{64}Cu -DOTA-EGFR F(ab)'₂ was developed with F(ab)'₂ fragmentation and chelator conjugation of a humanized monoclonal antibody to EGFR. Probe affinity was assessed using Ga-67 labeling and saturation binding studies with EGFR positive A345 cells. For in-vivo studies, Gli-36, an EGFR expressing GBM cell line transfected to express luciferase, was used. Nude (nu/nu) mice were injected intra-cranially with 5×10^4 Gli-36 cells. Prior to PET imaging, tumor growth was confirmed with bioluminescence. In vivo agent kinetics were established by imaging (n=3) mice at 4, 8, 16, and 22h after injection of 100 uCi of ^{64}Cu -DOTA-EGFR F(ab)'₂. Blocking studies were performed by injecting mice (n=3) with escalating doses of cetuximab 24h prior to agent administration.

RESULTS

CONCLUSION

Specific PET imaging of glioblastoma multiforme tumors that express EGFR is possible using the kinetically optimized novel PET imaging agent ^{64}Cu -DOTA-EGFR F(ab)'₂.

CLINICAL RELEVANCE/APPLICATION

A direct EGFR specific imaging agent for GBM tumors expressing EGFR may be able to confidently distinguish true progression from pseudoprogression, sparing patients the high surgical risks of biopsy.

SSJ15-02 • EGFR MAb-bioconjugated Superparamagnetic Iron Oxide Nanoparticles as a Specific MRI Contrast Agent for Detection of Brain Glioma In Vivo

Wenzhen Zhu MD, PhD (Presenter) ; Shun Zhang ; Ketao Mu PhD

PURPOSE

Superparamagnetic iron oxide nanoparticle (SPIONs) delivery system has become a model system in which to study the target molecule-specific biodistribution, rapid excretion and undesired side-effects using in vivo small animal MRI. As a cellular transmembrane receptor, EGFR regulates important cellular processes and is linked to a poor prognosis in various human cancers. In this study, we developed a potentially valuable new targeted nanocarrier based on SPIO delivery system, EGFRmAb-bioconjugated nanoparticles (EGFRmAb-SPIONs). The purpose of this study was to elucidate strategies for further improvement of this promising approach.

METHOD AND MATERIALS

EGFRmAb-SPIONs were prepared and characterized. The preferential accumulation of the EGFRmAb-SPIONs within gliomas and subsequent MRI contrast enhancement were demonstrated in vitro in C6 cells and in vivo in tumors of rat model. MRI scanning was performed using a 3.0T MRI scanner and a research coil insert designed specifically for imaging rats was used to MRI

RESULTS

The average particle size of about 10.21 nm, hydrodynamic diameter of about 161.5 nm, saturation magnetization of 55 emu/g Fe and T₂ relaxivity of 92.73 s⁻¹mM⁻¹ of the EGFRmAb-SPIONs suggested its applicability for MRI. MR T₂WI of iron uptake in C6 cells treated with the nanoparticles (EGFRmAb-SPIONs and SPIONs) of various iron concentrations were shown. This result demonstrated that EGFRmAb-SPIONs could efficiently and specifically label the C6 cells compared to SPIONs. Using a rat model of C6 glioma, EGFRmAb-SPIONs provided a better picture or more sensitivity to depict brain glioma on MR images than that of SPIONs. Significantly enhanced T₂-weighted images of brain glioma were documented in vivo with EGFRmAb-SPIONs until 48h after injection. The results from cytotoxicity, histopathology and blood toxicity assays suggested that the EGFRmAb-SPIONs had good biocompatibility and exhibited no toxicity.

CONCLUSION

EGFRmAb-SPIONs could be specifically and efficiently uptaken by C6 glioma cells, and selectively improve the detection of tumor by MRI; it could produce the remarkable contrast change of brain glioma in vivo following intra-carotid administration of EGFRmAb-SPIONs.

CLINICAL RELEVANCE/APPLICATION

EGFRmAb-SPIONs is suitable for use as negative MRI contrast agent, and had good biocompatibility and exhibited no toxicity, which was very important for the clinical application.

SSJ15-03 • Imaging Biomarker Evaluation of Cytoskeletal Stabilization Therapy for Traumatic Brain Injury

Donna J Cross PhD (Presenter) * ; Rodney Ho PhD * ; Todd L Richards PhD ; Vasily L Yarnykh PhD ; Greg Garwin ; Pierre Mourad ; David Cook ; Satoshi Minoshima MD, PhD *

PURPOSE

Currently, there is no effective pharmacological intervention to improve outcome in traumatic brain injury (TBI). The goal of this study is to evaluate a microtubule-stabilizing drug as a therapeutic intervention following TBI using neurological assessments and MR imaging biomarkers in a rodent model.

METHOD AND MATERIALS

Subjects, (C57BL6 mice, n=12, 10wks) had craniotomy plus controlled cortical impact (CCI) surgery under isoflurane anesthesia, (Leica Biosystems, Richmond, IL), followed by 200 ug/kg paclitaxel (n=6) or vehicle (n=6) applied to the brain injury site. Sham surgery (craniotomy no CCI) was performed on controls (n=3). At 2 days post surgery, subjects had gait assessment by CatWalk automated gait analysis (Noldus Information Tech, The Netherlands) followed by high-tesla MR imaging (14T MR Avance III Ultrashield, Bruker BioSpin, Billerica, MA). T₁-weighted and quantitative T₂ maps were obtained: MDEFT, FA:12°, TR:5000ms, TE:1.9ms, resolution 0.140x0.140x0.25mm³, 64 slices and, T₂ map: TR=2000ms, 16 echoes, spacing:6.7ms, TE 1: 6.7ms, TE 2: 13.4ms, resolution 0.12x0.12x1.0mm³, 15 slices. Manual VOI analysis of lesion volume and volume of edema related to injury was performed.

RESULTS

Lesion analysis on T₂ and T₁ images, blinded to therapeutic regimen, indicated 20% reduction in volume with paclitaxel treatment (9.96±2.3 versus 7.94±1.5mm³, p=0.05) and hyperintense voxels (edema) on quantitative T₂ maps were reduced 26% (11.92±3.0 versus 8.86±2.2mm³, p=0.05). Paclitaxel resulted in improved gait (computer-recorded objective analysis) for maximum print area (0.38±0.09 versus 0.29±0.08cm², p=0.05) and mean intensity (79.45±14.26 versus 66.38±5.52, p=0.05) over vehicle group.

CONCLUSION

The results indicate that administering drugs to stabilize axonal cytoskeleton following TBI improves outcome in neurological/gait assessment, also demonstrated as improvement on MR imaging biomarkers. This improvement appears to be mediated by reductions in size of lesion and corresponding post-injury edema. Evaluations of structural integrity on DTI and myelin degradation with magnetization transfer as well as western blot protein analysis are ongoing to better characterize the mechanisms of improved outcome after treatment.

CLINICAL RELEVANCE/APPLICATION

This study provides evidence of the efficacy for microtubule-stabilizing drugs to improve outcome following traumatic brain injury and

imaging assessment that can be translated to patient evaluation.

SSJ15-04 • Dual-modality Imaging of Exogenous Endothelial Progenitor Cells in Ischemic Stroke Mouse

Ying Ying Bai (Presenter) ; Sheng Hong Ju MD, PhD

PURPOSE

The objective was to noninvasively visualize the homing, migration and differentiation of exogenous EPCs in vivo using a dual-modality imaging probe, and to examine the effect of transplanted EPCs on the recovery of ischemic stroke.

METHOD AND MATERIALS

Bone-marrow derived EPCs were labeled with a multifunctional probe modified with gadolinium, Cy5.5 and rhodamine. EPCs(5×10^5) were transplanted via ipsilateral internal carotid artery into cortical ischemia mice induced by photothrombosis. Magnetic Resonance(MR) and near-infrared(NIR) optical imaging were performed at different time points. The infarct areas were determined by T2WI-MR and behavioral deficits were detected with cylinder tests, foot-fault tests and mNSS scores. The microvessel density, proliferation of immature neural cells and cell apoptosis were evaluated by immunofluorescence. Moreover, the expression of cytokines and related proteins during EPCs therapy in stroke area was detected by Western blot analysis.

RESULTS

After transplantation, the signal intensity enhancement was observed in stroke area on NIR imaging starting on day 1 and in perilesion region on MR imaging starting on day 3. The signal intensity reached their peak on day 5 in both imaging methods. Compared with unlabeled EPCs group, the fluorescent signal intensity had a remarkable increase from day 3 to 7(p

CONCLUSION

Exogenous EPCs can be detected non-invasively on both MR and NIR imaging by using this probe. Transplanted EPCs could home to the ischemic-angiogenic region and promotes stroke recovery. The paracrine effects of EPCs in ischemia area may contribute to angiogenesis and neurogenesis.

CLINICAL RELEVANCE/APPLICATION

EPCs treatment at 24 hours after the stroke onset when thrombolytic therapy doesn't work may promote the recovery of ischemic stroke patients.

SSJ15-05 • Axonal Degeneration in Alzheimer Disease: Functional Investigation with Dynamic Manganese-enhanced MR Imaging

Christopher A Potter MD (Presenter) ; Nathalie M Martin BA ; Greg Garwin ; Yoshimi Anzai MD ; Satoshi Minoshima MD, PhD * ; Donna J Cross PhD *

PURPOSE

Axonal dysfunction is an early feature of Alzheimer disease (AD). Research implicates altered axonal transport as a possible cause. We hypothesize that the axonal transport rate in the olfactory tracts will decrease with age in triple transgenic AD mice.

METHOD AND MATERIALS

2 groups of triple transgenic AD model and wild-type mice were imaged on a 14T Bruker MR magnet at 1.5 months, prior to pathology and at 5 months of age, after synaptic dysfunction, A-beta plaque, neurofibrillary tangle formation and axonal degeneration. Unilateral intranasal injection of MnCl₂ was administered. Mice were scanned dynamically using MDEFT (Modified Drive Equilibrium Fourier Transform) sequence for 45 min at 1 hour post MnCl₂ (TR/TE: 5000ms/1.9ms, resolution 0.140 x 0.140 x 0.25mm³) and again at 4 hours post for 60 min. Image processing was performed stereotactically in 3D atlas space (NEUROSTAT, UW Seattle) and pixel intensity normalized globally. VOI was used to measure average signal intensity change in the olfactory bulb. Uptake and rate of transport were estimated.

RESULTS

CONCLUSION

Compared with wild type mice, axonal transport significantly decreases in AD Tg mice as they age and develop known AD pathology. Although there is mild decrease in uptake and transport in aged WT mice, there is a significantly greater axonal transport decrease in AD Tg mice.

CLINICAL RELEVANCE/APPLICATION

Investigation of axonal transport provides critical insights into pathogenesis of AD and facilitates new imaging developments that can be applied in the clinic.

SSJ15-06 • Molecular Magnetic Resonance Immunoradiology Reveals Novel Effect of Interferon- β on Myeloid Cells in Murine Multiple Sclerosis

Benjamin Pulli MD (Presenter) ; Gregory R Wojtkiewicz MSc ; Lionel A Bure MD ; Muhammad Ali MBBS ; John Chen MD, PhD *

PURPOSE

Conventional contrast-enhanced MRI measures blood-brain-barrier breakdown, but not necessarily inflammation. We hypothesized that MPO-Gd (bis-5HT-DTPA-Gd), a molecular MRI probe sensitive and specific for the inflammatory enzyme myeloperoxidase (MPO), can detect therapeutic effects of Interferon- β (Ifn- β), a current first-line drug in MS and reveal changes in the immune response.

METHOD AND MATERIALS

Thirty-three female SJL mice were injected with proteolipid protein (PLP) to induce experimental autoimmune encephalomyelitis, a mouse model of MS, and treated with either Ifn- β (1 μ g/day) or saline. To determine effects of Ifn- β on MPO, mice underwent MRI at 4.7T with MPO-Gd at the disease peak (day 12). Lesion volumes and CNR at 10 and 60 minutes post MPO-Gd injection were quantified. MPO activity assay and MPO secretion experiments were performed.

RESULTS

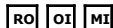
Disease severity was ameliorated with Ifn- β (p < 0.05; **figure, D**). Since Ifn- β is known to affect lymphocytes, we expected to see fewer lesions but not changes to MPO activity. Indeed, MPO-Gd enhanced MRI showed a smaller total (p < 0.05) and mean (p < 0.01) lesion volume with Ifn- β compared to saline (**A+B**). Surprisingly, while CNRs of lesions at 10 minutes post MPO-Gd injection, which mostly reflect blood-brain-barrier breakdown were similar (p = 0.47), CNRs at 60 minutes post injection, which reflect MPO activity, were significantly lower with Ifn- β treatment (p < 0.01; **A+B**). Lesion-by-lesion quantification confirmed these findings (p = 0.06 for 10 minutes and p < 0.001 for 60 minutes post MPO-Gd injection; **C**). Brain homogenates from mice treated with Ifn- β had markedly reduced MPO activity (p < 0.01; **E**), validating the imaging findings. Myeloid cells showed less MPO secretion when incubated with Ifn- β (p < 0.05; **F**), but Ifn- β did not directly inhibit MPO activity (p = 0.93; **G**).

CONCLUSION

Our results revealed a new mechanism: Ifn- β directly acts on myeloid cells to decrease MPO secretion, contributing to the efficacy of this widely used drug. MPO-Gd enhanced MRI can detect inhibition of MPO secretion by Ifn- β non-invasively. This study also demonstrated the unique capability of molecular imaging to probe immunology *in vivo*.

CLINICAL RELEVANCE/APPLICATION

Upon translation, MPO-Gd molecular imaging could be used to monitor treatment efficacy of Ifn- β and similar drugs in MS patients.

**SSK12 • AMA PRA Category 1 Credit™:1.5 • ARRT Category A+ Credit:1.5****Moderator****David A Mankoff**, MD, PhD**Moderator****Michael S Gee**, MD, PhD**SSK12-01 • Molecular Imaging Keynote Speaker: Molecular Imaging and Biomarkers in Cancer****David A Mankoff** MD, PhD (Presenter)**SSK12-02 • Molecular Ultrasound Imaging Using Microbubbles Targeted to Endoglin, VEGFR2 and Integrin****Ingrid Leguerney** (Presenter) ; **Jean-Yves Scoazec** ; **Laure D Boyer** ; **Nicolas Gadot** ; **Sandraa Robin** ; **Nathalie B Lassau** MD, PhD ***PURPOSE**

The aim of this study was to investigate the use of targeted contrast-enhanced high-frequency ultrasonography for molecular imaging to determine the expression levels of endoglin, α_v integrin and vascular endothelial growth factor receptor 2 (VEGFR2) biomarkers in murine melanoma tumor models.

METHOD AND MATERIALS

Melanoma-bearing nude mice (B16F10) were explored using dynamic contrast-enhanced ultrasonography with a VEVO2100 imaging system (Visualsonics, Canada). Microvasculature and expression levels of biomarkers were investigated at 20 MHz using specific contrast agents (CA) (MicroMarker™, Visualsonics). The lyophilized CA were conjugated with biotinylated rabbit anti-mouse endoglin, α_v integrin and VEGFR2 monoclonal antibodies. Specificity of these functionalized CA was evaluated in comparison with an isotope control antibody (immunoglobulin G) which was bounded on the surface of the CA. Boluses injections of each targeted CA were performed and ultrasound signal intensity from bounded CA was evaluated on the different groups of mice. Two groups of mice were evaluated, control and treated with sorafenib with a daily dose of 62 mg/kg. Tumor samples were harvested for analysis of endoglin, integrin and VEGFR2 expression levels by immunohistochemistry.

RESULTS

The mean ultrasound signal intensity amplitude caused by backscatter of the retained endoglin/integrin/VEGFR2-targeted ultrasound CA after fixation into the vasculature was assessed. Endoglin biomarkers were more expressed than α_v integrin and VEGFR2 in the tumor model. Endoglin tend to increase with time in the control group whereas a decrease in the level expression was observed in the sorafenib group between D0 and D3. These differences in biomarkers expression were also observed by immunostaining.

CONCLUSION

Targeted ultrasound CA coated with antibodies enable in vivo molecular imaging of biomarkers expression on the tumor vascular endothelium and may be used for noninvasive evaluation of tumor angiogenesis during growth or therapeutic treatment in preclinical studies. Endoglin protein which plays an important role in angiogenesis seems to be a target of interest for detecting cancer and for predicting therapy efficacy.

CLINICAL RELEVANCE/APPLICATION

Being able to propose to most appropriate therapy depending on biomarkers expression

SSK12-03 • Radiolabeled Antibody to gp41 HIV Glycoprotein Kills ART-treated Lymphocytes from HIV Patients and HIV-infected Monocytes in Human Blood Brain Barrier Model**Ekaterina Dadachova** PhD (Presenter) ; **Dina Tsukrov** ; **Alicia McFarren****PURPOSE**

Eliminating virally infected cells is an essential component of HIV eradication strategy. In addition, many patients on antiretroviral therapy (ART) suffer from HIV-associated neurocognitive disorders as the brain becomes a reservoir for infection. Thus, the drugs that can enter into the CNS and eradicate the infection are needed.

METHOD AND MATERIALS

Radioimmunotherapy (RIT), a clinically established method to kill cells using radiolabeled monoclonal antibodies (mAbs), was recently used to target the HIV gp41 glycoprotein expressed on the surface of infected cells. As gp41 expression by the infected cells is downregulated in patients on ART, we evaluated the ability of RIT to kill infected cells treated with ART in vitro using patients lymphocytes. We also tested the ability of the same radiolabeled mAb 2556 to gp41 to cross the blood brain barrier (BBB) and kill HIV infected monocytes in the CNS.

RESULTS

We found that RIT was able to specifically kill ART-treated lymphocytes and to reduce HIV p24 to undetectable levels. ART and RIT worked in concert to decrease viral production when compared to ART or RIT alone, indicating that expression of gp41 under ART was still sufficient to allow 2556 mAb binding and killing infected cells. A 4 μ Ci dose of 213Bi-2556 successfully killed over 80% of PBMCs (p9 compared to isotype control 1418 mAb pI of 8. 213Bi-2556 killed significantly more HIV infected than uninfected monocytes on the astrocyte side of the BBB in dose response manner (p

CONCLUSION

In conclusion, RIT in concert with ART eliminated infected cells. Co-treatment was effective in both Atripla and tenofovir/emtricitabine/atazanavir cohorts. We demonstrated the unique ability of 213Bi-2556 mAb to cross the BBB and specifically kill HIV infected monocytes. These findings demonstrate the feasibility of an RIT-based strategy for use with ART to achieve HIV eradication systemically and in CNS.

CLINICAL RELEVANCE/APPLICATION

HIV/AIDS remains an incurable disease. Our goal is to develop RIT-based strategies for therapy of systemic and CNS HIV for use with other anti-retroviral strategies to achieve complete HIV eradication

SSK12-04 • Early Multi-modal Tumor Perfusion Monitoring upon Anti-vascular tTF-NGR Therapy by USPIO-MRI, CE-US, SPECT, and FRI**Thorsten Persigehl** MD (Presenter) ; **Janine Ring** ; **Sven Hermann** ; **Wolfgang E Berdel** ; **Walter L Heindel** MD ; **Rolf Mesters** ; **Christoph B Bremer** MD ; **Christian Schwoppe****PURPOSE**

The purpose of this study was to investigate multi-modal USPIO-enhanced MR imaging (MRI), contrast-enhanced Ultrasound (CE-US), 123I-tTF-NGR-SPECT, and Fluorescence Reflectance Imaging (FRI) for early monitoring of anti-vascular treatment effects of the thrombogenic tTF-NGR protein with a specific binding to CD13 on tumor endothelial cells.

METHOD AND MATERIALS

Fibrosarcoma (HT1080) bearing nude mice (n=12/12/14) were injected with the thrombogenic tTF-NGR with and without earlier blocking

of CD13 by pure NGR peptide (GNGRAHA), or saline as control respectively. USPIO-enhanced MRI for determination of the relative blood volume (rBV), 123I-tTF-NGR-SPECT, and FRI for fluorescence imaging of Alexa-Fluor647-labelled fibrinogen were acquired about 4-8 hours after treatment initiation. CE-US was performed during and within 30 minutes after tTF-NGR application. Treatment response and blocking effectiveness were analyzed by histological grading of vascular thrombosis and/or necrosis (score: 0-5).

RESULTS

CONCLUSION

Multi-modal USPIO-MR, CE-US, SPECT, and FR imaging allow an early complementary assessment of treatment efficacy of the thrombogenic vascular targeting agent tTF-NGR.

CLINICAL RELEVANCE/APPLICATION

This study demonstrates the feasibility of a complementary early multi-model monitoring of anti-vascular therapies for better understanding of the molecular mechanism of action.

SSK12-05 • Whole-body Diffusion-weighted MRI with ADC Mapping in Patients with Diffuse Large B Cell and Hodgkin Lymphoma at Staging and during Treatment

Sarah M Toledano-Massiah (Presenter) ; **Emmanuel Itti** MD ; **Alain Luciani** MD, PhD * ; **Violaine Safar** ; **Sandrine Katsahian** ; **Chieh Lin** MD ; **Bertrand Bresson** ; **Anais Charles-Nelson** ; **Karim Belhadj** ; **Jehan Dupuis** ; **Pierre Zerbib** ; **Benhalima Zegai** ; **Julien Moroch** ; **Michel Meignan** MD, PhD ; **Corinne Haioun** MD ; **Alain Rahmouni** MD

PURPOSE

Evaluation of whole body diffusion weighted MRI (WB-DW-MRI) using apparent diffusion coefficient (ADC) parametric images for staging and response assessment in diffuse large B-cell lymphoma (DLBCL) and Hodgkin lymphoma (HL) by comparison with PET/CT as the reference standard.

METHOD AND MATERIALS

27 consecutive patients presenting with newly diagnosed DLBCL (n=15) and HL (n=12) prospectively underwent both WB-DW-MRI and 18-F FDG-PET/CT at staging, after 2 cycles of chemotherapy (26 patients at interim) and at the end of treatment (23 patients at closure). WB-DW-MRI analysis included size and visual ADC analysis - more or less restricted than muscle-, for the 23 defined nodal regions and the 6 defined organs allowing Ann Arbor staging at baseline and for response assessment. PET/CT data were analyzed using Deauville international criteria. WB-DW-MRI and PET/CT images were both independently analyzed by a junior and a senior reader. The baseline stages and the interim and closure responses based on WB-DW-MRI and PET/CT were compared. Agreement between junior and senior readings were compared on a per-site basis (Kappa).

RESULTS

At baseline, Ann Arbor stages were concordant between WB-DW-MRI and PET/CT in 22 patients: 4 patients were understaged on WB-DW-MRI because of overlooked lung (n=2), iliac node (n=1), and bowel involvement (n=1); one was overstaged (bone marrow involvement). Using size criteria, WB-DW-MRI and PET/CT showed concordant responses in 12/26 patients at interim and in 18/24 patients at closure; with combined size and visual ADC analysis, WB-DW-MRI was concordant with PET/CT in 19/26 patients at interim and in 21/23 patients at closure. At closure, only 1 patient had persistent low ADC with no abnormal uptake on PET/CT, and 1 patient had abnormal FDG uptake not detected on MRI (mediastinal mass). Interobserver agreement for PET/CT reading ranged 0.63-0.70 (good) while for WB-DW-MRI reading the range was 0.86-0.96 (excellent).

CONCLUSION

WB-DW-MRI with ADC mapping is a potentially valuable technique for initial staging, interim and final response assessment, with excellent interobserver agreement.

CLINICAL RELEVANCE/APPLICATION

Our study opens a path towards the use of WB-DW-MRI with ADC mapping complementary to PET/CT in lymphoma patient care; these results should be confirmed in a larger population.

SSK12-06 • A Hybrid Radioactive and Fluorescent Tracer for Sentinel Node Biopsy in Melanoma Patients

Nynke S Van Den Berg MSc ; **Gijs Kleinjan** MD ; **Martin Klop** ; **Omgo Nieweg** ; **Renato Valdes Olmos** ; **Fijs Van Leeuwen** (Presenter)

PURPOSE

The purpose of this study was to explore the value of the hybrid tracer indocyanine green (ICG)-99mTc-nanocolloid for the sentinel biopsy in a large cohort of melanoma patients. A comparison was made with optical detection of blue dye (conventional approach).

METHOD AND MATERIALS

One-hundred-and-four patients with melanoma of the head and neck (n=53), trunk (n=33) or an extremity (n=18) were evaluated. Lymphoscintigraphy with subsequent SPECT/CT was performed after intradermal administration of ICG-99mTc-nanocolloid. The operation was performed 3-27 hours after tracer injection. Patent blue dye was injected prior to the start of surgery, except in patients with a melanoma in the face (n=35). Intraoperatively, sentinel nodes were pursued via gamma ray tracing, followed by optical verification using fluorescence and/or blue dye. A portable gamma camera was used to confirm removal of all radioactive sentinel nodes.

RESULTS

Preoperative imaging revealed at least one sentinel node in all patients. Intraoperatively, in 17 patients (16%) a sentinel node could only be localized using fluorescence imaging; these sentinel nodes were mainly located near the injection site or in the parotid area. Of all harvested sentinel nodes (n=300), 97% of sentinel nodes exhibited fluorescence intraoperatively. In the patients in whom blue dye was used, only 60% of sentinel nodes were stained blue at the time of excision (p

CONCLUSION

ICG-99mTc-nanocolloid allowed for preoperative lymphoscintigraphy and SPECT/CT imaging as well as intraoperative radio- and fluorescence-guided sentinel node detection in all 104 included patients. Optical fluorescence-based identification of the sentinel node was particularly useful in head and neck melanoma with nodes located close to the injection site and/or in the parotid area.

CLINICAL RELEVANCE/APPLICATION

Fluorescence imaging, in addition to the conventional radioguided approach, may allow the accuracy with which sentinel nodes can be removed, possibly improving the false-negative rates.

SSK12-07 • Novel Fluorescent Nanoparticle Imaging Allows Non-invasive Assessment of Immune Cell Modulation within the Esophageal Tumor Microenvironment

Peiman Habibollahi MD (Presenter) ; **Todd Waldron** ; **Pedram Heidari** MD ; **Hoon Sung Cho** ; **David Alcantara** PhD ; **Timothy C Wang** ; **Anil Rustgi** ; **Umar Mahmood** MD, PhD

PURPOSE

Repeat endoscopic imaging combined with administration of fluorescent nanoparticles highly phagocytized by subpopulations of immune cells in the tumor microenvironment allows for their temporal evaluation. We employed this approach to understand changes in the myeloid derived suppressor cell (MDSC) immune cell subpopulation, a central modulator of tumor initiation and progression.

METHOD AND MATERIALS

A novel imaging probe (FH-CyAL5.5) was developed based on Feraheme, a monocrysaline dextran coated iron oxide nanoparticle, conjugated to a near infrared (NIR) fluorochrome, CyAL5.5. Two groups of L2Cre;p120ctnflox/flox mice (n=5 each), a transgenic mouse

model of esophageal squamous cell carcinoma, were imaged simultaneously for white light and fluorescent NIR signal using a custom-built dual channel upper GI endoscope 3 hrs after receiving the imaging probe, with or without dexamethasone (dex) pretreatment. Immune cell modulation was quantified by means of immunophenotyping (FACS), confocal microscopy and compared to the signal intensity during fluorescent endoscopy.

RESULTS

A high level of uptake of the fluorescent nanoparticles was observed in the esophageal lesions of L2Cre;p120ctnflox/flox mice which significantly decreased after dex treatment (TBR 2.65 ± 0.15 vs. 1.98 ± 0.09 , p

CONCLUSION

These observations suggest that FH-CyAL5.5 is highly taken up by the MDSC immune cell component of the esophageal tumor microenvironment and can be used for assessment of specific immune cell modulation in response to targeted or non-targeted therapies.

CLINICAL RELEVANCE/APPLICATION

This translatable technology may be used for the early detection of dysplastic changes as well as the serial assessment of immune-modulatory therapy in the esophageal tumor microenvironment.

SSK12-08 • 18F-fluorocholine PET/CT Detecting Prostate Cancer Recurrence: Is Dual-phase Imaging Really Beneficial?-Singapore Experience

Aaron K Tong MBBS, MRCP ; **Zoe X Zhang** PhD ; **Sean X Yan** MD (Presenter)

PURPOSE

In the last decade, choline PET/CT scan has been evaluated in diagnosing prostate cancer, particularly recurrence. The ability of choline PET /CT to detect prostate cancer recurrence may be enhanced by dual-phase acquisition presumably due to the different kinetics of choline in cancer tissue and in benign tissues. However, for this young imaging modality, the optimal protocol and the added value of performing dual-phase scan are still debatable. This study aimed to better define the imaging protocol for 18F-fluorocholine PET/CT.

METHOD AND MATERIALS

A total of 34 patients with suspected prostate cancer recurrence were scanned during the period of 04/2010 to 02/2013 in our hospital and were followed up for an average of 16 months. Final diagnosis was made on biopsy, correlating with other imaging modalities, PSA trend and clinical course. Each patient was given 5-10 mCi 18F-fluorocholine. Immediate acquisition (early phase, 20 min post injection) of the pelvis and subsequently whole body acquisition (late phase, 30 min post injection) were performed. Two blinded physicians read the scans independently with final consensus achieved in all cases. Standard Uptake Value (SUV) in the dominant lesions was recorded. Statistical analysis was done by SPSS program.

RESULTS

The accuracy of 18F-fluorocholine PET/CT for diagnosing prostate cancer recurrence was 85% with sensitivity of 81% and specificity of 100%. Uptrend change of SUV on the late phase vs early phase was significantly associated with recurrent cancer (P=0.05). The PSA level is closely associated not only with the likelihood of a positive scan (P=0.001), but also with the SUV (R²=0.51, P=0.000) and the change in SUV between two phases (R²=0.25, P=0.014).

CONCLUSION

18F-fluorocholine PET/CT is a useful imaging modality in evaluating prostate cancer recurrence. The dynamic change of SUV between early and late phase images facilitates differentiating malignancy from benignity. The value of dual-phase imaging in improving the performance of 18F-fluorocholine PET for detecting prostate cancer recurrence is confirmed.

CLINICAL RELEVANCE/APPLICATION

Dual-phase 18F-fluorocholine PET/CT scan is more accurate than single phase scan and is recommended in detecting prostate cancer recurrence.

SSK12-09 • [18F]-FLT PET to Predict Early Response to Neoadjuvant Therapy in Rectal Cancer

Eliot McKinley (Presenter) ; **Ronald C Walker** MD ; **Anuradha Bapsi Chakravarthy** MD * ; **M. Kay Washington** ; **Robert J Coffey** ; **H. C Manning** PhD

PURPOSE

Effective implementation of personalized medicine in oncology requires tailoring an individualized therapeutic regimen for a given patient based upon the molecular characteristics of their disease, and deploying effective biomarkers that predict responses early in the course of therapy. In this pilot study, we evaluated [18F]-FLT PET, a non-invasive molecular imaging biomarker of thymidine salvage pathway activity, as a means to predict response to neoadjuvant therapy that included cetuximab in wild-type KRAS rectal cancer patients.

METHOD AND MATERIALS

Baseline [18F]-FLT PET was collected prior to treatment initiation. Followup [18F]-FLT was collected after three weekly infusions of cetuximab, and following a combined regimen of cetuximab, 5-FU, and radiation. Imaging-matched biopsies were collected concomitantly with each PET study.

RESULTS

Diminished [18F]-FLT PET was observed in 3/4 of patients following cetuximab treatment alone and in all patients following combination therapy. Reduced [18F]-FLT PET following combination therapy predicted disease free status at surgery. Overall, [18F]-FLT PET imaging agreed with Ki67 immunoreactivity from biopsy samples and surgically resected tissue and was predictive of treatment-induced p27 levels.

CONCLUSION

To our knowledge, this study represents the first clinical evaluation of [18F]-FLT PET to predict response to neoadjuvant therapy that included EGFR blockade with cetuximab in patients with rectal cancer. Our results suggest that [18F]-FLT PET is a promising imaging biomarker of treatment response in this setting.

CLINICAL RELEVANCE/APPLICATION

This study reports the utilization of [18F]-FLT PET to predict early response to neoadjuvant therapy in patients with rectal cancer. Early detection of therapeutic efficacy can improve clinical outcome

Physics (Molecular Imaging)

Wednesday, 10:30 AM - 12:00 PM • S404AB



[Back to Top](#)

SSK21 • AMA PRA Category 1 Credit™:1.5 • ARRT Category A+ Credit:1.5

Moderator

Georges El Fakhri, PhD

Moderator

Scott Metzler, MD

SSK21-01 • Intravoxel Incoherent Motion Perfusion MRI: A Sensitive Imaging Biomarker of Tumor Oxygenation

PURPOSE

The overall poor perfusion rate caused by abnormal vascular architecture and increased flow resistance is an important contributor to hypoxia and resistance to therapies. The intravoxel incoherent motion (IVIM) effect observed by diffusion-weighted MRI offers a non-invasive, quantitative method to measure perfusion. In this study, we investigate the feasibility of using the perfusion parameters derived from IVIM MRI as a sensitive imaging biomarker of tumor oxygenation.

METHOD AND MATERIALS

Small pieces of tumor tissue (Dunning R3327- AT1 and MAT-Lu rat prostate sublines) were implanted subcutaneously in the thigh of six male Copenhagen rats. MRI was performed at 4.7 T with a 35 mm volume coil, tunable to 1H or 19F. Each animal breathed air followed by 100% oxygen and then carbogen (95% O₂, 5% CO₂), all delivered at 2 L/min. A multi-shot FSE DWI sequence was performed with TR/TEff = 2000/56ms, 40mm × 40mm FOV, 128×64 matrix, ETL = 8, and 2 NSA. Diffusion gradients were applied in 3 orthogonal directions with 10 b-values (0-1500s/mm²). ADC was computed by fitting all b-values to a monoexponential model and IVIM parameters were calculated using a biexponential model: $S/S_0 = fp \cdot \exp(-bDp) + (1-fp) \cdot \exp(-bDt)$. ADC_{civ} = ADC - Dt was also defined to quantify intravascular space. pO₂ (mmHg) was estimated using 19F FREDOM method through injection pO₂ reporter. Pearson correlation coefficients (r) between IVIM parameters and pO₂ were calculated.

RESULTS

The pO₂ measured in air correlated strongly and significantly with the mean of fp*Dp (r=0.88), as well as Dp in air (r=0.84), which indicates fp and fp*DP are sensitive to pO₂ in air. When gas challenge was given, Strong correlation with fp was found for ?pO₂cb (pO₂ in carbogen-pO₂ in air)(r=0.80) and ?pO₂o2(pO₂ in oxygen-pO₂ in air)(r=0.89). A similar strong and significant correlation was found between ADC_{civ} and ?pO₂cb and ?pO₂o2 (r=0.86 and r=0.92). It suggests that the baseline fp as well as ADC_{civ} determines the size of tumor response to gas challenge.

CONCLUSION

This study indicates that the perfusion parameters derived from IVIM MRI serve as a sensitive imaging biomarker of tumor oxygenation. IVIM Perfusion MRI may also be of value in the assessment of tumor microenvironment, monitoring tumor radiation therapy response.

CLINICAL RELEVANCE/APPLICATION

The IVIM Perfusion MRI provides a unique tool for assessment of tumor oxygenation and tumor microenvironment without the use of exogenous contrast.

SSK21-02 • Establishing Cell Structure-based Biomarkers of Disease Using Label-free Optical Quantification of Cell Mass, Volume, and Density in Early and Late Stage Colorectal Cancer Cell Lines

Sophia Bornstein MD, PhD ; Eric Anderson MD, PhD ; Melissa Wong PhD ; Owen McCarty PhD ; Kevin Phillips (Presenter)

ABSTRACT

Purpose/Objectives

Metastasis, the leading cause of all cancer-related deaths, is facilitated by the hematogenous transport of circulating tumor cells (CTCs) from the primary tumor site to distant organs. We have developed label-free optical tools to quantify the basic physical features of CTCs including their total dry mass content and subcellular density distribution. To interpret these biophysical signatures of cancer at the single cell level, we investigated these quantitative features as a function of tumorigenic potential in the patient-matched SW480/SW620 colorectal cancer cell lines as a model of early and late stage disease.

Materials/Methods

Using non-interferometric quantitative phase microscopy (NIQPM), a technique that can be carried out on commercial microscopes, we quantified the dry mass content and sub-cellular density distribution of cultured cell lines plated on microscope slides. The density distribution was fit with a bi-modal Gaussian distribution whose size parameters quantified the contributions of small and large density structures to the overall composition of the cells. The Jarque-Bera test was used to evaluate normality of all parameters. One-way analysis of variance with Bonferonni post hoc analysis was used to assess statistical significance among parameters across multiple normally distributed cell parameters.

Results

SW620 cells demonstrated a morphology-dependent total dry mass content. The relative amount of small and large micron-scale density contributions to cellular density was found to be morphology-dependent among SW480 cells. SW620 cells possess significantly denser small-scale structures in comparison to SW480 cells. The density contributions from large-scale structures are conserved across all the SW cell types.

Conclusions

Micron scale characterization of the SW cell types with NIQPM demonstrated a systematic bimodal distribution of the subcellular density distribution whose small-scale peak was sensitive to tumorigenic potential of the SW620 cells. Total mass was also specific to SW620 cells. This work quantitatively elucidates distinct cellular architectural phenotypes of early and late stage colorectal cancer in an in vitro setting. These results provides a rational for the use of label-free optically derived metrics to be tested clinically as biomarkers capable of monitoring responses among CTCs to radiological interventions.

SSK21-03 • Comparison of Quantitative Approaches to Identify Patients with Parkinsonism Using Dopamine Transporter Scans

Kenneth Nichols PhD (Presenter) * ; Maria B Tomas MD ; Christopher J Palestro MD

PURPOSE

Presynaptic dopamine transporter ¹²³I-ioflupane (DaT) SPECT imaging facilitates the differentiation of Parkinsonism from essential tremor (ET). Some groups advocate quantitative analyses of caudate (C) or putamen (P) counts for improved differentiation of these two entities, while others recommend applying normal limits to background-corrected counts. This investigation was undertaken to determine which data analysis approach agrees most strongly with a final diagnosis of Parkinsonism.

METHOD AND MATERIALS

We performed a retrospective analysis of ¹²³I-FP-CIT SPECT data for 50 pts (age 64±12 years; 28 F; 22 M) who were evaluated for movement disorders. Data were reconstructed by OSEM (12 iterations, 8 subsets) and corrected for attenuation by the Chang method. BASGAN software (Eur J Nucl Med Mol Imaging 2007;34:1240-53) generated ratios of automated caudate (AC) and automated putamen (AP) counts per pixel versus background counts per pixel, and dichotomous abnormal values for caudate (DC) and putamen (DP) by applying recently updated age- and sex-adjusted normal limits (Eur J Nucl Med Mol Imaging 2013;40:565-73). In separate processing sessions, a medical physicist manually drew regions of interest to determine maximum caudate (MC) and maximum putamen (MP) counts, without knowledge of other clinical or quantitative results. The diagnosis of the patient's official report served as the reference standard. ROC analysis determined optimal discrimination thresholds and kappa statistics evaluated strength of agreement.

RESULTS

Twenty-seven pts had Parkinsonism and 23 had ET. Highest agreement with final diagnoses was found for MP (? = 0.72), followed by DC, MC, AC, AP and DP (? = 0.67, 0.64, 0.64, 0.63 and 0.41, respectively). MP also had highest accuracy (86%), with sensitivity of 78% and specificity of 96%. Pixel averaging and statistical noise of background counts were likely reasons that automated output from BASGAN software underperformed manual determinations of maximal counts.

CONCLUSION

We conclude that, in the analysis of presynaptic dopamine transporter SPECT scans, a straightforward detection of abnormally suppressed putamen counts is the single quantitative measure that agrees most strongly with a diagnosis of Parkinsonism.

CLINICAL RELEVANCE/APPLICATION

While quantitation of DaT scans can bolster visual determinations of disease states, use of quantitative measures should be applied judiciously in influencing final diagnoses.

SSK21-04 • Spectral CT with K-edge Detection of Targeting Gold-nano-Particles: An Experimental Study

Thorsten R Fleiter MD (Presenter) ; Marie-Christine Daniel PhD ; Omer Aras MD

PURPOSE

To determine the specific detectability of targeting Gold-Nano-particles using K-edge CT imaging for the selective and quantitative imaging of the Gold cores.

METHOD AND MATERIALS

Mice with over-expression of the Angiotensin - converting Enzyme (ACE) were prepared with Lisinopril-Gold-Nano-particles. The Gold core diameter of the conjugates was measured with 10-15 nm. The animals were euthanized and frozen at 2, 4, 6 and 10 min after the injection of the conjugates. A control group of mice was prepared with conventional Lisinopril ahead of the injection of Lisinoprol-Gold-Nano-particles to block the binding sites for the conjugate and therefore to analyze the targeting capabilities of the Conjugate. The mice were scanned with a photon counting full spectral CT with data sampling 5KeV above and below the K-edge of Gold at 80.7 KeV. The difference of these two measurements was used to reconstruct images that contained the Gold signal only. Additional data sampling was performed over the residual x-ray spectrum and used for the reconstruction of the anatomical background for the Gold specific images.

RESULTS

The highest signal to noise and Gold to anatomical background ratios were achieved at 10 min after the injection of the Lisinopril-Gold-Nano-particles. The highest signal was measured in the heart muscles and the lung parenchyma. The anatomical background was completely eliminated in the k-edge images of the Gold. The signal to noise ratio in these images was >5:1. An overlay of the anatomical images and the Gold images better demonstrated the distribution of the Gold particles. There were no gold signals detectable in mice that were pre-treated with Lisinopril prior to the conjugate injection.

CONCLUSION

K-edge imaging to detect targeting Gold-Nano-Particles with Computed Tomography is feasible. The specific Gold-images can be used for a fast assessment of the distribution of the particles and therefore the density of the bindings sites for the molecule.

CLINICAL RELEVANCE/APPLICATION

K-edge imaging with Spectral CT can be used to track Nano-particles with high Z cores like Gold that could be designed to specifically display e.g. tumors or cardiac scars.

SSK21-05 • Direct Visualization of miRNA-22 Biogenesis in Isoproterenol-induced Cardiac Hypertrophy by Bioluminescence Imaging In Vitro and In Vivo

Yingfeng Tu (Presenter) ; Bao-Zhong Shen

CONCLUSION

These findings elucidate the feasibility of using our constructed miRNA reporter imaging system to monitor the location and magnitude of expression level of miRNA-22 in CH and to appraise the function of antagomir-22 in silencing the cardiac endogenous miR-22 expression in vitro and in vivo.

Background

Evidence from recent studies has shown that miRNAs play key roles in cardiac hypertrophy (CH). To measure the expression level of endogenous miRNAs is very conducive to understanding the importance of miRNAs in CH. However, current methods to monitor endogenous miRNA level, such as northern blotting, quantitative real-time polymerase chain reaction (qRT-PCR), and miRNA microarrays can not provide real-time information of miRNA biogenesis in CH. Here, we constructed a novel miRNA reporter imaging system to monitor the miR-22 expression in CH in which three copies of the antisense of miR-22 (3×PT_miR-22) was cloned immediately into the downstream region (3'UTR region) of the gaussia luciferase (Gluc) reporter genes, driven by a cytomegalovirus (CMV) promoter.

Evaluation

In this current study we found that with prolongation of isoproterenol (ISO) stimulation in vitro and in vivo, the expression level of miR-22 in cardiomyocytes was gradually increased. Accordingly, the bioluminescence imaging analysis revealed that the fluorescence signals of the miRNA reporter imaging system (CMV/Gluc/3×PT_miR-22) gradually decreased under conditions where miRNA-22 was up-regulated by ISO stimulation. However, the firefly luciferase (Fluc) activity of CMV/Fluc, as a positive control, was not affected with ISO treatment. Furthermore, knockdown of miR-22 by antagomir-22 could reverse the repressed Gluc activities in vitro and in vivo.

Discussion

The development of imaging strategies related to miRNAs will be critical to advance our understanding of the interactions of miRNAs with their target genes and signaling pathways, and eventually to evaluate the use of miRNAs as a novel class of diagnostics and therapeutic targets in cardiovascular disease.

SSK21-06 • Volume of Drug Distribution as a Function of Time for Adaptive Gamma Variate Fits to Plasma Concentrations Curves

Michal J Wesolowski PhD, MSc (Presenter) ; Surajith N Wanasundara PhD, MSc ; Richard C Puetter PhD ; Maria T Burniston PhD ; Paul S Babyn MD ; Carl A Wesolowski MD, FRCPC

CONCLUSION

While it is often assumed that the distribution of a drug in the body is complete after 1-2 hours, this does not appear to be the case for patients having a GFR marker study and a high incidence of ascites for whom it may take several days to reach 95% of the final volume of distribution.

Background

In studies of renal function and glomerular filtration rate (GFR) it is commonly assumed that the distribution of drug in the body is complete within the first 1-2 hours after a single injection or institution of a continuous infusion of a GFR marker. If incorrect, this may lead to inaccuracy in the calculation of plasma clearance and affect patient care. To test the validity of this assumption, a time dependent volume of drug distribution term was derived from the mass conservation equation in the Tikonov adaptively fit gamma variate (Tk-GV) model of plasma clearance.

Evaluation

Following a single intravenous injection, the plasma concentration of a radioactively labeled glomerular filtration marker, ⁵¹Cr-EDTA, was monitored over 24 hours (up to 16 samples) in thirteen patients being evaluated for liver transplantation. For each patient, the volume of drug distribution as a function of time, from adaptive gamma variate fits to plasma concentration versus time curves, was obtained. Plasma clearance and the time required to reach 95% of the final GFR marker volume of distribution were calculated.

Discussion

In these patients, the time required to reach 95% of the final volume of distribution ranged from 0.79 to 11.08 days, which is significantly longer than is commonly assumed. In fact, the GFR marker appears to be eliminated faster than the completion of the volume distribution expansion implying that a steady state volume cannot be reached in practice. Finally, it is shown that on average, 7% of the value of plasma clearance can be attributed solely to this volume expansion. We therefore propose that extrarenal clearance, which has often been invoked to explain discrepancies observed between plasma and urinary clearance values, may largely originate in this time dependent volume expansion term.

SSK21-07 • Prognostic Value of Metabolic Tumor Volume Measured by Differing Methods on Staging 18F-fluorodeoxyglucose Positron Emission Tomography in Esophageal Cancer

Vinod Malik MBBCh, MA (Presenter) ; **Ciaran J Johnston** MD ; **Julie A Lucey** PhD ; **John V Reynolds** MD

PURPOSE

Metabolic tumor volume (MTV) a volumetric parameter obtained on ¹⁸F-fluorodeoxyglucose positron emission tomography/computed tomography (¹⁸F-FDG PET/CT) has been shown to be an independent prognostic factor for survival in patients with esophageal cancer. This study ascertained if different methods of calculating MTV would have an effect on its utility as a prognostic factor.

METHOD AND MATERIALS

From December 2008 to May 2011, 150 patients with biopsy-proven cancer of the esophagus or esophagogastric junction underwent staging ¹⁸F-FDG PET/CT. Maximum standardized uptake value (SUVmax) and MTV of the primary tumor was recorded at different thresholds (absolute cut-offs of SUV 2.5 and 3.5, threshold values of 42% and 50% SUV max and a variable method depending on the SUV max of the primary tumor). Survival analysis was performed using Kaplan-Meier and independent prognostic factors determined using Cox regression multivariate analysis.

RESULTS

¹⁸F-FDG PET/CT SUVmax < 4.1 (p=0.0014), ¹⁸F-FDG PET/CT MTV (absolut cut-off SUV 2.5 method)< 14.5cm³ (p=0.001), ¹⁸F-FDG PET/CT MTV (absolut cut-off SUV 3.5 method) < 7.5cm³ (p=0.0013), ¹⁸F-FDG PET/CT MTV (threshold value of 42% method)< 5.9cm³ (p=0.0005), ¹⁸F-FDG PET/CT MTV (threshold value of 50% method)< 4.4cm³ (p=0.0004), ¹⁸F-FDG PET/CT MTV (variable method)< 4.7cm³ (p=0.0008) were all significantly associated with outcome on analysis.

CONCLUSION

Regardless of the method used to measure MTV, it consistently was able to predict survival even when simple quantative analysis only is performed.

CLINICAL RELEVANCE/APPLICATION

MTV is a valuable prognostic factor in patients with esophageal cancer even when performed with simple quantitative analysis which is available on all clinical scanners.

SSK21-08 • Determining the Minimal Required Radioactivity of F-18 FDG for Reliable Semi-quantification in PET-CT Imaging: A Phantom Study

Ming-Kai Chen MD, PhD (Presenter) ; **David H Menard** ; **David W Cheng** MD, PhD *

PURPOSE

The aim is to investigate minimal required radioactivity of F-18 FDG and corresponding imaging time for reliable semi-quantification in PET-CT imaging in an effort for dose reduction

METHOD AND MATERIALS

We performed F-18 FDG PET-CT study using an ECT phantom containing various spheres (diameter: 3.4, 2.1, 1.5, 1.2, 1.0 cm) filled with a fixed concentration of 165 kBq/ml and background 23.3 kBq/ml (total 156.8 MBq) at multiple time points up to 20 hrs of radioactive decay. The images were acquired for 10 min/bed at each time point using 3-D mode in a hybrid GE Discovery 690 scanner equipped with LYSO detectors and a 64-slice CT. The images were reconstructed in 1, 2, 3, 4, 5, and 10 min per bed using ordered-subset expectation maximum (OSEM) algorithm with 24 subsets and 2 iterations. The standardized uptake values (SUV) of the spheres with both maximal and average were measured by applying volume of interests (VOI) in serial PET images. The minimal required activity concentrations at various acquisition time were determined as well as the minimal product of activity concentration and acquisition time.

RESULTS

The minimal required activity concentration for precise SUVmax quantification in spheres (

CONCLUSION

Our phantom study provided guidance for minimal required activity and acquisition time for precise semi-quantification in F-18 FDG PET imaging. We can further reduce dose and radiation exposure to patients at reasonable acquisition time in clinical studies.

CLINICAL RELEVANCE/APPLICATION

(dealing with PET-CT) Based on the data, we can further reduce the administrative dose of F-18 FDG in clinical studies.

SSK21-09 • Detecting Osteoporosis Using Photoacoustic Spectroscopy

Behnoosh Tavakoli (Presenter) ; **Xiaoyu Guo** ; **Shadpour Demehri** MD ; **Abdullah Muhit** PhD ; **John A Carrino** MD, MPH * ; **Emad Boctor** PhD, MSc *

CONCLUSION

Photoacoustic spectroscopy is technically for detecting the osteoporosis at no radiation cost. This method may be sensitive to the micro structural changes in the bone. In addition with multi spectral imaging, it is possible to analyze different components of the bone tissue such as calcium by decomposing the photoacoustic spectrum to the standard tissue absorbers optical spectrums.

Background

Osteoporosis, is the most common metabolic bone disorder. Monitoring the micro architectural deterioration of the bone tissue and the decrease of the bone mineral density are necessary for early detection the osteoporosis. Broadband attenuation of ultrasound signal is correlated with bone mineral density and its microstructure. In addition, the optical absorption spectrum of the bone tissue analyzes its mineral, water, lipid and oxy-deoxy hemoglobin content. Therefore photoacoustic spectroscopy as a hybrid functional method that combines both optical and ultrasound information is a promising technique for determination of osteoporosis in early stages.

Evaluation

In this study, the quantitative ultrasound calcaneal phantoms of normal and osteoporotic bone were imaged in the transmission mode and the corresponding photoacoustic spectrums were obtained. Our photoacoustic imaging system includes a tunable Q-switch Nd:YAG laser followed by an OPO system generating pulses at the wavelength range of 690 nm-950 nm. The photoacoustic signal is detected with the FDA approved Sonix RP ultrasound system including a data acquisition device for recording the raw data. Multiple points of each phantom were evaluated using a linear US probe with 128 elements. Finally the maximum raw data was extracted from the elements and the value was normalized to the illuminating laser energy.

Discussion

The result revealed a general decrease in the spectrum of the osteoporotic phantom compared to the normal one. The trend matches the optical spectrum of the calcaneus bone tissue. In this test, there was about two times contrast between the normal and osteoporotic case. These phantoms were modeling the bone microstructure and more contrast is expected in the real bone tissue including other tissue absorbers.

PET Imaging of Neuroendocrine Tumors-Clinical State of the Art

Wednesday, 12:15 PM - 12:45 PM • S503AB

CL-MIE-WE5A

Shadi A Esfahani , MD, MPH
Pedram Heidari , MD
Umar Mahmood , MD, PhD

[Back to Top](#)

PURPOSE/AIM

18F-FDG, despite its widespread use in oncologic assessment, has limited application in imaging of neuroendocrine tumors (NET) a broad range of PET tracers has been developed for NET to address this unmet need. We will discuss i) the major classes of targeted compounds that have been used for imaging of NET; ii) detail of the most promising tracers in each class.

CONTENT ORGANIZATION

1. Importance of PET imaging in NET 2. Limitations of 18F-FDG in imaging of NET 3. Various classes of receptor PET tracers including small molecules, and peptides 4. A detailed description (including advantages and limitations) of tracers in each class with potentially higher clinical impact in NET 5. Future directions in development of novel PET tracers for NET.

SUMMARY

PET has become a powerful tool in diagnosis and follow up of cancer patients including NET. Since 18F-FDG has a number of limitations in NET, a wide variety of PET tracers have been developed that range from small molecules to labeled peptides. This overview encompasses limitations of FDG PET in NET, groups of compounds that can be used as probes for NET PET imaging, and detailed examples of more promising tracers in each class.

Molecular Imaging - Wednesday Posters and Exhibits (12:15pm - 12:45pm)

Wednesday, 12:15 PM - 12:45 PM • S503AB

[Back to Top](#)



CL-MIS-WEA • AMA PRA Category 1 Credit™:0.5

Host

Donna J Cross, PhD *

CL-MIS-WE1A • Preliminary Study of Oxygen-enhanced Longitudinal Relaxation in MRI: A Potential Novel Biomarker of Oxygenation Changes in Multiple Myeloma

Ettore Squillaci MD (Presenter) ; Francesca Bolacchi ; Marco Nezzo MD ; Marco Antonicoli ; Giovanni Simonetti MD

PURPOSE

To investigate the significance of the oxygen-enhanced longitudinal relaxation in MRI (R1) of diffuse spinal bone marrow infiltration in patients with Multiple Myeloma

METHOD AND MATERIALS

Twenty-one patients with diffuse multiple myeloma underwent measurement of lumbar bone marrow R(1) while breathing medical air (21% oxygen) followed by 100% oxygen (oxygen-enhanced MRI). Gadolinium-based dynamic contrast-enhanced MRI was also performed. Peak enhancement percentage (Emax), enhancement slope (ES), and time to peak (TTP) were determined from a time-intensity curve (TIC) of lumbar vertebral bone marrow. Ten subjects were enrolled as controls.

RESULTS

Baseline deltaR(1) showed statistically significantly higher with respect to control subjects (0.058 vs 0.021 s⁻¹). Peak enhancement percentage (Emax) showed a positive correlation with DeltaR(1) (r = 0.62, p < 0.01). No correlation was found between ES and DeltaR(1) (p > 0.05). A negative correlation was found between the TTP values and DeltaR(1) (r = -0.58, p < 0.01). A decrease in the Emax and DeltaR(1) values was observed with increased TTP values after treatment in all of the 16 patients who responded to treatment with respect to non responders (p < 0.01). Baseline deltaR(1) values also showed a negative correlation with recovery time as assessed by laboratory data (r = -0.756, 95% CI = -0.938 - -0.241, P = 0.011)

CONCLUSION

These results provide evidence that oxygen-enhanced longitudinal relaxation can monitor changes in tumor oxygen concentration. The technique shows promise in identifying hypoxic regions within tumors and may enable spatial mapping of change in tumor oxygen concentration.

CLINICAL RELEVANCE/APPLICATION

Oxygen-enhanced longitudinal relaxation in MRI of the bone marrow can monitor changes in tumor oxygen concentration and can be used as a prognostic biomarker for response evaluation in MM.

CL-MIS-WE2A • A Peptide Based Molecular Probe for CXCR4 Targeted Oncological MR Imaging

Liang Zhu MD (Presenter) ; Jing Lei ; Yonglan He MD ; Huadan Xue MD ; Zhengyu Jin MD

PURPOSE

To construct a CXCR4 targeted iron oxide nanoparticle for cancer MR imaging, and to evaluate its binding specificity to various cancer cells and its ability to quantify CXCR4 expression level by altering MR T2/T2* signal in vitro.

METHOD AND MATERIALS

A novel CXCR4 binding peptide (Pep12) was introduced for targeted MRI. Immuno-fluorescence studies and flow cytometry were introduced to test its binding affinity to tumor cells expressing CXCR4, with CXCR4 monoclonal antibody as a positive control, and a random peptide as a negative control. Iron oxide nanoparticle was synthesized and conjugated to Pep12. Its cellular toxicity was tested by MTS. Pullulan stain were done to confirm its binding specificity to various cancer cells (A549, PANC-1 and MCF-7). Pep12-USPIO incubated with cancer cell suspensions were scanned at 1.5T MR.

RESULTS

Pep12 had great binding affinity to tumor cells expressing CXCR4, which is comparable to CXCR4 monoclonal antibodies. Pep12-USPIO forms stable aqueous colloid in water/PBS solution. The hydro diameter was 80.5 nm. MTS tests proved its low cellular toxicity. Pullulan stain showed pep12-USPIO could bind to tumor cells in a concentration dependent way, while USPIO alone could not. A significant T2/T2* signal dropdown was observed in Pep12-USPIO incubated cell suspension, and the value of T2/T2* change has positive correlation to the expression level of CXCR4 in different cancer cells.

CONCLUSION

A peptide based MR contrast agent was developed for CXCR4 targeted imaging, it could specifically bind to CXCR4 expressing cells and produce MR signal change. The value of T2/T2* change might be used for the prediction of CXCR4 expression and somehow, tumor metastasis potential. Further studies will be carried out in mice xenograft models, to see its pharmacokinetics, biological toxicity and ability to detect tumor metastasis potential in vivo.

CLINICAL RELEVANCE/APPLICATION

peptide based MR magnetic nanoparticles could be used in oncological MR imaging, with some advantages over antibody based MR molecular probes.

CL-MIS-WE3A • A Preliminary Study Evaluating the Functional Diffusion Map for Early Evaluation of TACE Treatment Response in Patients with Liver Carcinoma

Yu-Fang Chen (Presenter) ; Yong-Bo Yang ; He Wang PhD ; Dong Chen ; Xing-An Long ; Hong-Yan Cheng

PURPOSE

To investigate the value of Functional Diffusion Map (FDM) in the early evaluation of Transarterial Chemoembolization (TACE) treatment response in patients with liver carcinoma as it was typically evaluated by traditional imaging methods several months later.

METHOD AND MATERIALS

A total of 45 patients with liver carcinoma were enrolled, and they are all treated with TACE. T1-weight and Diffusion Weighted Imaging (DWI, $b=600$) were performed before and 4 weeks after treatment. The three-color FDM was obtained from the registration of DWI images to their own pre-treatment T1-weighted images by a 12-degree of freedom transformation using FSL (FMRIB, Oxford, UK). In FDM, the Red voxels (VR) have the ADC increased significantly, blue voxels (VB) have the ADC decreased significantly, and green voxels (VG) have the ADC did not change significantly, where total voxels ($VT=VR+VB$) for which the ADC changed significantly. Each patient was examined by dynamic contrast-enhanced CT or MRI every 3 months during the follow-up.

RESULTS

CONCLUSION

FDM could evaluate the early therapeutic response in patients with liver carcinoma after TACE, and showed a fairly close association with those by the long-term conventional means of imaging. It could be a powerful and promising biomarker and may provide an early and important reference for the clinical protocols.

CLINICAL RELEVANCE/APPLICATION

FDM could be a powerful and promising biomarker for the early evaluation of TACE treatment response and may provide early and important reference for the clinical protocols.

Molecular Imaging - Wednesday Posters and Exhibits (12:45pm - 1:15pm)

Wednesday, 12:45 PM - 01:15 PM • S503AB

[Back to Top](#)



CL-MIS-WEB • AMA PRA Category 1 Credit™:0.5

CL-MIS-WE1B • Immune Cell Trafficking during Radiation Therapy-A Potential Predictive Marker for Therapeutic Response

Bryan Bednarz PhD (Presenter) ; **Sean B Fain** PhD * ; **Jeremy Gordon** ; **Myriam Bouchlaka** ; **Christian Capitini** MD

PURPOSE

Given the cross talk between cancer and the host immune system, there is a compelling need to monitor immunogenic responses in vivo during radiotherapy treatment. Over the last year our collaboration has been working toward (1) developing the nonradioactive isotope fluorine-19 (^{19}F), as a novel, clinically applicable tracking agent for immune cells using magnetic resonance imaging (MRI), and (2.) investigating if local irradiation of tumors augments expression of "danger signals" that recruit and activates immune cells using ^{19}F MRI.

METHOD AND MATERIALS

Using a high-resolution Varian 4.7 Tesla small animal MRI scanner several we have developed and optimize a ^{19}F MR imaging platform that uses a volumetric fluorine coil. We have labeled human NK cells with ^{19}F -PFPE and injected these labeled cells intravenously in immunocompromised mice. The mice were scanned ~1, 24, 48, 72, 120 hours after injection.

RESULTS

Initial optimization experiments have demonstrated excellent SNR uniformity provided by the volume coil. Excellent signal linearity was demonstrated by acquiring images of phantom vials with increasing concentrations of ^{19}F -PFPE. We have also demonstrated the ability to perform whole-body NK cell trafficking. We have verified that NK cells injected into immunocompromised mice trafficked to the liver and spleen.

CONCLUSION

We are currently investigating the immunogenic response following irradiation of subcutaneous tumors in mice. The ability to monitor immune cell trafficking during therapy will help optimize the synergistic effects of radiation cytotoxicity and the host immune system.

CLINICAL RELEVANCE/APPLICATION

The ability to monitor the host immune system response during radiation therapy will help elucidate a more optimal treatment course for individual patients.

CL-MIS-WE2B • In Vivo Magnetic Resonance Tracking of Endothelial Progenitor Cells Trafficking to Sites of Hepatoma Angiogenesis

Xiao Li Mai MD, PhD ; **Bao Xin Li** (Presenter) ; **Hai Jian Fan** ; **Bin Han**

PURPOSE

The goal of this study was to use Micro-MR to track the migration and incorporation of intravenously injected, magnetically labeled rat peripheral blood endothelial progenitor cells (EPCs) into the blood vessels in a rapidly growing hepatoma model.

METHOD AND MATERIALS

This study was approved by the Institutional Committee on Animal Research. Transplanted hepatoma in 18 BALB/c nude mice was induced with injected 1×10^6 cells from a H22 mouse hepatoma cell line into left hepatic lobe. Rat EPCs labeled ($n=9$) and unlabeled ($n=9$) with superparamagnetic particle Fe_2O_3 -poly-L-lysine (PLL) complexes were injected intravenously, and MR imaging was obtained 3, 7, and 10 days after transplantation. Hepatoma-to-muscle contrast-to-noise ratios (CNRs) on T_2^*WI were measured and compared to histomorphologic studies.

RESULTS

Rat EPCs could be efficiently labeled. Migration and incorporation of transplanted labeled cells into tumor neovasculature were documented with in vivo MR as low signal intensity at the tumor periphery as early as 3 days after EPCs administration in preformed tumors. However, low signal intensities were not observed in tumors implanted at the time of EPC administration until tumor size reached 1 cm at 10 to 14 days. CNRs on T_2^*WI decreased significantly in the hepatoma 12 days after injected of EPCs. Prussian blue staining showed iron-positive cells at the sites corresponding to low signal intensity on MRI. The labeled cells initially localized in the edge of tumor. No free nano-particles were found in the interstitial substance or macrophage. Confocal microscopy showed incorporation into the neovasculature, and immunohistochemistry confirmed the transformation of the administered EPCs into endothelial cells.

CONCLUSION

Rat EPCs could be effectively labeled with Fe_2O_3 -PLL. MRI demonstrated the incorporation of magnetic labeled rat EPCs into the neovasculature of implanted hepatoma.

CLINICAL RELEVANCE/APPLICATION

tracking the labeled cells with micro-MR can demonstrate neovasculature of tumors in vivo and is recommended as part of a MR study prior to tumor treatment.'

CL-MIS-WE3B • Image Features Derived from Contrast Enhanced CT Can Predict BAP1 Loss in Patients with Clear Cell Renal Carcinoma: Results of a Feasibility Study

PURPOSE

To identify image-derived features on contrast-enhanced CT scans in patients with Clear Cell Renal Carcinoma (CRCC) that are predictive of BAP1 deletion.

METHOD AND MATERIALS

We performed a feasibility study on contrast enhanced CT scans from a set of 39 patients (11 with BAP1 deletion) from The Cancer Genome Atlas (TCGA) KIRC database. We created tumor segmentation masks using the open-source software, Medical Image Interaction Tool Kit (mitk.org). Three-dimensional textural features (such as Laws texture features, Wavelet transforms, and Haralick texture measures), volumetric features, and ratios of features at different image resolutions were computed using MATLAB. A total of 73684 different imaging features were extracted for each phase of the CT (non-contrast (nc), cortico-medullary (cm), nephrographic(neph) and excretory(ex)), and correlated to the BAP1 loss (derived from the TCGA database). Feature association with mutation status was tested using the Wilcoxon rank-sum test. Multiple testing correction for p-values was done using Benjamini-Hochberg FDR correction. A statistical random forest classifier was trained on features significant at an unadjusted p-value of 0.05 to predict mutation status. Receiver Operating Characteristics (ROC curves) were obtained using a five-fold cross-validation procedure.

RESULTS

The number of features that were significantly different in tumors with BAP1 loss were: 3994 in the non-contrast phase; 475 in the cortico-medullary phase; 1844 in the nephrographic phase; and 3907 in the excretory phase. Out of these features, nephrographic and excretory phases had 182 and 273 features that were significantly different after FDR correction (q-value < 0.05). Area Under the Curve (AUC) values from the classifier based on the features (from unadjusted p-value < 0.05) identified nephrographic and non-contrast phases as reliable predictors of BAP1 loss (AUC:1, and AUC:0.8 respectively).

CONCLUSION

Our initial feasibility study suggests that it is possible to predict BAP1 status from analysis of imaging features derived from contrast enhanced CT. Nephrographic and non-contrast phases seem to be most predictive in this initial analysis.

CLINICAL RELEVANCE/APPLICATION

BAP I deletion is associated with high grade CRCC and poor prognosis. We demonstrate a non-invasive way of predicting this on contrast enhanced CT scans.

CL-MIS-WE4B • Assessing Tumor Vasculature Using a Liposomal CT/MRI Bimodal Contrast Agent

Guanshu Liu PhD (Presenter) ; **Yuguo Li** PhD ; **Yuan Qiao** MD, PhD ; **Shibin Zhou** MD, PhD ; **Peter C Van Zijl** PhD * ; **Michael T McMahon** PhD

PURPOSE

To develop a liposomal system that encapsulates clinically-used iodinated CT/X-ray contrast agent iodixanol to be a CT/MRI bimodal contrast agent, simply using the Chemical Exchange Saturation Transfer (CEST) contrast from the CT agent.

METHOD AND MATERIALS

Iodixanol encapsulated liposomes (CT-lipo) were prepared according to literatures using a formulation of DPPC:cholesterol: DSPE-PEG-2000=57:40:3. The size, concentration and encapsulation ratio of CT-lipo were measured following our previous published methods. 24 hours before MRI and CT studies, 500 µL overnight-dialyzed liposomes (1000 mgI/kg) were injected to the tail vein of Balb/c mice carrying subcutaneous CT26 murine colon tumors. In vivo CEST MR images were acquired using previous published methods. 6 3D CT images were acquired using an IVIS Spectrum CT system (Perkin Elmer) with the following parameters: 50 kVp, 1 mA, and 50 msec exposure, totally 720 projections.

RESULTS

The results showed that iodixanol, both in liposomal (~160 nm) and non-liposomal forms, can also be detected using CEST MRI with a relatively high sensitivity at 4.3 ppm. The detection limit is estimated to be ~ 2nM liposomes, or ~1.4mM encapsulated iodixanol. At 24 hours after i.v. injection, mice injected with CT-lipo showed marked enhancement in tumor region, while those injected with blank liposomes (blank-lipo) did not show significant contrast enhancement. In MRI, the tumor of CT-lipo injected mice showed remarkable but non-uniform CEST contrast enhancement at 4.3 ppm as compared to those injected with blank-lipo, with a average tumor contrast enhancement (MTR_{asym}) of 0.8% (n=2 for each group). More studies of CT and MRI acquisitions on additional animals and immunohistological validation are underway.

CONCLUSION

The present work demonstrated the feasibility of engineering a multimodality imaging system by encapsulating nanosized liposomes with a single clinically used CT contrast agent iodixanol. Our results showed that both CT and MRI could detect reliably the presence of iodixanol-encapsulating liposomes in tumors, enabling the bimodal assessment of tumor vasculature.

CLINICAL RELEVANCE/APPLICATION

The present nanoparticle system can be easily translated to the Clinical for imaging the vasculature of tumors and monitoring the effect of anti-angiogenic drugs using both MRI and CT.

Molecular Imaging (Imaging Probes)

Wednesday, 03:00 PM - 04:00 PM • S504CD



[Back to Top](#)

SSM12 • AMA PRA Category 1 Credit™:1 • ARRT Category A+ Credit:0.5

Moderator

Umar Mahmood, MD, PhD

Moderator

King C Li, MD

SSM12-01 • Building Nanoparticles from Small Molecules in Situ in Dying Tumor Tissue to Track Chemotherapy Response by MRI

Adam J Shuhendler PhD (Presenter) ; **Deju Ye** PhD ; **Prachi Pandit** PhD ; **Kimberly D Brewer** PhD ; **Brian K Rutt** PhD ; **Jianghong Rao** PhD

PURPOSE

Apoptosis is a major cellular pathway for chemotherapy-induced tumor death, the early monitoring of which could lead to evidence-based and personalized therapy planning. We report a novel small molecule for chemotherapeutic response monitoring by MRI based on the caspase-3-triggered formation of nanoparticles in dying tumor tissue.

METHOD AND MATERIALS

Our modular probe design comprises a biocompatible intramolecular condensation reaction, a two-step activation requiring both active caspase-3 and disulfide reduction, and an exchangeable reporter moiety. For MRI, this reporter moiety is a gadolinium chelate, resulting in a caspase-sensitive nano-aggregation MRI (**C-SNAM**) probe. **C-SNAM** was tested in female nude mice bearing subcutaneous HeLa tumors receiving i.v. doxorubicin (DOX) chemotherapy. MR imaging was performed following **C-SNAM** administration prior to treatment and following three rounds of therapy on a Bruker Icon 1T desktop scanner. Additionally, the mechanism of probe activation was

demonstrated using a fluorescent version of the probe (**C-SNAF**), which was used with both super-resolution microscopy and whole animal imaging.

RESULTS

Apoptosis requires the activation of caspase-3, which cleaves the *L*-DEVD peptide capping group of **C-SNAM**. Coupled to the reducing environment of the tumor, this two-step activation results in the formation of a hydrophobic macrocycle. This macrocycle self-assembles *in situ* into ~80 nm nanoparticles, providing enhanced imaging contrast in regions of apoptotic tumor through high local reporter moiety concentrations and prolonged retention in tumor tissue. Additionally, nanoparticle formation resulted in a ~223% increase in r_1 relaxivity at 1T (**C-SNAM** $r_1 = 12.57 \text{ mM}^{-1}\text{s}^{-1}$; nanoparticle $r_1 = 28.02 \text{ mM}^{-1}\text{s}^{-1}$). *In vivo* studies showed that both probe accumulation and retention were significantly greater post-treatment, demonstrating the utility of **C-SNAM** for therapeutic response monitoring.

CONCLUSION

Our novel, biocompatible and bioorthogonal self-assembling contrast agent chemistry results in *in situ* probe nano-aggregation and contrast enhancement that allows for the successful tracking of chemotherapeutic response with MRI.

CLINICAL RELEVANCE/APPLICATION

In vivo self-assembly is a new strategy for smart molecular imaging, where this first-of-kind demonstration of *in situ* nanoparticle formation pushes the frontier of probe and tracer design.

SSM12-02 • High r_1 Relaxivity Sub-5 nm Suprasmall Iron Oxide Nanoparticles (sSIOs) as Contrast Agent for MRI Angiography

Hui Mao PhD (Presenter) ; **Jing Huang** ; **Liya Wang** MD

PURPOSE

A new class of high r_1 relaxivity, sub-5 nm, super small iron oxide nanoparticles with oligosaccharide coating as T1-weighted MRI contrast agents while providing reverse T2 contrast was used in MRI angiography.

METHOD AND MATERIALS

The sSIO nanoparticles were obtained from the encapsulation of iron oxide core in a thin oligosaccharide shell through *in situ* polymerization. SIO solutions with different concentrations were examined by a 3T MRI scanner using T1- and T2-weighted fast spin echo sequences, inversion recovery turbo spin echo sequence and multi-echo T2-weighted spin echo sequence. R1 and R2 relaxivities were calculated by fitting signal changes in multi-IR T1 and multi-TE T2 images using simple exponential equations. SIO with different sizes and Gd-BOPTA were intravenously administered into mice. Fat suppressed T1-weighted spin echo images were obtained to investigate the contrast changes in liver, kidney and iliac artery at the different time points.

RESULTS

The prepared sSIO has an r_1 value of $4.2 \text{ mM}^{-1}\text{s}^{-1}$ and a high r_1/r_2 ratio (0.28), which is competitive with commercial Gd-based contrast agent. Significant T1 contrast enhancement in the kidney and iliac artery were evidenced in *in vivo* MRI after intravenously administration of sSIO in mice, similar to that observed in Gd-BOPTA enhanced MRI. The positive contrast enhancement is attributed to the small size and the reduced susceptibility of the nanoparticles, as well as the excellent colloidal stability in physiological environment. Such T1 contrast enhancement is not obvious when using a larger size SIO-10 or 20. Interestingly, uptake of SIO-3 in liver led to strong T2 effect or signal drop in liver further improves the image quality for visualizing liver tissue and hepatic vasculature in T1 weighted MRI. Furthermore, SIO-3 has a much longer blood retention time than small molecule Gd for prolonged imaging time for organs of interest, providing a potential long half time T1 weighted imaging agents for imaging of vasculature of disease tissues.

CONCLUSION

sSIO-3 has a much longer blood retention time than small molecule Gd for prolonged imaging time for organs of interest, providing a potential long half time T1 weighted MR imaging agents for MRI Angiography.

CLINICAL RELEVANCE/APPLICATION

The suprasmall SIOs exhibit excellent T1 contrast in *in vivo* MRI studies, especially for kidney and iliac artery, providing a potential long half time blood pool MR imaging agents.

SSM12-03 • In Vivo Mesenchymal Stem Cell Labeling Using FDA Approved Iron Oxide: Ferumoxytol

Aman Khurana MD (Presenter) ; **Fanny Chapelin** MS ; **Graham Beck** ; **Jessica Donig** BA ; **Solomon Messing** ; **Heike E Daldrop-Link** MD

PURPOSE

To develop an immediately clinically applicable approach for labeling of bone marrow derived mesenchymal stem cells (MSC), which would not require *ex vivo* manipulations of harvested MSC.

METHOD AND MATERIALS

Sprague Dawley rats were injected with IV ferumoxytol (0.5mmol/kg). 48 hours later, MSC were extracted from long bones (femur & tibia) as per established protocols. The labeling efficiency of these *in vivo* labeled cells was compared with traditional *ex vivo* labeling procedures using fluorescence, confocal and electron microscopies. These *in vivo* labeled stem cells were cultured for 7 days before imaging them on 7T GE MR scanner (T-2 ME/SE; TE-15, 30, 45, 60 TR-4000; NEX: 1) along with unlabeled controls to calculate T2 relaxation times and generate T2 maps. Day-7 labeled *in vivo* cells were subsequently transplanted in osteochondral defects of 12 knees of 6 nude Sprague Dawley rats and followed up for 4 weeks using MR imaging. Quantitative T2 relaxation times were compared for significant differences between labeled cells and controls using t-tests. MR imaging data were correlated with histopathology of cell samples and implants.

RESULTS

Fluorescent & confocal microscopy confirmed presence of iron oxides in *in vivo* labeled cells, with 3.2 times higher intracellular quantities than standard *ex vivo* labeled cells. Electron microscopy localized iron oxide nanoparticles in secondary lysosomes. *In vivo* labeled cells demonstrated significant T2 shortening effects both *in vitro* & *in vivo* when compared to unlabeled controls (T2 times *in vitro*: 8.2 vs 33.6 ms, *in vivo*: 15.4 vs 24.4ms; p

CONCLUSION

To the best of our knowledge, this is the first report of *in vivo* stem cell labeling with an immediately clinically applicable iron supplement. This method eliminates risks of *ex vivo* contamination and alterations of stem cell due to manipulations between harvest and transplantation and thus could be rapidly translated to the clinic via off label use of the FDA-approved Ferumoxytol.

CLINICAL RELEVANCE/APPLICATION

In vivo labeling could be widely used for tracking of MSC in various target tissues as it involves no additional cell manipulation between harvest & transplantation & provides strong MR signal *in vivo*

SSM12-04 • Optical Imaging with a Novel Cathepsin-B Activated Probe for Enhanced Detection of Colorectal Cancer

Shadi A Esfahani MD, MPH (Presenter) ; **Pedram Heidari** MD ; **Umar Mahmood** MD, PhD

PURPOSE

Despite significant advances in diagnosis and treatment, colorectal cancer (CRC) is still the fourth most common cause of cancer death with a global incidence rate of greater than 1 million people per year. Although the colonoscopy is a routine method for CRC screening, it has limited sensitivity for detection of lesions in the early stages. We assessed the ability of a novel protease activatable probe (Lumicell-33) selective for Cathepsin B (CTSB) with improved kinetics in the early detection of CRC tumors.

METHOD AND MATERIALS

An orthotopic CRC model was developed with crossing APCKKO, KrasLSL-G12D and p53flox/flox mice to generate APCKOKrasLSL-G12Dp53flox/flox (AKP) mice (n=8). Cre expressing adenovirus (AdCre) was administered focally in descending colon of the mice to cause recombination; mice were followed by colonoscopy for tumor development. Also in a human CRC model HT-29 cells were implanted subcutaneously (SC) in the flank of 8 adult nu/nu mice. Multispectral epifluorescence imaging was performed over 48 hours following IV injection of Lumicell-33 probe in SC mice. Signal intensity of the probe was measured in the tumor, and tumor to background ratio (TBR) were calculated. AKP mice were sacrificed 6 hours after injection of the probe. Ex vivo imaging of the colon was performed using NIRF imaging system. IHC evaluation of CTSB expression in both human and murine CRCs was performed.

RESULTS

CONCLUSION

Multispectral epifluorescence imaging revealed increased fluorescent signal in both human and mouse tumors, and in both xenografts and spontaneous tumors. This protease probe has the potential to improve CRC tumor detection by fluorescently highlighting neoplastic regions.

CLINICAL RELEVANCE/APPLICATION

Cathepsin B activatable probe has the potential in early detection of colorectal cancer. By fluorescently highlighting neoplastic regions, it could provide an adjunct to standard WL colonoscopy.

SSM12-05 • PET Imaging of Periostin, a Novel Extracellular Matrix Protein Target in the Tumor Microenvironment

Shadi A Esfahani MD, MPH (Presenter) ; Pedram Heidari MD ; Nazife S Turker ; Peiman Habibollahi MD ; Timothy C Wang ; Anil Rustgi ; Umar Mahmood MD, PhD

PURPOSE

Periostin, a secreted extracellular matrix protein, plays a key role in cell adhesion and motility within the tumor microenvironment, and is correlated with metastases. Periostin is highly upregulated in esophageal squamous cell carcinoma (ESCC), one of the two major subtypes of esophageal cancer worldwide. We developed a novel PET tracer that specifically targets periostin, and tested it in murine models of ESCC.

METHOD AND MATERIALS

Human ESCC cell lines were subcutaneously implanted in nu/nu mice (n = 10). TE-11 cells with high expression and TT cells with minimal expression of periostin were used to generate the positive and control tumor models. We additionally tested the probe in a genetically engineered mouse model (GEMM) of ESCC by conditionally deleting the cell adhesion molecule p120ctn (L2-cre;p120ctnLoxP/LoxP); the model demonstrates a trend of increasing periostin concentration in serum, and its enhanced expression in distal esophagus and forestomach with progression of ESCC. An anti-periostin-F(ab)2 was generated from a monoclonal antibody by enzymatic digestion and conjugated with p-SCN-Bn-DOTA. The conjugate was labeled with ⁶⁴Cu. PET/CT scanning and quantitative analysis were performed at 6, 12, and 24 h after IV injection of the probe. Results were compared to ¹⁸-F FDG PET/CT images in the GEMM. Organ specific biodistribution was performed at 24h after tracer injection.

RESULTS

CONCLUSION

We demonstrated that specific imaging of periostin in the ECM of ESCC is feasible using a novel targeted PET tracer. Detection of periostin in the tumor microenvironment may help with early detection, post-surgical follow up, and with in situ characterization of primary and metastatic lesions.

CLINICAL RELEVANCE/APPLICATION

PET imaging of periostin in the ECM could be used for tumor characterization and to assess novel targeted anti-metastatic therapies.

SSM12-06 • Monocyte Specific Single Photon Emission Computed Tomography (SPECT) Imaging Reveals Local Inflammation Activity In-vivo

Michel Eisenblaetter MD (Presenter) ; Rebekka Hueting ; Margaret Cooper ; Walter L Heindel MD ; Thomas Vogl PhD ; Christoph B Bremer MD ; Tobias R Schaeffter PhD

PURPOSE

The release of the protein S100A8/A9 by activated monocytes has been shown to reflect local disease activity in numerous inflammatory disorders. Monocytes are among the initial drivers of inflammation and S100A8/A9 has in this context been shown to act as a proinflammatory cytokine, crucial for maintenance of inflammation. Having shown the feasibility to specifically visualise S100A8/A9 using optical imaging (OI), we now demonstrate the first specific SPECT imaging of monocytes activity in order to overcome the limitations of OI with regards to complex disease models or translational purposes. For this first approach, we used a well established model of local innate immune response.

METHOD AND MATERIALS

Local inflammation was induced at the right ears of female Balb/c mice by application of 2% croton oil (n=10). A S100A9-antibody (aS100A9) was conjugated to DTPA and labelled with In111. The labelling efficacy and purity of the compound was assessed using HPLC. Mice received the labelled tracer iv in doses, corresponding to about 10 MBq activity 24 h after induction of inflammation. An equivalently labelled IgG of irrelevant specificity in mice was used to control for unspecific tracer distribution. SPECT was performed immediately after tracer injection and repeatedly up to 48 h later. Tracer biodistribution was assessed after in-vivo imaging. For correlation of imaging findings, S100A9 serum levels were determined at the imaging time points and immunohistochemistry for S100A9 was performed.

RESULTS

SPECT imaging immediately after tracer injection did not reveal a specific tracer uptake in the region of inflammation but already allowed for estimation of perfusion properties. 24 h later however, the diseased area showed a significant uptake of aS100A9 with excellent contrast to the healthy control side and other tissues, as confirmed by ex-vivo biodistribution measurements (%ID/g ♦ right ear: 51.9; left ear: 3.1; liver: 2.5; spleen: 8.5). Control experiments and histology supported the in-vivo imaging results.

CONCLUSION

In a first approach using a well established and controllable model, S100A9-mediated imaging of monocytes activity appeared to be a promising tool for specific visualisation of inflammation.

CLINICAL RELEVANCE/APPLICATION

Inflammation is widely accepted as the driving pathomechanism behind multiple diseases. Understanding and specific monitoring of the underlying cellular processes is therefore of utmost importance.

Molecular Imaging (Oncology and Subspecialties)

Thursday, 10:30 AM - 12:00 PM • S504CD



SSQ12 • AMA PRA Category 1 Credit™:1.5 • ARRT Category A+ Credit:1.5

Moderator

Hubert J Vesselle, MD, PhD *

[Back to Top](#)

SSQ12-01 • Biochemical MRI with gagCEST (Glycosaminoglycan Chemical Exchange Saturation Transfer Imaging) of Finger Joint Cartilage in Rheumatoid Arthritis

Christoph Schleich (Presenter); Anja Lutz; Benedikt Ostendorf; Philipp Sewerin; Gerald Antoch MD*; Falk R Miese MD

PURPOSE

Rheumatoid arthritis (RA) frequently involves finger and hand joints. Joint damage may result in severe physical disability. gagCEST has recently been demonstrated to visualize biochemical alterations of cartilage in knee joints of patients following cartilage repair surgery as well as in intervertebral discs. The purpose of our study was to test the feasibility of gagCEST imaging in finger joint cartilage in healthy volunteers and patients with RA.

METHOD AND MATERIALS

Six volunteers (mean age 33; range: 21-45 years) and four patients (age 58; range: 52-64 years) were examined at a 3T MR scanner (Siemens Magnetom Trio) using two loop coils (4 cm diameter), one fixed on the palmar, the other on the dorsal side of the second metacarpophalangeal joint (MCP). For gagCEST imaging, CEST effects were prepared by a train of Gaussian RF pulses followed by signal readout with a 3D RF spoiled GRE sequence. The CEST curves were calculated for each pixel and were shifted for the water resonance to appear at 0 ppm of the Z-Spectrum. The MTR asymmetry curves were determined. The CEST effect of the cartilage was measured with the glycosaminoglycan saturation transfer [ST = CEST (+1.3 ppm) - CEST (-1.3 ppm)/CEST (+1.3 ppm)]. Joint space width (JSW) as a morphologic feature of cartilage integrity was measured.

RESULTS

Cartilage ST values were significantly lower in patients compared to healthy volunteers (13.58 ± 6.11 vs. 27.38 ± 4.52 ; $p=0.011$). Cartilage CEST curves showed a decrease of CEST effect between 1.2 and 2.2 ppm, which corresponds to the resonance frequency of hydroxyl protons of glycosaminoglycans. There was no significant difference in JSW between healthy volunteers and RA patients.

CONCLUSION

CEST imaging revealed alterations in finger cartilage of RA patients compared to healthy controls in the absence of cartilage thinning. The decreased CEST effect in the spectral range of glycosaminoglycan resonances points towards depletion of glycosaminoglycans in RA.

CLINICAL RELEVANCE/APPLICATION

Biochemical imaging with gagCEST of cartilage composition is feasible at finger joints in RA.

SSQ12-02 • Application of 59Fe Labeled Triglyceride-rich Lipoproteins for Quantitative Activity Measurements of Brown Adipose Tissue at 7T MRI

Caroline Jung (Presenter); Barbara Freund; Markus Heine; Michael G Kaul; Jorg Heeren; Harald Ittrich MD; Gerhard B Adam MD

PURPOSE

The aim was to determine metabolic activity of brown adipose tissue (BAT) with MRI at 7T using radioactively labeled superparamagnetic iron oxide nanoparticles (SPIO) embedded into the lipoprotein layer for visualisation of lipoprotein distribution and BAT metabolism after intravenous (iv) and intraperitoneal (ip) injection.

METHOD AND MATERIALS

59Fe labeled SPIOs were embedded into the lipid core of Triglyceride-rich lipoproteins (TRL; 59Fe SPIO-TRL). Cold exposed (24h), BAT activated mice (n=10) and thermoneutral control mice (n=10) were starved for 4 hours before 59Fe-SPIO-TRL application. MRI was performed before, 1 and 24 hours after ip (n=10) and iv (n=10) injection at a 7T small animal MRI using a T2*w Multiecho-GRE sequence (TR/TEfirst 400/2ms, ETL 12, ES 1ms, FA 25°, NSA 4, 10 slices, eff. voxel volume 160x160x600 μm³). R2* and ?R2* in liver and BAT were estimated. Ex vivo the biodistribution of 59Fe SPIO-TRL was analyzed using a large volume Hamburg whole body y counter (HAMCO). The amount of TRL in liver and BAT was calculated according to the results of percentage TRL accumulation arrived from activity measurements and correlated with MRI measurements. Uptake of TRL into tissue was confirmed by histological (Prussian blue) and TEM analyses.

RESULTS

CONCLUSION

CLINICAL RELEVANCE/APPLICATION

SSQ12-03 • Macrophage Tracking with Heteronuclear Proton MRI

Rebecca Schmidt MD (Presenter); Nadine Nippe; Klaus Strobel*; Max Masthoff; Olga Reifscheider DIPLPHYS; Daniela Delli Castelli; Cord Sunderkotter MD; Uwe Karst PhD; Silvio Aime; Christoph B Bremer MD; Cornelius Faber

PURPOSE

To explore the feasibility of imaging Thulium (Tm)DOTMA labeled cells in a murine inflammation model by ultra-short echo time imaging (UTE).

METHOD AND MATERIALS

Bone marrow derived macrophages (BMDM) were labeled with 15 μmol TmDOTMA/10⁶ cells by incubation for 24h. Cell viability and activity were tested by determination of cell death, adhesion, phagocytosis and NO production. Fluorescence microscopy due to the self-fluorescence of TmDOTMA (ex. 253nm; em. 460nm) and MR spectroscopy determined labeling efficiency. Inflammation was induced by s.c. injection of 100 μl polyacrylamide (PAG) gel in both flanks of 3 nude mice. To intensify inflammation, lipopolysaccharide (30 μg/100 μl PAG) was added to one PAG pellet per mouse. 3.6x10⁶ labeled BMDMs were injected i.v. 24h after gel implantation. MRI was performed on a Bruker Biospec 94/20 with a 35mm ¹H volume coil over a period of 8 days using 3D UTE sequence. On day 8, PAG-pellets, livers and spleens were explanted. Selective macrophage staining (MAC 3) and laser ablation inductively-coupled plasma mass spectrometry (LA-ICP-MS) were performed for correlation with the MR data.

RESULTS

Neither cell viability nor activity were affected by TmDOTMA labeling. Fluorescence microscopy showed an intracellular uptake of the complex. MR spectroscopy of labeled cells revealed an average of $8.97 \pm 0.85 \times 10^{10}$ TmDOTMA molecules per cell. *In vivo*, TmDOTMA signal was detected in the bladder (day 1) and in liver, spleen and gel pellets over 8 days. Within 2h scan time, signal-to-noise values within the PAG-pellets ranged between 1.49 and 3.98. From a reference tube with a 0.25 mM TmDOTMA solution, the *in vivo* detection limit was estimated to be slightly below 10⁴ BMDMs. Origin of the signal from migrated BMDMs was confirmed by histology and LA-ICP MS showing both BMDMs and Tm around the injected gel.

CONCLUSION

The highly shifted signal of the equivalent methyl protons of TmDOTMA can be detected independently from the water signal by UTE resulting in an increased sensitivity. This approach of heteronuclear proton MRI may provide a versatile tool for MR cell tracking *in vivo* and thus facilitate the application of molecular MRI without the need for extra MR equipment.

CLINICAL RELEVANCE/APPLICATION

Detection and tracking of labeled cells by means of noninvasive molecular imaging has become essential part of both preclinical research

and medical diagnostics related to cellular therapies.

SSQ12-04 • In Vivo Ultrasound Imaging of Pancreatic Islets

Jose L Paredes MD (Presenter) ; George Gittes ; Jiamjung Wang ; Flordeliza Villanueva

PURPOSE

Imaging and quantifying pancreatic islets in vivo could revolutionize the treatment of diabetes mellitus. Currently, insulin levels and hemoglobin A1C are our main methods for determining beta cell mass in diabetic patients. These insensitive measures are grossly inadequate for proper guidance of therapy. An office-based, non-invasive method for determining islet mass serially in diabetics has long been sought-after, but with no success. Here we show that a sub-harmonic ultrasound probe, in conjunction with microbubble intravenous contrast, allows islets visualization in the mouse pancreas based on the increased blood flow compared to surrounding pancreatic tissue.

METHOD AND MATERIALS

RESULTS

The subharmonic ultrasound visualization rendered clearly delineated large blood vessels of the scanned region in the pancreas. We were also able to identify discrete, three-dimensional hyper-perfused areas that were of the size, number, and distribution of islets. To validate that these hyperperfused areas were indeed islets, we scanned the pancreas of transgenic mice that express GFP under the mouse insulin promoter

CONCLUSION

Using a mouse model, we now have strong evidence to show the potential feasibility of using ultrasound combined with intravenous administration of microbubbles to visualize and quantify islet mass.

CLINICAL RELEVANCE/APPLICATION

Imaging and quantifying pancreatic islets in vivo could revolutionize the treatment of diabetes mellitus.

SSQ12-05 • Automated Analysis of Metastatic Involvement in Bone Using Anatomical and Functional Information from FDG PET/CT Images

Omer Demirkaya (Presenter) ; Abdulaziz Alsugair MD ; Mohei M Abouzied MD

PURPOSE

Although overall incidence of bone metastasis is not known, over half of people who die of cancer in the US each year are thought to have bone involvement. In this study we developed a method to quantify the metabolic and anatomic changes induced by bone metastases in cancer patients using PET/CT images. The quantitative parameters along with the structural changes seen by CT bone window may serve as a useful tool in assessing the response of bone metastases to therapy.

METHOD AND MATERIALS

Seventy three patients with no prior history of chemo or radiotherapy who had bone metastases documented by PET/CT (Discovery ST, GE) and other conventional modalities were selected for the study. PET/CT images were resampled to the same pixel size. Then the bone structure was segmented using a threshold of 150 HU. After the segmentation, the 50% of the maximum SUV within the bone mask was used to identify bone lesions in each slice. Using the ROIs defined at 70% of the max, the lesion characteristics including the mean HUs were computed from the PET/CT images. The lesions were subjected to the visual confirmation by an experienced PETCT physician who also categorized them based on the appearances in the CT bone window as lytic, sclerotic, mixed, or no-change type. The lesion characteristics were compared using statistical methods.

RESULTS

340 lesions in 73 patients with different cancer types were analyzed. The lesions were categorized into four anatomical groups. The spine hosts the largest number of lesions, while thoracic cage bones had the least. The lumbar bones were the most preferential sites within the spine. Quantitatively, the mean SUVmax for the lytic, no-change, mixed and sclerotic lesions with no structural changes were 7.4, 6.1, 8.2 and 7.2, respectively. Comparison of SUVs showed that only no-change type was statistically different from the mixed type. Statistical comparison of CT values indicated that the difference between no-change and lytic types was significant. Uptake period did not seem to have an impact on no-change and sclerotic types as much as it did on the others.

CONCLUSION

The quantitative method for analysis of bone metastases may serve as a useful tool in monitoring and assessing therapy response.

CLINICAL RELEVANCE/APPLICATION

A quantitative method provides a convenient way to analyze the functional and structural characteristics of bone lesions and may serve as a useful tool for assessing the response to therapy.

SSQ12-06 • A Dual Isotope Hybrid MCT-PET System Reveals Functional Heterogeneity of Bone Lining Cells and Longitudinal Changes in Marrow from Local Radiation and Chemotherapy

Masashi Yagi (Presenter) ; Luke Arentsen BS, ARRT ; Yutaka Takahashi PhD ; Leslie Sharkey ; Masahiko Koizumi MD, PhD ; Cory Xian ; Clifford J Rosen ; Douglas Yee MD ; Jerry W Froelich MD ; Susanta K Hui PhD

PURPOSE

We report the skeletal and marrow response to clinically relevant local radiation and chemotherapy using 18 F-CT-PET and reveal a potentially important role for bone lining cells in mediating the skeletal response to local and systemic injury.

METHOD AND MATERIALS

Mice were given systemic methotrexate (MTX, 2.5mg/kg, 3 days) or 16Gy local radiation to legs. Longitudinal FDG (days -4, 2) and NaF (days -3, 3, 7, 14, 29) 18 F-CT-PET scans were performed. Eight skeletal regions were monitored. Distal femora were harvested for cellular histology.

RESULTS

We observed significant functional heterogeneity throughout the skeleton for bone mineral remodeling as measured by NaF (

CONCLUSION

Dual isotope 18 F-CT-PET revealed functional heterogeneity of the skeleton in response to local radiation or chemotherapy. These studies demonstrate an important role for bone lining cells in mediating the skeletal and possibly the marrow response to injury. This methodology also establishes a translational model for studying the skeletal health of cancer survivors.

CLINICAL RELEVANCE/APPLICATION

Dual isotope 18 F-CT-PET revealed functional heterogeneity of the skeleton in response to radiation or chemotherapy and establishes a translational model to study the skeletal health of cancer survivors.

SSQ12-07 • Direct Water Proton Saturation (DWS) Imaging of Prostate Cancer

Guang Jia PhD (Presenter) ; Saba N Elias MSc ; Wenbo Wei ; Daniel J Clark MSc ; Jinyuan Zhou PhD ; Michael V Knopp MD, PhD

PURPOSE

Conventional magnetization transfer (MT) can be used to study the interaction of free water protons to macromolecular protons in the

prostate. However, MT only shows weak contrast between prostate cancer and benign regions due to a large frequency offset. Direct water proton saturation (DWS) may provide a stronger contrast by applying a smaller frequency offset. This study is to evaluate DWS imaging for prostate cancer detection.

METHOD AND MATERIALS

A total of 20 patients with prostate cancer were prospectively enrolled in this sub-study. All patients were imaged on a 3 Tesla MR system (Achieva, Philips Healthcare). DWS imaging was based on single-slice single-shot TSE sequence. The saturation pre-pulse was composed of a train of sixteen block pulses, each with a pulse length of 31 ms and a flip angle of 720° to 1800°. The single slice image was acquired with saturation pre-pulse at 33 different frequencies (8 to -8 ppm with an interval of 0.5 ppm) and the scan time was 3 min. Magnetization transfer ratio (MTR) at 8 ppm was calculated on tumor regions, non-cancerous peripheral zone, and central gland at four different saturation pre-pulse powers (1.6, 2.4, 3.2, and 4.0 \diamond T). Student t-test was used to compare MTR(8ppm) in the histology identified tumor region and non-cancerous regions.

RESULTS

The measured MTR at 8 ppm in prostate cancer was 10.2% \pm 0.6% at 1.6 \diamond T, 20.7% \pm 1.9% at 2.4 \diamond T, 29.0% \pm 3.0% at 3.2 \diamond T, and 37.2% \pm 3.6% at 4 \diamond T, indicating a linear relationship between MTR(8ppm) and the saturation pre-pulse power. Non-cancerous peripheral zone showed significantly smaller MTR(8ppm) at all four powers (7.3% \pm 2.3% at 1.6 \diamond T, 14.7% \pm 2.9% at 2.4 \diamond T, 21.4% \pm 4.7% at 3.2 \diamond T, and 28.2% \pm 5.6% at 4 \diamond T, $P < 0.01$). Non-cancerous central gland exhibited similar MTR(8ppm) values to prostate cancer regions (11.1% \pm 2.2% at 1.6 \diamond T, 20.1% \pm 2.0% at 2.4 \diamond T, 28.9% \pm 2.0% at 3.2 \diamond T, and 37.1% \pm 4.9% at 4 \diamond T, $P > 0.05$).

CONCLUSION

Direct water proton saturation imaging can generate a contrast that is different from T1 or T2 contrast. Malignant tumors consistently reveal higher MTR(8ppm) due to increased magnetization transfer and direct water saturation effects. By optimizing the saturation pre-pulse power and frequency offset, image contrast in the prostate can be substantially enhanced.

CLINICAL RELEVANCE/APPLICATION

The DWS-MRI approach has the potential to improve imaging of cancerous tissue within organs such as the prostate by better tissue contrast.

SSQ12-08 • Enhanced Delineation of Primary Pancreatic Adenocarcinoma Following Neoadjuvant Therapy Using -Ferumoxylol: Preliminary Findings with Histopathologic Correlation

Sandeep S Hedgire MD (Presenter) ; Mari Mino Kenudson MD ; Carlos Fernandez-Del Castillo MD ; Sarah Thayer ; Ralph Weissleder MD, PhD ; Mukesh G Harisinghani MD

PURPOSE

To evaluate role of MRI with ferumoxylol in delineating primary tumor in pancreatic adenocarcinoma patients undergoing preoperative neoadjuvant therapy.

METHOD AND MATERIALS

In institutional review board approved, HIPPA compliant prospective study, 10 patients with biopsy proven pancreatic adenocarcinoma were enrolled with the primary intention of detecting lymph node metastasis following administration of ferumoxylol. MRI scans were performed at baseline, immediate post and at 48 hrs time points with quantitative T2* sequences using single shot, monopolar, multiecho gradient echo (TE = 4.8 \diamond 24.8, TR = 169 ms, thickness = 4 mm). The patients were categorized into those who received preoperative neoadjuvant therapy (group A) and those who did not (group B). The T2* of primary pancreatic tumor and adjacent parenchyma was recorded at baseline and 48 hrs time point in both groups and the difference between T2* values was calculated. After Whipple surgery, the primary tumors were assessed histopathologically for fibrosis and inflammation.

RESULTS

Five of the 10 (50 %) patients had presurgical neoadjuvant therapy. The mean T2* of tumor and adjacent parenchyma at 48 hrs in group A were 22.11 ms and 16.34 ms respectively. In group B, these values were 23.96 ms for tumor and 23.26 ms for adjacent parenchyma. The T2* difference between the tumor and adjacent parenchyma in group A was more pronounced compared to group B. The tumor margins were subjectively more distinct in the group A compared to group B. Histopathologic evaluation showed prominent fibrosis with scattered residual tumor glands with therapeutic effects, and a rim of dense fibrosis with atrophic acini at the periphery of the lesion in the group A. Conversely, intact tumor cells/glands were present at the periphery of the tumor in the group B. Two patients didn't undergo Whipple surgery due to hepatic metastasis detected preoperatively.

CONCLUSION

Ferumoxylol may have potential application in depicting post neoadjuvant therapy induced fibrosis (especially at the periphery of the tumor) and thereby improving the ability for precise delineation of tumor margins.

CLINICAL RELEVANCE/APPLICATION

Indistinct tumor margin poses a challenge to the surgeon. MRI with ferumoxylol may be used for better delineation of the pancreatic cancer thereby affecting surgical planning and overall prognosis.

SSQ12-09 • Quantification of ADC and SUV Values in Tumors and Lymph Node Metastases of Patients with Cervical Carcinoma in a Simultaneous PET-MRI System

Philipp Brandmaier MD (Presenter) ; Sandra Purz MD ; Martin Reinhardt MD ; Henryk Barthel ; Osama Sabri MD ; Thomas K Kahn MD ; Patrick Stumpp MD, PhD

PURPOSE

Previous studies have shown discrepancies between standard uptake value (SUV) and apparent diffusion coefficient (ADC) parameters of different tumor entities with non simultaneous measurements on examination modalities such as PET-CT and MRI. The objective of this study was the quantitative evaluation of SUV and ADC values in patients with primary and recurrent cervical cancer and suspicious lymph nodes in a simultaneous PET-MRI system to exactly deteriorate an expectable correlation.

METHOD AND MATERIALS

We included 15 patients with histologically confirmed cervical carcinoma and lymph node metastases (total of 38 lesions; primary tumor n= 14; positive lymph nodes n=24) who all underwent a simultaneous whole body 18F-fluorodeoxyglucose (FDG) PET-MRI (T2-HASTE, TIRM, EPI-DWI with b values of 0 and 800 mm/s²) including a dedicated pelvic examination (EPI-DWI with b values of 0,50,400,800 mm/s², T2 - TSE, T1-weighted TSE native and post-contrast \pm fat suppression). Reader defined volume-of-interest (VOI; 0.2-0.5 mm³) for ADC and SUV were placed in suspicious tumor lesions and FDG-positive lymph nodes (short axis diameter > 5mm) in regions with maximum FDG-uptake. ADC_{min}, ADC_{mean}, relative ADC value (ratio of ADC_{mean} / ADC_{reference tissue}) and SUV_{mean} was calculated with the M.gluteus maximus serving as reference tissue. Evaluation was performed by simultaneous analysis of specific lesions on a dedicated workstation (syngo.via, Siemens Medial Solutions \diamond , Erlangen, Germany). A value of

RESULTS

Local tumor lesions and lymph nodes showed average SUV_{mean} values of 12.7 (SE \pm 1.63), respectively 9.4 (SE \pm 1.59); corresponding ADC_{mean} averages amounted to 1.020 x 10⁻³ mm/s² (SE \pm 0.104) and 1.094 x 10⁻³ mm/s² (SE \pm 0.12). A significant difference to reference tissue (SUV 0.72 \pm 0, 17 SE, ADC 1.58 \pm 0.12 SE) was seen.

CONCLUSION

The present work demonstrates the ability of acquisition of quantitative parameters (ADC and SUV) in a simultaneous PET-MRI system. Values of ADC and SUV in tumor tissue apparently show an opposite behaviour to ADC and SUV values in non-tumor tissue.

CLINICAL RELEVANCE/APPLICATION

Simultaneous quantification of SUV and ADC parameters in PET-MRI show an opposite behaviour which might be useful for evaluation of

Characterization of Breast Cancer Using PET Molecular Imaging: A Clinical Perspective

Thursday, 12:15 PM - 12:45 PM • S503AB

[Back to Top](#)

CL-MIE-TH5A

Amir Imanzadeh , MD
Pedram Heidari , MD
Sarvenaz Pourjabbar , MD

PURPOSE/AIM

18F-FDG, despite its widespread use in oncologic assessment, has limited application in breast cancer (BrCa) characterization; a broad range of PET tracers has been developed for BrCa to address this unmet need. We will discuss i) the major classes of targeted compounds that have been used for imaging of BrCa; ii) detail the most promising tracers in each class.

CONTENT ORGANIZATION

1. Importance of PET imaging in BrCa 2. Limitations of 18F-FDG in characterization of BrCa 3. Various classes of receptor PET tracers including small molecules, peptides, antibody fragments 4. A detailed description (including advantages and limitations) of tracers in each class with potentially higher clinical impact in BrCa 5. Future directions in development of novel PET tracers for BrCa.

SUMMARY

PET has become a powerful tool in diagnosis and follow up of cancer patients including BrCa. Since 18F-FDG has a number of limitations in characterization of BrCa phenotype, a wide variety of PET tracers have been developed that range from small molecules to intact antibodies. This overview encompasses limitations of FDG PET in BrCa, groups of compounds that can be used as probes for BrCa PET imaging, and detailed examples of more promising tracers in each class.

Molecular Imaging - Thursday Posters and Exhibits (12:15pm - 12:45pm)

Thursday, 12:15 PM - 12:45 PM • S503AB

[Back to Top](#)



CL-MIS-THA • AMA PRA Category 1 Credit™:0.5

Host
Umar Mahmood , MD, PhD

CL-MIS-TH1A • Simplified Two-timepoint FDG-PET/CT for Diagnosis of Pancreatic Lesions. Is It Helpful in Determining Pancreatic Lesions?

Freimut Juengling MD, PhD (Presenter) * ; Christian Bieg MD ; Ralph Peterli MD ; Markus Von Flue MD ; Markus Gass MD

PURPOSE

Predicting the dignity of pancreatic lesions is still a diagnostic challenge. Fusion of FDG-PET/CT with diagnostic computed tomography offers new possibilities, nevertheless the differentiation between benign changes in chronic pancreatitis from pancreatic cancer remains difficult. Therefore the aim of this study was to evaluate, whether early two-timepoint kinetics of pancreatic lesions in FDG PET may be helpful to differentiate pancreatic lesions

METHOD AND MATERIALS

We prospectively analyzed 64 patients (pancreatic cancer n=45, chronic pancreatitis n=19) scheduled for two-timepoint FDG-PET/CT scan for pancreatic lesions in our hospital between 2005-2011. Studies were performed 60 and 90 minutes after application of the radioactive substance. Histological samples were collected for all patients, either by resection or by biopsy. Semi-quantitative analysis was performed using the minimal, the maximal and the average standardized uptake value (SUV) from the two different sets of images and a SUV change was calculated as difference between the two measurements in percent. SUV changes of patients with pancreatic cancer and chronic pancreatitis were compared using the student t-test.

RESULTS

Mean change of SUV_{min} was 12.04 % for pancreatic cancer vs. -4.66 % for chronic pancreatitis respectively (p=0.00012). Mean change of SUV_{avg} was 12.13 % for pancreatic cancer vs. -5.65 % for chronic pancreatitis respectively (p

CONCLUSION

The present analysis shows a statistically highly significant difference comparing the changes in SUV_{min}, SUV_{avg} and SUV_{max} in early two-timepoint PET/CT images of pancreatic cancer and chronic pancreatitis. This is the first analysis of two-timepoint PET/CT performed as early as 30 minutes after the first images. The additional time and effort is minimal and fits perfectly into the existing, clinical and diagnostic workflow. Therefore, in patients with suspicious pancreatic lesions the simplified two-timepoint FDG-PET/CT represents an excellent diagnostic option and is helpful in characterizing pancreatic lesions.

CLINICAL RELEVANCE/APPLICATION

In patients with pancreatic lesions simplified two-timepoint FDG-PET/CT can help to differentiate between malignant and chronic inflammatory disease and is recommended in initial diagnostic evaluation

CL-MIS-TH2A • Functional Diffusion Map, a Preferable Biomarker versus Mean ADC Value for Early Evaluation of TACE Treatment Response in Patients with Liver Carcinoma

Yong-Bo Yang (Presenter) ; Yu-Fang Chen ; He Wang PhD ; Dong Chen ; Xing-An Long ; Hong-Yan Cheng

PURPOSE

To compare the efficacy of Functional Diffusion Map (FDM) and mean ADC in the early evaluation of Transarterial Chemoembolization (TACE) treatment response in patients with liver carcinoma, as it was typically evaluated by traditional imaging methods several months later.

METHOD AND MATERIALS

A total of 45 patients with liver carcinoma were enrolled and treated with TACE. T1-weight and DWI (b=600) were performed before treatment and 4 weeks later. The three-color FDM was obtained from the registration of DWI images to their own pre-treatment T1-weighted images and a 12-degree of freedom transformation using FSL (FMRIB, Oxford, UK). Red voxels (VR) for which the ADC increased significantly, blue voxels (VB) for which the ADC decreased significantly, and green voxels (VG) for which the ADC did not change significantly, where total voxels (VT= VR+VB) for which the ADC changed significantly. The mean ADC values were measured on the diffusion MRI images in one week ahead of TACE and one month after the treatment. Each patient was examined by dynamic contrast-enhanced CT or MRI every 3 months during the follow-up.

RESULTS

CONCLUSION

FDM showed better efficacy than the mean ADC value in the early evaluation of therapeutic response in patients with liver carcinoma after TACE, and a fairly close association with those by the long-term conventional means of imaging. It will be a powerful and promising

biomarker and could provide an early and important reference for the clinical protocols.

CLINICAL RELEVANCE/APPLICATION

FDM may be a robust biomarker with better efficacy than the mean ADC value in the early evaluation of therapeutic response and could provide important reference for the clinical protocols.

CL-MIS-TH3A • Hybrid 18F-FDG PET-MRI of the Hand in Rheumatoid Arthritis

Falk R Miese MD (Presenter) ; Hubertus Hautzel MD ; Benedikt Ostendorf ; Gerald Antoch MD * ; Axel Scherer MD ; Hans Herzog

PURPOSE

18F-FDG-PET is highly sensitive to inflammatory activity in Rheumatoid Arthritis (RA). However, it is MRI that is the imaging method of choice for the visualization of joint damage in RA due to its high soft tissue contrast and superior spatial resolution. The purpose of the present study was to test the feasibility of true hybrid PET-MRI of the hand in RA and to compare the assessment of synovitis in PET and MRI.

METHOD AND MATERIALS

True hybride 18F-FDG PET-MRI was acquired in four patients. All patients were female with an average age of 48 years, range 24-58 years. Two presented with early therapy-naïve RA, two presented prior to therapy escalation. PET-MRI were acquired on a APD-based magnetoinsensitive BrainPET Detector (Siemens Healthcare, Erlangen, Germany) in a 3 T MRI scanner (Magnetom Trio, Siemens). The MRI data were evaluated according to the RAMRIS synovitis criteria. The PET of the same joints was categorized semiquantitatively. Additional findings, not included in the RAMRIS criteria, such as tenovaginitis or synovitis of joints not applicable for the RAMRIS were recorded.

RESULTS

All patients were positive for synovitis in MRI and PET. On a joint base, 21/26 (81%) of joints were MRI-positive, and 18/26 (69%) were positive on PET. In three joints that demonstrated synovitis on MRI, normal glucosid utilization was noted (14%). Synovitis severity as measured in PET and MRI correlated significantly ($r = 0.672$; $P < 0.001$). In 6/10 additional abnormal findings there was concordance between MRI and PET.

CONCLUSION

The results of this feasibility study point towards the validity of 18F-FDG PET-MRI of the hand in RA. 18F-FDG PET-MRI may possibly be a tool for further research on inflammatory activity, therapy control and joint destruction in RA.

CLINICAL RELEVANCE/APPLICATION

Inflammation and joint destruction in RA can proceed under therapy. 18F-FDG PET-MRI may be a research tool for the assessment of both, inflammatory activity and joint destruction in RA.

CL-MIS-TH4A • Ultra-high Relaxivity Gd Nanoparticles for Molecular Imaging

Ananth Annapragada PhD * ; Eric Tanifum PhD * ; Ketan B Ghaghada PhD (Presenter) *

PURPOSE

: T1 based Magnetic Resonance (MR) molecular imaging requires molecularly targeted, high relaxivity contrast agents. The Solomon-Bloembergen-Morgan equations predict that the T1 relaxivity of Gd-based agents at clinically relevant field strengths can be increased by increasing the rotational correlation time of the Gd. The purpose of this work was therefore to design Gd-presenting nanoparticles that increased the rotational correlation time, and to test them in vitro and in vivo.

METHOD AND MATERIALS

Gd-presenting liposomal nanoparticles were designed with Gd chelates either on, or off hydrophilic tethers that modulated the in-membrane flipping of the Gd. Lipid anchors were varied to modulate the in-membrane rotation. Relaxivity measurements were made at field strengths from 1.4T to 9.4T. MR angiography was performed in C57BL/6 mice to study signal intensity as a function of gadolinium dose in the vasculature, and immobilized in tissue.

RESULTS

The liposomal nanoparticle enabled association of 25,000-100,000 gadolinium chelates per nanoparticle. Inhibiting Gd chelate rotation resulted in at least a 5 fold increase in T1 relaxivity compared to conventional contrast agents. MRA studies demonstrated a long blood half-life (~24 hours) of the nanoparticle contrast agent compared to the conventional agents. The high T1 relaxivity of the nanoparticle agent resulted in a substantially higher signal-to-noise ratio and improved feature conspicuity.

CONCLUSION

This study demonstrates an ultrahigh T1 relaxivity nanoparticle contrast agent for use in MR molecular imaging. Combined with the multiplex ability of the particle encapsulating a large number of Gd atoms, a signal enhancement of at least 125,000 over traditional Gd chelates is achieved. This could facilitate the use of such a particle in MR molecular imaging.

CLINICAL RELEVANCE/APPLICATION

The development of a high T1 relaxivity Gadolinium-based nanoparticle contrast agent will enable MRI-based interrogation of molecular targets.

Molecular Imaging - Thursday Posters and Exhibits (12:45pm - 1:15pm)

Thursday, 12:45 PM - 01:15 PM • S503AB



CL-MIS-THB • AMA PRA Category 1 Credit™:0.5

CL-MIS-TH1B • Qualitative Assessment in Radiotherapy of Lung Cancer Using Gemstone Spectral Imaging

Weihua Li MD, PhD (Presenter) ; Dan Wang ; Beiqiu Han MD ; Bao-Zhong Shen

PURPOSE

To evaluate tumor responses in patients treated with radiotherapy for medically inoperable non-small cell lung cancer (NSCLC) by assessing intratumoral changes and damage of nearby tissues using gemstone spectral imaging (GSI).

METHOD AND MATERIALS

26 cases of early-stage, biopsy-proved, medically inoperable lung cancer (NSCLC) underwent gemstone spectral imaging before and 1-6 weeks after radiotherapy. The CT images before and after radiotherapy were obtained and iodine concentration, water concentration and spectrum energy curve and CT values at 40-50 keV were measured. All the data were post processed by using GSI viewer software. Tumor response was evaluated by comparing tumor dimensions, volumes and damage of nearby tissues before and after radiotherapy with standard PET/CT evaluation criteria. Those measurements between pre- and post-treatment and two methods were compared by using SPSS 17.0.

RESULTS

[Back to Top](#)

Mean CT values of tumor and iodine content of the tumor region of interest (ROI) in post-therapy were significant lower than that in pre-therapy (50.13±7.50 vs. 78.82±11.81 (HU), 0.91±0.32 vs. 2.65±0.35 (g/L), P

CONCLUSION

Gemstone spectral CT imaging is a noninvasive, precise and rapid screening method. By spectral imaging and material separation technology, it could provide more qualitative and quantitative assessment in radiotherapy of lung cancer.

CLINICAL RELEVANCE/APPLICATION

Gemstone spectral CT imaging could provide valuable information for the diagnosis and monitoring of tumor responses in patients treated with radiotherapy for non-small cell lung cancer.

CL-MIS-TH3B • 3T Cellular Imaging of Liver Inflammation in a Murine Model of Induced Hepatitis

Cindy Fayard (Presenter) ; **Vanessa Deveaux** ; **Florence Gazeau** ; **Adrien Guillot** ; **Lambros C Tselikas MD** ; **Julien Calderaro** ; **Sophie Lotersztajn** ; **Alain Rahmouni MD** ; **Alain Luciani MD, PhD ***

PURPOSE

To design and optimize a 3T MRI protocol for liver inflammation detection and quantification following USPIO IV injection in a murine model

METHOD AND MATERIALS

All experiments complied to current ethical regulations; P904 (Guerbet, Aulnay, France) was used as USPIO contrast agent. 47 C57BL6 male mice were injected with increasing doses of P904 in order to determine the optimal P904 dose. 30 additional C57BL6 mice were randomized in 3 distinct groups. In two groups distinct states of inflammation were induced by injection of lipopolysaccharides (LPS) at respective 1 and 2 mg / g dose, while the last group served as control. The effect of P904 injection on liver signal variance was tested on a 3T MRI, and correlated with the quantification of liver macrophages on immunohistochemistry (F4/80), to pro-inflammatory markers quantification by RT-PCR, and to the absolute iron quantification.

RESULTS

P904 injection induced an increase in the variance of the liver signal proportional to the dose injected. The optimal dose of P904 for the study of liver inflammation was 150µmol/kg. There was a significant correlation (r = 0.86, p

CONCLUSION

It is possible to detect and quantify liver inflammation following USPIO injection using 3T MRI.

CLINICAL RELEVANCE/APPLICATION

Non-invasive assessment of liver inflammation using clinical 3T scanners could contribute to the optimized detection and follow-up of chronic liver disease on MRI.

Ultrasound/Opto-Acoustic Molecular Imaging

Thursday, 04:30 PM - 06:00 PM • S504CD



[Back to Top](#)

RC717 • AMA PRA Category 1 Credit™:1.5 • ARRT Category A+ Credit:1.5

Moderator

Juergen K Willmann, MD *

LEARNING OBJECTIVES

In this course, attendees will learn the principles and applications of molecular imaging using ultrasound and photoacoustic imaging techniques. In the first part, principles and applications of ultrasound molecular imaging will be reviewed. In the second part, principles and applications of molecular imaging using photoacoustic imaging techniques will be presented. In the third part, ultrasound guided drug delivery approaches will be reviewed. At the end of this course, the attendees will understand the principles and potential clinical applications of ultrasound and optoacoustic molecular imaging as well as of ultrasound guided drug delivery.

RC717A • Photoacoustic Imaging

Stanislav Emelianov PhD (Presenter) *

LEARNING OBJECTIVES

1) Understand the fundamental principles of photoacoustic imaging and major components of photoacoustic imaging system. 2) Knowing how photoacoustic images are formed and how to interpret photoacoustic images. 3) Understand how imaging contrast agents or imaging probes affect contrast, penetration depth and specificity in photoacoustic imaging. 4) Understand the ability of photoacoustic imaging system to visualize anatomical, functional and molecular properties of imaged tissue. 5) Identify the role of photoacoustic imaging in pre-clinical and clinical applications.

ABSTRACT

Photoacoustic imaging or tomography is a non-ionizing, non-invasive, real-time imaging technique capable of visualizing optical absorption properties of tissue at reasonable depth and high spatial resolution, is a rapidly emerging biomedical and clinical imaging modality. Photoacoustic imaging is regarded for its ability to provide in-vivo morphological and functional information about the tissue. With the recent advent of targeted contrast agents, photoacoustics is capable of in-vivo molecular imaging, thus facilitating further molecular and cellular characterization of tissue.

This presentation is designed to provide both a broad overview and a comprehensive understanding of photoacoustic imaging. With a brief historical introduction, we will examine the foundations of photoacoustics, including relevant governing equations, optical/acoustic properties of the tissues, laser-tissue interaction, system hardware and signal/image processing algorithms. Specifically, penetration depth and spatial/temporal resolution of photoacoustic imaging will be analyzed. Integration of photoacoustic and ultrasound imaging systems will be discussed. Techniques to increase contrast and to differentiate various tissues in photoacoustic imaging will be presented. Furthermore, design, synthesis and optimization of imaging probes (typically, nanoconstructs or dyes) to enable molecular/cellular photoacoustic imaging will be presented. Special emphasis will be placed on contrast agents capable of multiplexed imaging, multi-modal imaging and image-guided therapy including drug delivery and release. The presentation will continue with an overview of several commercially available and clinically-relevant systems capable of photoacoustic imaging. Regulatory aspects of photoacoustic imaging systems and imaging contrast agents will be presented. Finally, current and potential biomedical and clinical applications of photoacoustics will be discussed.

RC717B • Ultrasound Molecular Imaging

Juergen K Willmann MD (Presenter) *

LEARNING OBJECTIVES

1) To understand the acquisition and quantification principles of ultrasound molecular imaging. 2) To understand the characteristics and biodistribution of molecularly targeted ultrasound contrast agents. 3) To understand the role of ultrasound molecular imaging in preclinical and clinical applications.

ABSTRACT

Ultrasound imaging is a widely available, relatively inexpensive, and real-time imaging modality that does not expose patients to radiation and which is the first-line imaging modality for assessment of many organs. Through the introduction of ultrasound contrast

agents, the sensitivity and specificity of ultrasound for detection and characterization of focal lesions has been substantially improved. Recently, targeted contrast-enhanced ultrasound imaging (ultrasound molecular imaging) has gained great momentum in preclinical research by the introduction of ultrasound contrast agents that are targeted at molecular markers over-expressed on the vasculature of certain diseases. By combining the advantages of ultrasound with the ability to image molecular signatures of diseases, ultrasound molecular imaging has great potential as a highly sensitive and quantitative method that could be used for various clinical applications, including screening for early stage disease (such as cancer); characterization of focal lesions; quantitative monitoring of disease processes at the molecular level; assisting in image-guided procedures; and, confirming target expression for treatment planning and monitoring. In this refresher course the concepts of ultrasound molecular imaging are reviewed along with a discussion on current applications in preclinical and clinical research.

RC717C • Sonographically-guided Drug Therapy

Alexander L Klibanov PhD (Presenter) *

LEARNING OBJECTIVES

1) To identify the basic principles of ultrasound energy deposition as applied to molecular imaging and image-guided therapeutic interventions. 2) To combine the general physical principles of ultrasound-microbubble interaction, drug-carrier systems pharmacokinetics and ultrasound contrast imaging, apply this knowledge for the development of triggered delivery approaches in the setting of personalized medicine. 3) To understand advantages and disadvantages of ultrasound application in the potential image-guided intervention designs. 4) To identify and compare potential clinical applications of ultrasound-guided drug delivery.

ABSTRACT

The reason of ultrasound use in drug delivery is to enhance drug action specifically in the area of disease. The design of such therapeutic intervention should assure that drug deposition or action enhancement take place only in the disease site, with the general goal to improve the therapeutic index. There are several approaches to ultrasound-assisted drug delivery. The first approach, closest to clinical practice, takes advantage of existing ultrasound contrast agents (intravenous gas microbubbles approved in US for cardiac imaging). When these bubbles are co-injected intravenously with the drugs, and ultrasound energy applied to the areas of disease, localized energy deposition leads to endothelium activation or transient 'softening' of blood brain barrier (BBB). Drugs (including antibodies or liposomes) can thus transit BBB and achieve therapeutic action. Ultrasound imaging can be used for targeted focusing of ultrasound energy in the areas of disease. Second approach suggests attaching microbubbles to the drug or a drug carrier (including nucleic acid drugs). Microbubbles can be complexed with drug or gene carrier nanoparticles, so that local action of ultrasound would result in triggered drug release/deposit or transfection in the ultrasound-treated area. Third approach involves targeted microbubble design, as in ultrasound molecular imaging. Combination of targeted microbubbles with drug carrier makes possible unfocused ultrasound use, to act only in the areas of the target receptor expression, where microbubbles adhere and ultrasound energy is then deposited. Lately, formulation moved from microbubbles to smaller nanodroplet drug carriers, to reach interstitium, where drug release could take place upon ultrasound treatment. Overall, combination of ultrasound imaging, including contrast (molecular) imaging, focused ultrasound, and drug carrier systems will lead to novel image-guided therapies, especially applicable in the era of personalized medicine.

Essentials of Molecular Imaging

Friday, 08:30 AM - 10:00 AM • S505AB



[Back to Top](#)

RC817 • AMA PRA Category 1 Credit™:1.5 • ARRT Category A+ Credit:1.5

Moderator

Steven M Larson, MD *

RC817A • Molecular Imaging as a Guide for Better Cancer Therapies

Steven M Larson MD (Presenter) *

LEARNING OBJECTIVES

1) The participants will learn the definition of theranostic radiotracer. 2) The participants will learn the role of MEK in non-avid thyroid cancer. 3) The participants will learn why expression of Prostate Specific Membrane antigen (PSMA) offers potential for improved diagnosis and therapy of prostate cancer. 4) The participants will learn the contribution of radioactive nanoparticles both now and in the future for staging and drug delivery.

RC817B • Pediatric Molecular Imaging

Heike E Daldrop-Link MD (Presenter)

LEARNING OBJECTIVES

1) To understand advantages and limitations of radiation-free whole body diffusion MRI techniques for tumor staging in children. 2) To recognize the value of immediately clinically applicable iron oxide nanoparticles for tumor staging and tumor characterization in pediatric patients. 3) To learn about clinically relevant PET/MR applications in pediatric patients.

ABSTRACT

Pediatric Molecular Imaging

How much does Molecular Imaging matter in our clinical environment? Molecular Imaging spurs the discovery of fundamentally new targets for imaging diagnoses, thereby leading to new knowledge and new concepts that substantially advance our approach to detecting, characterizing and treating disease. Translational molecular imaging approaches are increasingly integrated into the clinical care of adult patients, but applications in pediatric patients are still limited due to safety considerations and regulatory and administrative hurdles. The clinical need for more specific information along with the success of molecular imaging techniques in adult patients will ultimately penetrate into pediatric applications. New, child-adapted molecular imaging approaches are currently utilized to improve our knowledge of the biology of pediatric diseases, and to support personalized diagnostic and therapeutic approaches. This presentation will show three immediately clinically applicable molecular imaging applications for pediatric patients: (1) Novel approaches for radiation-free whole body staging, (2) Improved tumor characterization with clinically approved iron oxide nanoparticles and (3) clinically relevant MR/PET applications in pediatric patients. Further developments aim to integrate the advantages of multi-modality molecular imaging tools towards more comprehensive and quantitative diagnoses that can direct early decision making, guide individualized clinical care procedures, and ultimately, accelerate and improve positive treatment outcomes.

RC817C • Molecular Imaging of Breast Cancer: Clinical and Biologic Insights

David A Mankoff MD, PhD (Presenter)

LEARNING OBJECTIVES

1) Review breast cancer clinical and biologic concepts relevant to treatment. 2) Discuss how molecular imaging may be used to guide targeted breast cancer therapy. 3) Describe future directions in breast cancer biomarker imaging.

ABSTRACT

This talk will review molecular imaging in the context of current knowledge of breast cancer biology and the increasing trend towards individualized and targeted breast cancer therapy. The discussion will emphasize molecular imaging, especially PET, and biomarker applications to guide treatment selection. Insights gained into the in vivo biology of breast cancer from quantitative molecular imaging

will also be discussed.

RC817D • New Tools and Targets for Molecular Imaging

Martin G Pomper MD, PhD (Presenter) *

LEARNING OBJECTIVES

1) Discuss emerging molecular imaging agents. 2) Discuss new targets for molecular imaging. 3) Focus on translation of molecular imaging agents to the clinic.

ABSTRACT

We will discuss how one goes about identifying a suitable target for molecular imaging and then actually generates the imaging agent - for a variety of modalities, whichever is appropriate to answer the question at hand. There will be a focus on clinical translation and discussion of combined diagnostic/therapeutic (theranostic) agents.

Disclosure Index

A

Alsop, D. C. - Research support, General Electric Company Royalties, General Electric Company
Anderson, N. G. - Stockholder, MARS Bioimaging Ltd
Annapragada, A. - Founder, Marval Biosciences Inc Stockholder, Marval Biosciences Inc Founder, Alzeza Biosciences LLC Stockholder, Alzeza Biosciences LLC Founder, Sensulin LLC Stockholder, Sensulin LLC Stockholder, Abbott Laboratories Stockholder, Johnson & Johnson Stockholder, Merck & Co, Inc
Antoch, G. - Speaker, Siemens AG Speaker, Bayer AG

B

Basilion, J. P. - Co-founder, AKrotome Imaging Inc Scientific Advisory Board, AKrotome Imaging Inc
Beer, A. J. - Speaker, Siemens AG
Bettinger, T. - Employee, Bracco Group
Boctor, E. - Co-founder, Clear Guide Medical LLC
Brenner, W. - Research Consultant, Bayer AG
Brown, R. - Investor, RadExchange, LLC
Butler, A. P. - Director, MARS Bioimaging Ltd

C

Carrino, J. A. - Research Grant, Siemens AG Research Grant, Carestream Health, Inc Research Consultant, General Electric Company
Chakravarthy, A. - Research Grant, Bayer AG Research Grant, Onyx Pharmaceuticals, Inc
Chen, J. - Research Grant, Pfizer Inc
Cheng, D. W. - Consultant, Bayer AG Consultant, Navidea Biopharmaceuticals, Inc
Cho, S. - Research support, Amgen Inc Research support, Peregrine Pharmaceuticals, Inc Research support, Algeta ASA
Cobas, C. - Co-founder and President, Mestrelab Research SL
Cornelius, R. S. - Spouse, Stockholder, Bristol-Myers Squibb Company
Cross, D. J. - Research Grant, Hitachi, Ltd Research Grant, Astellas Group

D

Drzeczga, A. - Research Consultant, Bayer AG Research Consultant, Eli Lilly and Company Research Consultant, General Electric Company Research Consultant, Piramal Enterprises Limited Speakers Bureau, Bayer AG Speakers Bureau, Eli Lilly and Company Speakers Bureau, General Electric Company Speakers Bureau, Siemens AG Research Grant, Bayer AG

E

Emelianov, S. - Co-founder, NanoHybrids Inc.

F

Fain, S. B. - Research Grant, General Electric Company Research Consultant, Marvel Medtech, LLC
Fayad, Z. A. - Research Grant, Merck & Co, Inc Research Grant, Pfizer Inc Research Grant, F. Hoffmann-La Roche Ltd Research Grant, Takeda Pharmaceutical Company Limited Research Grant, DAIICHI SANKYO Group Research Grant, Siemens AG Research Grant, VIA Pharmaceuticals, Inc Research Grant, Guerbet SA Research Consultant, Merck & Co, Inc Research Consultant, VIA Pharmaceuticals, Inc Research Consultant, BG Medicine, Inc
Forsberg, F. - Equipment support, Toshiba Corporation Equipment support, Siemens AG Research collaboration, General Electric Company Research collaboration, Ultrasonix Medical Corporation Research collaboration, Toshiba Corporation Advisory Board, Siemens AG Advisory Board, Toshiba Corporation
Frey, K. A. - Consultant, MIMVista Corp Consultant, General Electric Company Consultant, Eli Lilly and Company Consultant, Bayer AG Research funded, General Electric Company Research funded, Eli Lilly and Company Stockholder, General Electric Company Stockholder, Novo Nordisk AS Stockholder, Bristol-Myers Squibb Company Stockholder, Merck & Co, Inc

G

Gagnon, D. - Employee, Toshiba Corporation
Ganeshan, B. - Scientific Director, TexRAD Limited
Ghaghada, K. B. - Research Grant, Marval Biosciences Inc Consultant, Marval Biosciences Inc Shareholder, Marval Biosciences Inc
Greenspan, B. S. - Consultant, CareCore National
Groves, A. M. - Investigator, GlaxoSmithKline plc Investigator, General Electric Company Investigator, Siemens AG Advisory Board, Merck & Co, Inc
Guimaraes, A. R. - Speakers Bureau, Siemens AG Expert Witness, Siemens AG
Guracar, I. - Employee, Siemens AG

H

Hahn, P. F. - Stockholder, Abbott Laboratories Stockholder, Covidien AG Stockholder, CVS Caremark Corporation Stockholder, Kimberly-Clark Corporation Stockholder, Landauer, Inc
Haines, E. - Employee, Toshiba Corporation
Halpern, H. J. - Consultant, Bruker Corporation
Ho, R. - Scientific Advisory Board, Impel NeuroPharma, Inc
Hristov, D. - Research Grant, Koninklijke Philips Electronics NV Partner, SoniTrack Systems, Inc
Hruska, C. B. - Institutional license agreement, Gamma Medica, Inc
Hugg, J. W. - Employee, Gamma Medica, Inc Officer, Gamma Medica, Inc
Huynh, P. T. - Research Grant, Siemens AG Consultant, Siemens AG

J

Ji, C. - Employee, Toshiba Corporation
Juengling, F. - Consultant, Siemens AG

K

Katzman, G. L. - Author, Amirsys, Inc Stockholder, Amirsys, Inc
Kieper, D. A. - Vice President, Dilon Technologies LLC
Klibanov, A. L. - Research Grant, Koninklijke Philips Electronics NV Stockholder, Targeson, Inc Grant, Targeson, Inc
Kundra, V. - License agreement, Introgen Therapeutics Inc
Kuo, M. D. - Shareholder, Confluence Life Sciences, Inc

L

Larson, S. M. - Owner, Clinical Silica Technologies Advisory Board, ImaginAb, Inc Advisory Board, Molecular Imaging, Inc Scientific Advisor, Takeda Pharmaceutical Company Limited Advisory Board, Perceptive Informatics, Inc Scientific Advisor, Progenics Pharmaceuticals, Inc
Lassau, N. B. - Speaker, Toshiba Corporation Speaker, Bracco Group Speaker, Novartis AG Speaker, Pfizer Inc Speaker, F. Hoffmann-La Roche Ltd
Liu, J. - Research Grant, GluMetrics, Inc
Luciani, A. - Research Consultant, General Electric Company

M

Macura, K. J. - Research Grant, Siemens AG
Mason, R. P. - Stockholder, AstraZeneca PLC Stockholder, GlaxoSmithKline plc Stockholder, Smith and Nephew plc Stockholder, Unilever
McConathy, J. E. - Research Consultant, GLG Consulting Speakers Bureau, Eli Lilly and Company Research Consultant, General Electric Company
Miles, K. - Director, TexRAD Limited Shareholder, TexRAD Limited
Minoshima, S. - License agreement, General Electric Company Research Grant, Koninklijke Philips Electronics NV Research Grant, Hitachi, Ltd Research Consultant, Hamamatsu Photonics KK Grant, Nihon Medi-Physics Co, Ltd Research Grant, Astellas Group Research Grant, Seattle Genetics, Inc

N

Nichols, K. - Royalties, Syntermed, Inc Consultant, Gilead Sciences, Inc
Niu, X. - Employee, Toshiba Corporation
Ntziachristos, V. - Stockholder, iThera Medical GmbH

O

O'Connor, M. K. - Research Grant, General Electric Company Royalties, Gamma Medica Ideas, Inc
Ozaki, C. K. - Grant, Smith & Nephew plc

P

Padhani, A. R. - Consultant, IXICO Limited Advisory Board, Acuitus Medical Ltd Advisory board, Siemens AG
Pomper, M. G. - Co-founder, Cancer Targeting Systems, Inc Royalties, Li-Cor Biosciences Grant, Li-Cor Biosciences Grant, Eli Lilly and Company Royalties, Progenics Pharmaceuticals, Inc Grant, Bind Therapeutics, Inc Royalties, Bind Therapeutics, Inc Grant, Gamma Medical Technologies, LLC Royalties, Gamma Medical Technologies, LLC

Q

Quon, A. - Speakers Bureau, Lilly USA/Avid Pharmaceuticals Research Consultant, Phillips Healthcare

R

Rockall, A. G. - Speaker, Novartis AG Speaker, Guerbet SA
Rosen, B. R. - Research Consultant, Siemens AG
Rybicki, F. J. III - Research Grant, Toshiba Corporation Research Grant, Bracco Group

S

Shamdasani, V. - Employee, Koninklijke Philips Electronics NV
Strobel, K. - Employee, Bruker Corporation

T

Tanifum, E. - Stockholder, Alzeca Biosciences LLC
Teshigawara, M. - Employee, Toshiba Corporation
Tsai, L. L. - Co-founder, Agile Devices Inc Stockholder, Agile Devices Inc Research Consultant, Agile Devices Inc Scientific Board, Agile Devices Inc

V

Vachon, C. M. - Consultant, Pfizer Inc
Van Zijl, P. C. - Speakers Bureau, Koninklijke Philips Electronics NV License agreement, Koninklijke Philips Electronics NV
Vesselle, H. J. - Consultant, MIM Software Inc

W

Wacker, F. K. - Research Grant, Siemens AG Research Grant, Pro Medicus Limited
Wang, W. - Employee, Toshiba Corporation
Waxman, A. D. - Research Grant, Gamma Medica, Inc
Weigert, J. M. - Speakers Bureau, Dilon Technologies LLC Speakers Bureau, General Electric Company Stockholder, Tractus, Inc
Willmann, J. K. - Research Consultant, Bracco Group Research Grant, Siemens AG Research Grant, Bracco Group
Wright, K. C. - Shareholder, IDev Technologies, Inc Royalties, IDev Technologies, Inc
Wu, A. M. - Stockholder, ImaginAb, Inc Research Grant, ImaginAb, Inc Consultant, ImaginAb, Inc. Consultant, DAIICHI SANKYO Group Consultant, sanofi-aventis Group

X

Xia, T. - Employee, Toshiba Corporation

Y

Yap, J. T. - Research Grant, Toshiba Corporation Medical Advisory Board, Toshiba Corporation Research Grant, Bristol-Myers Squibb Company Research Grant, Bayer AG Research Grant, Pfizer Inc

Ye, H. - Employee, Toshiba Corporation